Université de Montréal

A study of chymotrypsin immobilization conditions for improved peptide mapping

Fatma Omar Elshalale

Département de chimie
Faculté des Arts et Sciences

Mémoire présenté à la Faculté des études supérieures et postdoctorales
en vue de l'obtention du grade de Maître ès science (M.Sc.)
en Chimie

March, 2014

Résumé

La cartographie peptidique est une technique de grande importance utilisée lors de l'identification des protéines et la caractérisation des modifications post-traductionnelles des protéines. Deux méthodes sont utilisées afin de couper les protéines en peptides pour la cartographie : les méthodes chimiques et les méthodes enzymatiques. Dans ce projet, l'enzyme chymotrypsine a été utilisée pour l'hydrolyse (la digestion) des liens peptidiques. Cependant, l'autoprotéolyse des enzymes peut augmenter la complexité des échantillons, rendant ainsi ardue l'obtention de pics résolus suite à l'apparition de pics non-désirés dans la carte peptidique. Par conséquent, nous avons utilisé la réticulation des enzymes protéolytiques par réaction avec le glutaraldéhyde (GA) donnant une enzyme insoluble afin de réduire l'autoprotéolyse. L'immobilisation de la chymotrypsine par GA a été effectuée selon une méthode rapportée précédemment par le groupe Waldron. L'électrophorèse capillaire (CE) couplée à l'absorption UV-visible a été utilisée pour la séparation et la détection de peptides et pour obtenir ainsi une cartographie peptidique.

Deux tampons différents ont été évalués afin d'obtenir les meilleures conditions pour la digestion de substrats protéiques par la chymotrypsine libre (soluble) ou la GA-chymotrypsine et l'analyse par CE. Les cartes des peptides autoprotéolytiques ont été comparées entre les deux formats de chymotrypsine. Afin d'améliorer la cartographie peptidique, nous avons évalué trois méthodes de conditionnement du capillaire CE et deux méthodes pour stopper la digestion. Le bicarbonate d'ammonium s'est avéré être le tampon optimal pour la digestion en solution et l'utilisation d'un bain d'acétone et de glace sèche s'est avérée être la méthode optimale pour stopper la digestion. Une solution de SDS, 25 mM, dans l'étape de rinçage a été utilisée après chaque analyse CE et a permis d'améliorer la résolution des cartes peptidiques. La comparaison entre l'autoprotéolyse de la chymotrypsine libre et de celle immobilisé par GA a été effectuée par des tests utilisant une gamme de six différentes combinaisons de conditions afin d'évaluer le temps (30 et 240 min) et la température de digestion (4, 24 et 37°C). Dans ces conditions, nos résultats ont confirmé que le GA-chymotrypsine réduit l'autoprotéolyse par rapport à l'enzyme libre.

La digestion (à 37°C/240 min) de deux substrats modèles par la chymotrypsine libre et immobilisée en fonction de la température de dénaturation du substrat a été étudiée. Avant

la digestion, les substrats (l'albumine de sérum bovine, BSA, et la myoglobine) ont été dénaturés par chauffage pendant 45 min à trois températures différentes (60, 75 et 90°C). Les résultats ont démontré que la dénaturation par chauffage du BSA et de la myoglobine n'a pas amélioré la cartographie peptidique pour la GA-chymotrypsine, tandis que la digestion de ceux-ci en présence de la chymotrypsine libre a amélioré de façon quantifiable à des températures élevées. Ainsi, le chauffage du substrat à 90°C avec l'enzyme soluble facilite le dépliement partiel du substrat et sa digestion limitée, ce qui a été mieux pour la myoglobine que pour la BSA.

Mots-clés : Cartographie peptidique / Réticulation / Glutaraldéhyde / Chymotrypsine / Électrophorèse capillaire

Abstract

Peptide mapping is an important technique used in conjunction with other methods to identify proteins and characterize post-translational modifications. To cleave proteins into small peptides for mapping, chemical and/or enzymatic methods are used. In the present study, the enzyme chymotrypsin was used for hydrolysis (digestion) of peptide bonds. A drawback of using soluble enzyme is autoproteolysis, the formation of peptides coming from chymotrypsin, giving unwanted peaks in the peptide map of the protein substrate. Therefore, making chymotrypsin immobile by cross-linking it with glutaraldehyde (GA) to avoid unwanted autoproteolysis peaks has been used in the present work. GA cross-linking for enzyme immobilization was carried out based on a method described previously in the Waldron group. Capillary electrophoresis (CE) was used for separation of the peptides (i.e., peptide mapping) as a way to evaluate digestion efficiency of soluble versus immobilized chymotrypsin.

To investigate the best conditions for digestion of protein substrate by free (soluble) versus GA-cross-linked chymotrypsin prior to analysis by CE, two different buffers were evaluated (ammonium bicarbonate and Tris-HCl). The maps of autoproteolysis peptides were compared between the two chymotrypsin formats. To improve the peptide maps obtained by CE, again using autoproteolysis of chymotrypsin without substrate present, three methods for capillary conditioning and two methods for terminating the digestion were investigated. Ammonium bicarbonate was found to be the best digestion buffer and a dry ice/acetone bath was the best method for stopping the digestion, with both of these giving better CE-based peptide maps. Adding 25 mM SDS in the post-conditioning capillary rinse was demonstrated to further improve peptide mapping. The autoproteolysis of soluble and GA-chymotrypsin were compared under 6 different conditions of digestion time (30 and 240 min) and temperature (4, 24 and 37ºC). Under these conditions, our results confirmed that the GA-cross-linking reduces chymotrypsin autoproteolysis compared to the free enzyme.

Digestion (at 37ºC/240 min) of two model substrates with free or immobilized chymotrypsin as a function of heat-induced denaturation of substrate was studied. Prior to digestion, the substrates (bovine serum albumin, BSA, and myoglobin) were denatured by heating for 45 min at three different temperatures (60, 75, and 90ºC). The results showed

heat-induced denaturation of BSA and myoglobin did not improve peptide maps when using GA-chymotrypsin digestion compared to using free chymotrypsin, although the latter improved with heat-induced denaturation at higher temperatures. Therefore, heating the substrate to 90ºC and using soluble enzyme provided some unfolding of substrate and limited digestion, which was better for myoglobin than for BSA.

Keywords: Peptide mapping / Cross-linking / Glutaraldehyde / Chymotrypsin / Capillary electrophoresis

Table of Contents

List of Tables

List of Figures

List of Annex Figures

List of Annex Tables

Abbreviations:

BSA	Bovine serum albumin
BGE	Background electrolyte
CE	Capillary electrophoresis
CZE	Capillary zone electrophoresis
CIEF	Capillary isoelectric focusing
CITP	Capillary isotachophoresis
CGE	Capillary gel electrophoresis
CT	Chymotrypsin
DAD	Diode array detector
EOF	Electroosmotic flow
f.s.	Fused silica
GA	Glutaraldehyde
GA-CT	Glutaraldehyde cross-linked chymotrypsin
HPLC	High performance liquid chromatography
HPLC-MS/MS	High performance liquid chromatography-tandem mass spectrometry
IEC	Ion exchange chromatography
ID	Inner diameter
LC	Liquid chromatography
L_t	Total length
L_d	Total length to capillary detector
MALDI-TOF-MS	Matrix assisted laser desorption/ionization time-of-flight mass spectrometry
MECC	Micellar electrokinetic capillary chromatography
MS	Mass spectrometry
O.D.	Outer diameter
RSD	Relative standard deviation
SDS	Sodium dodecyl sulfate
SDS-PAGE	Sodium dodecylesulfate-polyacrylamide gel electrophoresis
s	Standard deviation
Tris-HCl	Tris (hydroxymethyl) amino methane hydrochloride

UV	Ultra-Violet
Vis	Visible
v_{eo}	Electroosmotic velocity
v_{ep}	Electrophoretic velocity
v_{app}	Apparent velocity
μ_{EOF}	Electroosmotic mobility

I dedicate my dissertation work to my family especially mama, you always said
" work hard now and enjoy later".
with all this hard work, I guess it is my time to enjoy.

I also dedicate this work and give special thanks to my best husband Dr. Ben zabeh and my wonderful kids Salima, Faraj, Sundoos and Omar for being there for me throughout the entire master's program.

Acknowledgements

I would like to express the deepest appreciation to my supervisor Professor Karen C. Waldron, who has supported me continually during my research and progressive improvement of my scientific knowledge. Without her supervision and constant help this dissertation would not have been possible.

I would like to thank our group members, Golfam, Denis, Samantha, Antoine and Brain who helped me to achieve my goal and provided me with valuable scientific recommendations. Without help and support of my classmates, this achievement would not be complete.

Also, I would like to extend my appreciation for their continual support and help to the group members of Professor Rochefort; John Forgie, Árann McMahon, Bruno Gèlinas, Arash Atashi, Imene Benrazek, Soumia El Khakani, etc.

I wish to thank my committee members, Pr. Pierre Thibault and Pr. Alexis Vallée-Bélisle, for their expertise, precious time and extensive corrections.

On a more personal note, I would like to thank my mother, sisters, and brothers for believing in me and my capabilities to complete this dissertation. Their support and encouragement gives me enough strength and power to complete my work.

Last but not least, I would like to dedicate my thesis to my lovely husband, Dr. Muftah Ben zabeh, who has provided me a stable life socially and emotionally, and to my children, Salima, Faraj, Sundoos, and Omar who continually enlighten my life and are my source of power used to overcome any challenge.

Chapter 1. General Introduction

1.1. Proteomics and peptide mapping

Proteomics is the study of proteins, specifically the characterization of their function and structure. Proteins are macromolecule complexes (polypeptides), which are composed of linear amino acid sequences linked by peptide bonds and then folded and connected by mostly non-covalent interactions. Proteins play important roles in different biological processes and represent the final expression product of transcribed genes. Proteomic experiments generally focus on the identification and quantification of proteins [1-3]. Proteomics can lead to insights into biological systems to further understand disease progression, and to identify biomarkers associated to disease or the effectiveness of therapeutic treatment [3-5].

One method commonly used as tool in proteomic studies is peptide mapping, where protein digestion is followed by analytical separation of peptide fragments, i.e., polypeptides. The resulting peptide fragments are a fingerprint or map of the original protein [6, 7]. In other words, the peptide map obtained after the digestion will be unique and will allow the user to identify the parent protein. Bio-analysts often use peptide mapping to characterize proteins and to identify post-translational modifications or amino acid substitution (mutation). This thesis touches the topic of peptide mapping, which relates to the primary sequence of proteins. The following section describes the general structure of proteins, and then the details for determination of primary structure are described in Section 1.1.2. The two techniques used for peptide mapping in this thesis, immobilized enzymes for digestion and capillary electrophoresis (CE) for analytical separation of peptides, are presented in Sections 1.2 and 1.3.

1.1.1. Protein structure

This topic is a matter of interest because the structure of a protein is modified during denaturation and cleavage (also called digestion), and the structure of a protein determines its functions. There are four different types of protein molecular structure: primary, secondary, tertiary and quaternary [8].

- The *primary protein structure* is the linear sequence of amino acids that are connected by covalent bonds called "peptide bonds." It starts at the N-terminal of the amino acid group and ends at the C - terminal of the carboxyl acid (Fig. 1a).
- The s*econdary protein structure* is the shape of the peptide chain caused by intermolecular and intermolecular hydrogen bonding. Two main structures are observed, called α-helices and β-pleated sheets (Fig. *1*b).
- The *tertiary protein structure* refers to the three-dimensional conformation of the long polypeptide chains. There are two general classes of proteins based on tertiary structure: fibrous and globular (Fig. 1c).
- The *quaternary protein structure* is the way in which multiple polypeptide chains interact in a large protein [8-10]. The different levels of protein structure are illustrated in Fig. 1, and the cumulative effect is called folding (Fig. 1d).

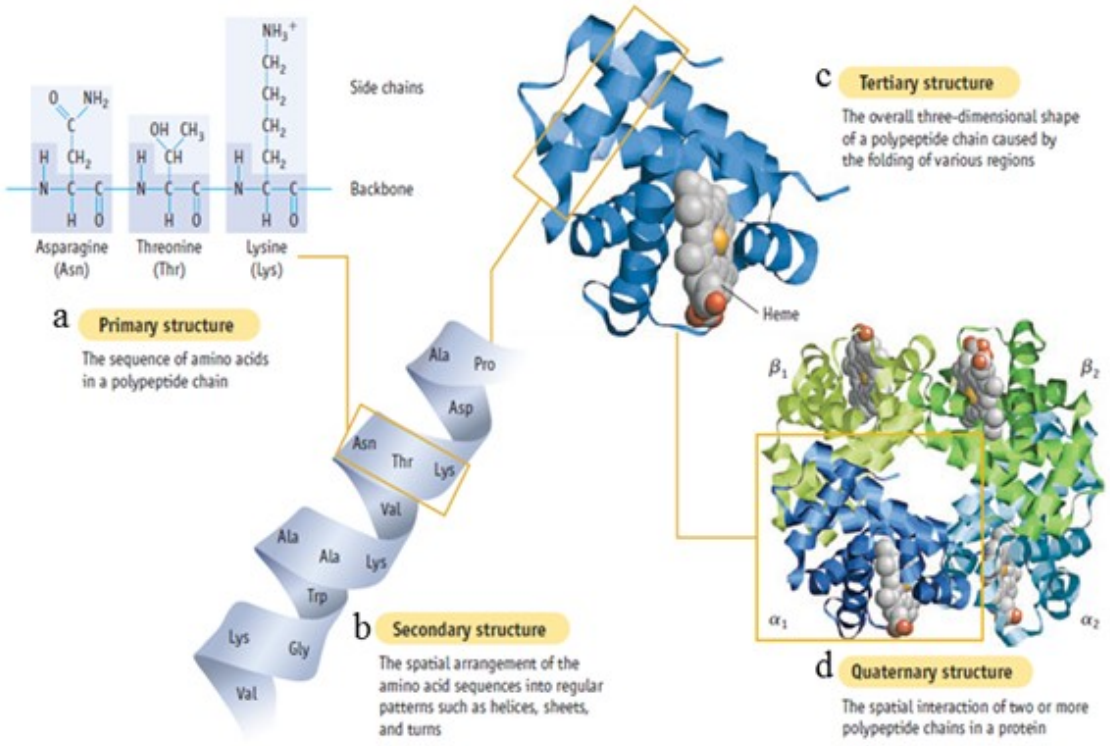

Figure 1. *Three-dimensional structure of hemoglobin [9].*

In general, the stability of the three dimensional structure of proteins depends on the types of bonds at each level of structure in the protein such as hydrogen bonds, electrostatic attractions, hydrophobic interactions (non polar) and disulfide bridges [8]. A small modification of the primary structure of the protein can lead to a significant change in the shape and function of the entire molecule. For example, Pauling explains sickle cell anemia as being the result of a modification of the primary structure of hemoglobin [8]. His studies showed that a glutamic acid group is replaced by a valine group, leading to the modification of the larger structure. In other words, the substitution of a single amino acid led to the modification of the three dimensional structure and then to the malfunction of the protein and thus disease.

The secondary, tertiary and quaternary structures are held together mainly by hydrogen bonds and electrostatic attractions [8]. These can be changed by modifying the environment of the protein. Hydrogen bonds are weak bonds, but in a long polypeptide chain there are numerous amino acids that participate in this type of interaction, resulting in the overall stability of the protein. The electrostatic attraction between the positive and negative charges on the backbone of the polypeptide chain is stronger than hydrogen bonds, when present. These charges can be found on amino acids with basic or acidic side chains like in histidine, lysine, arginine, glutamic acid, aspartic acid, cysteine, asparagine, glutamine and even tyrosine.

The tertiary structure of a protein can also include a third type of interaction, disulfide bonding, which is a covalent bond and thus stronger than electrostatic attraction. A disulfide bridge (disulfide bond) is the result of a covalent bond between the thiol groups of two cysteine residues [8]. Lastly, weaker hydrophobic interactions between amino acid side chains also contribute to the folding of proteins.

1.1.2. Determination of primary protein structure

To determine the structure of a protein and its function, it is important to know the primary sequence of amino acids as shown in Fig. 1a. In cells, very large sequences of DNA coding for specific genes are transcribed into mRNA in the ribosome. The nuclear pores in

cells facilitate the movement of mRNA in the ribosome to form the structure of the protein. The protein's function is based on its structure; any change in the sequence of protein, i.e., primary structure, can affect function [8]. To define the primary structure, two main techniques exist: Edman degradation [11-13] and peptide mapping by high performance liquid chromatography-tandem mass spectrometry (HPLC-MS/MS) or by matrix assisted laser desorption/ionization time-of-flight mass spectrometry (MALDI-TOF-MS) [14-17]. These two MS methods are now routinely used to characterize and identify proteins. Peptide separations can also be performed by sodium dodecylsulfate-polyacrylamide gel electrophoresis (SDS-PAGE), HPLC, ion exchange chromatography (IEC), or capillary electrophoresis (CE), where these last three are coupled with various detection methods like UV-Vis absorbance or fluorescence spectroscopy or mass spectrometry (MS). Without MS detection, these separation methods can be used to compare two peptide maps, but cannot define primary amino acid sequence. In this work, peptide mapping refers to the CE separation of proteolytic peptides. In CE with UV detection, although the identity of the individual peaks may not be known and would require sequencing for proper identification, comparisons between peptide maps can be informative.

Peptide mapping is often used to characterize proteins by identification of post-translational modifications or anomalies within the polypeptide chain. Any change in migration time of a single peptide peak or band on the electropherogram confirms that one or more amino acids have been altered in the peptide [18, 19]. In some cases, such modifications can lead to diseases.

The focus of our group's research has been to develop analytical techniques to improve peptide mapping. Peptide mapping involves three steps:

1) Protein denaturation, reduction and alkylation (if needed);
2) Protein cleavage by an enzyme, or chemical reagent;
3) Separation of the peptides.

These concepts are shown in Fig. 2. The first step, protein denaturation with reduction and alkylation, is a process in which a protein's overall 3-dimensional structure is disassembled to make linear polypeptide chains. This usually involves chemical or heat treatment, discussed further below. In general, large proteins require chemical denaturation to break

hydrogen and electrostatic bonds using, for example, urea or SDS. Then they require reduction of the resulting -SH groups from the disulfide bonds and alkylation because such proteins are highly folded and the enzyme will not otherwise be able to cut (digest) them. Some proteins do not require this step or may only require heat-induced denaturation if there is not much folding present [8], although this processes is often reversible upon cooling the protein solution.

The second step involves using proteases (enzymes) to cleave proteins into smaller polypeptides [20, 21]. Common enzymes used for proteolytic cleavage include trypsin, chymotrypsin and pepsin [22, 23]. Trypsin cleaves proteins at the carboxyl terminal side of the amino acids lysine (K) and arginine (R) [7]. Chymotrypsin cleaves peptide bonds at the carboxyl terminal side of tryptophan (W), tyrosine (Y) and phenylalanine (F); in other words, at an amino acid containing an aromatic ring in its side chain [22-25]. Some cleavage on the C-terminal side of leucine (L) and methionine (M) is also possible with chymotrypsin. Finally, pepsin cleaves peptide bonds between hydrophobic and also at aromatic amino acids.

In this study, chymotrypsin (CT) was used as an alternative to trypsin, currently the most commonly used enzyme for proteomic studies. Trypsin is favored because it cannot cut at as many positions on the protein, which leads to more selective cleavage and thus peptides terminating only in lysine and arginine residues [6, 26, 27]. A greater amount of peptides will be observed when using CT because of its ability to cut at more amino acid positions on a protein than trypsin [23]. Pepsin is a less common enzyme than trypsin, for similar reasons. Chemical cleavage involves using reagents like cyanogen bromide to cut proteins into polypeptides; however, only enzymatic methods were investigated in this study.

For the third step, separation, possible methods include HPLC, MS, HPLC-MS, IEC and CE [2, 26]. In this study, the technique of CE coupled with UV absorbance detection was employed [23, 27-29]. CE has many advantages compared to other separation techniques, such as speed, the small amount of sample injected, its low solvent consumption, and a high separation efficiency [23, 27, 28, 30].

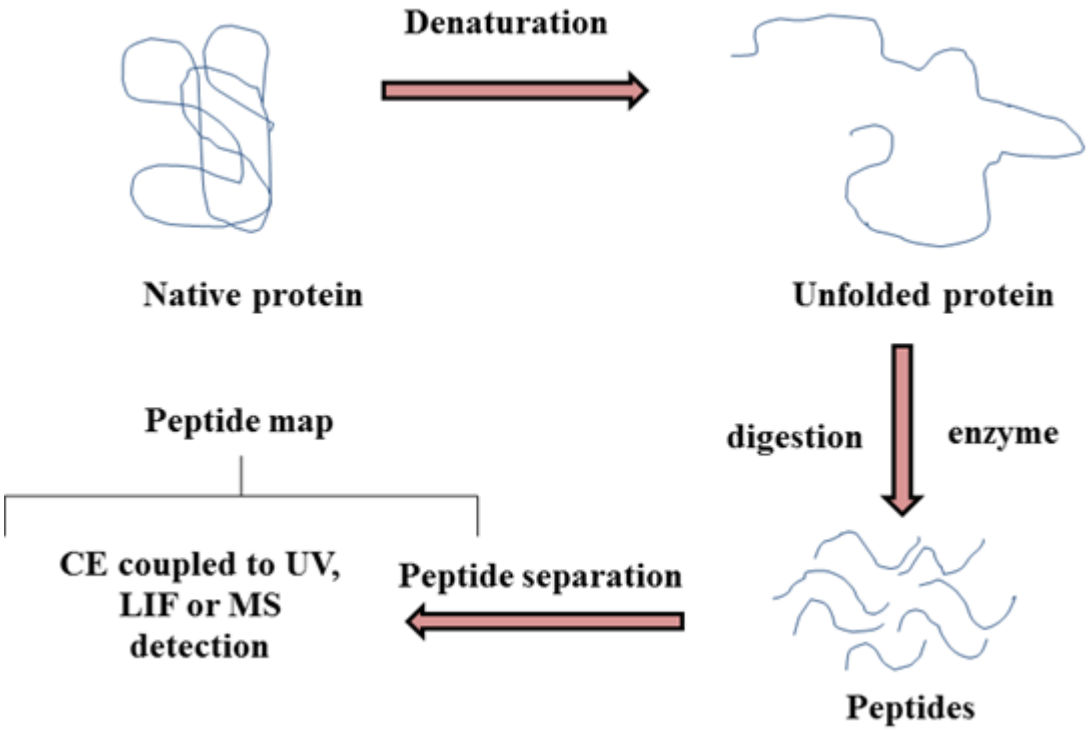

Figure 2. *Schematic showing the procedure for peptide mapping of a protein used in this study or others from the Waldron research group.*

Bovine serum albumin (BSA) and myoglobin were used as model substrates in this study. Fig. 3 shows the structure of BSA from Bovine Serum Albumin, and Fig. 4 shows the structure of Sperm Whale myoglobin. However, as mentioned above, the specific conformation of a native protein depends on the physical and chemical conditions of the protein environment. A distortion of the three dimensional structure of a protein is called denaturation, and this will be explained further below.

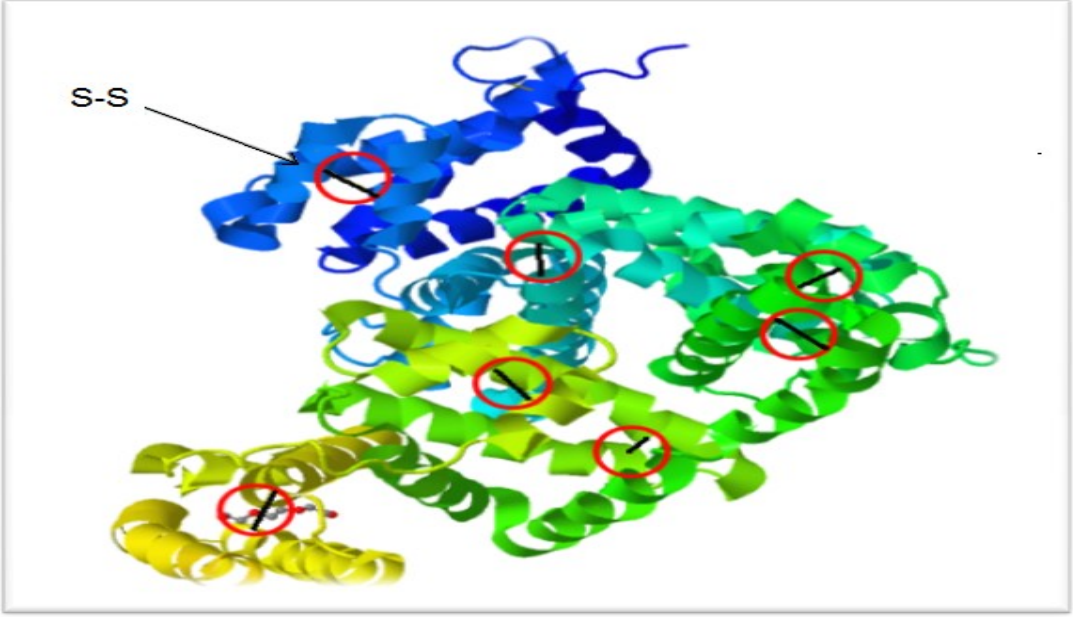

Figure 3. *Structure of BSA (Bovine Serum Albumin). A few of the 17 disulfide bridges (-S-S- bonds) are circled in red [31].*

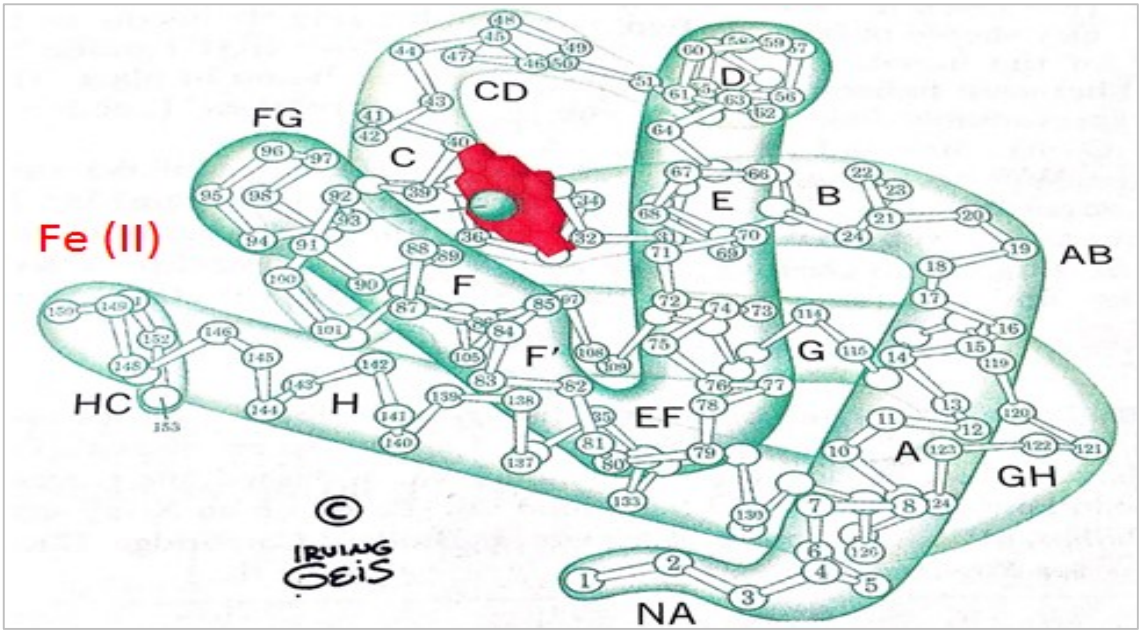

Figure 4. *Structure of Sperm Whale myoglobin [8], which has no disulfide bridges.*

Protein denaturation involves the alteration of the native secondary, tertiary, and/or quaternary structures, and is usually caused by changes in the protein's environment [8]. These changes include variations in pH, temperature and pressure or the addition of chemical

denaturants such as urea, guanidine hydrochloride and SDS [8, 32, 33]. Most commonly, protein denaturation is followed by reduction and alkylation [2, 22, 33, 34].

Heat-induced denaturation is the change of conformation of the secondary and tertiary protein structure. Heating can cause the breakdown of hydrogen bonds and non-polar hydrophobic interactions: this causes the folded protein to partially unfold. A protein's conformation does not generally change until the temperature passes a certain threshold [8]. The process is, however, reversible upon cooling for most proteins. In the present study, the effect of heat-induced denaturation on peptide mapping by soluble and immobilized CT was explored; the results are presented in Chapter 3.

Denaturation can also be achieved by changes in the pH, which can lead to ionization of amino acid side chains (Lysine, Arginine, Histidine, Aspartic acid, Glutamic acid, Tyrosine and Cysteine), a breakdown of H-bonding and a change in the molecular charge distribution [8]. Chemically-induced denaturation is caused by adding a chemical reagent to the protein in solution. Adding surfactants like SDS to a protein can affect interactions within the protein resulting in its unfolding [35].Urea is also widely used as a chemical agent in protein denaturation by breaking hydrogen bonds between polypeptide chains of a protein [8, 23, 32, 36].

After denaturation, the disulfide bridges within a protein can then be reductively cleaved by the addition of dithiothreitol. Iodoacetamide is usually added after this to prevent reformation of disulfide bridges between cysteine groups by alkylating the thiol side chains [36, 37]. This aspect of protein treatment by reduction and alkylation was not studied in this project, as described further in Section 1.4.

The proteolytic digestion of proteins at 37ºC for a given period of time can be carried out by adding a soluble enzyme to the protein after heat-induced denaturation, reduction and alkylation [38]. Trypsin is the most commonly-used proteolytic enzyme for protein digestion in solution [23, 39]. The enzyme is typically added to a denatured and reduced/alkylated protein in solution a low enzyme to substrate ratio (1:25) so that autoproteolysis products from the enzyme are in low abundance compared to peptides from the substrate.

However, the digestion of proteins in solution has some disadvantages. For example, the enzyme samples can only be used once (owing to the inability to separate the enzyme

from the digestion mixture), there is a slow rate of digestion because of the low enzyme concentration, and there is a decrease in enzyme activity due to autoproteolysis [23]. It also has some advantages on the other hand, such as the rapid preparation of the soluble enzymes, and the ability to carry out digestion directly on gels when using proteins that have been purified using gel electrophoresis [40, 41].

1.2. Immobilized or solid phase enzymes

Recently, immobilized enzymes have become a topic of considerable interest in the literature. The number of methods to immobilize enzymes is increasing steadily [7, 42-44]. In our group, immobilized enzymes are studied because we can easily separate them from the digestion mixture, resulting in a purer peptide map. The other advantage of immobilized proteolytic enzymes is their increased stability and their reusability.

Current methods for enzyme immobilization can be divided into two general classes: chemical methods and physical methods [45]. Chemical methods add covalent bonds, which are formed between the enzyme and the support, such as a silica or polymeric particle [46]. Physical methods can include adsorption to mesoporous silicates [47] adsorption to modified silica gel [48], and sol-gel entrapment [9, 49] without creating covalent bounds. There are different methods used to immobilize enzymes on a carrier (solid particle), such as Cross-linking Enzyme Crystals (CLECs) or by Cross-linking Enzyme Aggregates (CLEA) [45]. Porter *et al.* [50] studied immobilized enzymes such as pepsin, trypsin and α-chymotrypsin bound to controlled pore glass (CPG) beads and determined enzyme activity by monitoring the digestion of plant and animal proteins. Also, immobilized enzyme platforms can be produced by using microencapsulation methods such as that used to make paper-based biosensors [51].

Previous studies by Migneault *et al.* [43] were done to determine the efficiency when comparing two procedures for immobilizing trypsin via linkage of the enzyme to CPG beads or by the cross-linking reaction (i.e., without solid support) with glutaraldehyde (GA). Human hemoglobin was used as a substrate for peptide mapping by CE as the separation technique. Bonneil *et al.* [6] studied the activity of an immobilized trypsin microreactor made using commercial CPG-trypsin beads. The substrates used by Bonneil *et al.* were β-casein

and insulin chain B and CE-UV was used as a separation technique for peptide mapping. Nguyen [22] used a similar method to immobilize chymotrypsin via GA cross-linking with CE-UV as the separation technique for the analysis of peptides from human hemoglobin. Ghafourifar *et al*. [23] used an immobilized enzyme reactor based on GA-cross-linking of chymotrypsin (CT) into a fused silica (f.s) capillary for the analysis of myoglobin by CE-UV and CE-MS. Ghafourifar *et al.* [23] also used GA-CT particles for peptide mapping of fluorescently labelled β-casein by CE-laser induced fluorescence (LIF). The advantage of using CE-LIF as an alternative method to CE-UV is because it is a very sensitive detection method [52, 53]. However, the kinetics of fluorescent labelling of peptides in a digest is concentration limited. This means that if the substrate concentration is too low, the peptides will be too diluted for labelling. Therefore, this limits the studying of immobilized enzyme efficiency at very low substrate concentrations (i.e., if they are < 1 μM) by both CE-LIF and CE-UV peptide mapping. It is possible instead to use diluted fluorescent substrates to study immobilized enzymes by mapping their fluorescent peptides by CE-LIF, which has nanomolar or better detection ability. Unfortunately, this leads to another drawback for the most common proteolytic enzyme, trypsin: many fluorophores are attached to proteins at their lysine amino groups and thus the lysines are no longer recognized as a tryptic cleavage site. This is the reason our group is studying immobilized chymotrypsin, which can digest fluorescent proteins labelled at lysine groups and at concentrations that would be too low to detect by CE-UV.

In the present study, chemical immobilization was achieved using GA as a cross-linking agent for chymotrypsin. This choice was made because GA reacts rapidly with primary amines, and thus with lysine residues as well as the N-terminus of proteins [54]. Various methods of enzyme immobilization have been described in the literature [7, 44 , 55, 56]. To restrict the mobility of enzymes, GA is the most common reagent used for cross-linking proteins [54]. The same procedure that was previously used in our lab for trypsin immobilization by GA cross-linking [43] has also been used for chymotrypsin immobilization [22, 23]. Fig. 5 shows the structure of GA.

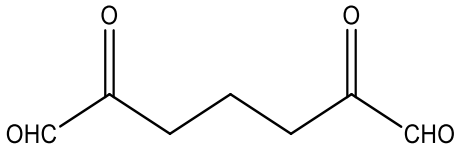

Figure 5. *Structure of glutaraldehyde (GA) (1,5-pentanedial).*

Glutaraldehyde immobilization has one major advantage, which is its rapid bonding with the primary amine groups present in proteins. Fig. 6 details how the reaction occurs between the protein (Enz-N) and the cross-linker, GA. Cross-linking can cause significant changes in enzyme activity, which may be disadvantageous in some circumstances [22].

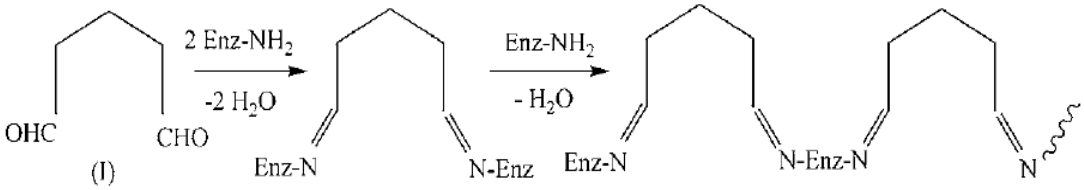

Figure 6. *Cross-linking of proteins with glutaraldehyde gives a quaternary pyridinium compound [7], which is in-soluble at pH > 5.*

1.3. Capillary electrophoresis (CE)

1.3.1. Instrumentation for capillary electrophoretic analysis

To follow the digestion of a protein by an enzyme, many different separation methods can be used. In this work, CE was used as a separation method, but HPLC is most commonly employed [57-59]. CE has some significant advantages such as improved speed and resolution [10, 27, 28]. Multiple separation mechanisms can be used (described below), and CE only requires nanolitre-sized sample injection [60].

There are several different modes of CE: capillary zone electrophoresis (CZE), capillary isoelectric focusing (CIEF), capillary isotachophoresis, micellar electrokinetic capillary chromatography (MECC), and capillary gel electrophoresis (CGE). CZE is the simplest and most commonly used mode of CE because of its efficiency and high resolution [61, 62]. Fig. 7 shows a diagram of a general CE instrumental setup.

CZE was used in this study, and the separation buffer was composed of sodium phosphate salt at a pH of 2.5. This buffer is commonly used in CE separation of peptides because of its resolution power [63]. In this project, the highest selectivity is found at pH 2.5 for the separation, because almost all peptides are cations at this pH and small differences in the carboxylate pK_a of aspartic acid (D), glutamic acid (E) and the C-terminus will allow peptide isomers to be separated [64]. CZE is most often used without an internal capillary coating, as in this project. A special coating can be applied to the capillary walls before carrying out CZE to stop proteins or highly cationic peptides from adsorbing onto the inner surface [65]. However, the separations in this study only involved peptides from BSA and myoglobin, which are less likely to adsorb, so a capillary coating was not used.

Finally, a DAD (diode array detector) was used as a detector. This type of multi-wavelength detector can be very useful when observing molecules with different absorption maxima, but this advantage was not exploited in this study because a single wavelength of 200 nm was used. Absorption at this wavelength is typical for peptide bonds.

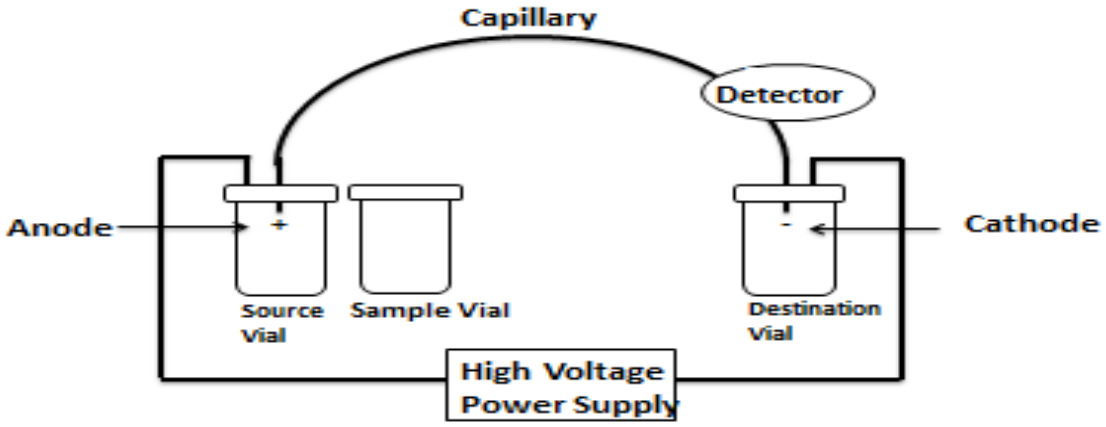

Figure 7. *A schematic diagram of a capillary electrophoresis instrument.*

1.3.2. Analyte migration in CZE

The movement of charged analytes through the capillary is governed by two phenomena: electrophoresis and electroosmosis. Briefly, electrophoresis is the movement of a charged molecule in solution when a voltage is applied, while electroosmosis is the

movement of the bulk solution allowing neutral molecules to be detected at the cathodic end of the capillary [66].

The movement of analytes in the capillary is affected by electroosmotic flow (EOF). In fused silica capillaries, the surface is composed of silanol groups (-SiOH). A negative charge forms on the inner surface when the pH is higher than 2.7. A layer of cations from the buffer solution will begin to build up at the surface in order to keep the bulk solution neutral. When a voltage is applied, the dissolved cations begin to migrate toward the cathode, and drag with them the entire bulk solvent. In other words, all the dissolved molecules will move towards the cathode, causing the EOF.

The sum of these two movements (electrophoresis and electroosmosis) under an electric field, is illustrated in the next figure (Fig. 8), where v_{eo} is defined as the electroosmotic velocity, v_{ep} the electrophoretic velocity, and v_{ep} the apparent velocity.

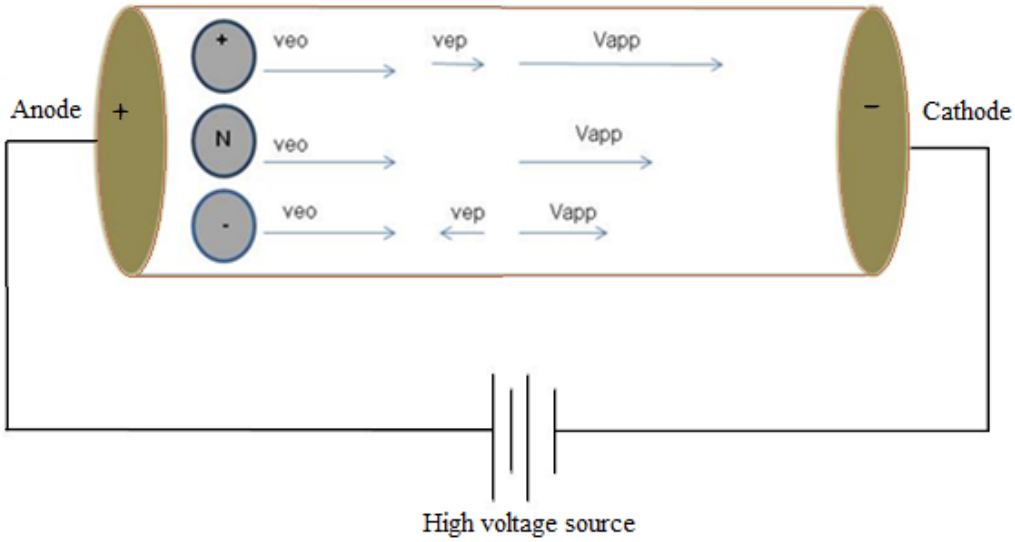

***Figure 8**. A representation of analyte migration as a function of charge (cations, neutals and anions) during CE. The terms v_{eo}, v_{ep} and v_{app} represent the electroosmotic, electrophoretic and apparent velocities, respectively.*

The flowing equation describes the velocity of electrophoretic mobility, v_{ep}, which depends on analyte charge (q) and hydrodynamic radius (r):

$$v_{ep} = \frac{q}{6\pi\eta r} E \qquad (1)$$

where v_{ep} is electrophoretic velocity (cm/s), E is the applied electric filed (V/cm) and η is the viscosity of the buffer. The equation of electroosmotic velocity (v_{eo}), or EOF' is not shown here but can be explained as the flow of buffer in a f.s. capillary tube when an electric field is applied as shown in Fig. 8. The apparent velocity, v_{app}, is the sum of the the electrophoretic and electroosmotic velocities.

The separation of cations and anions is based on differences in their apparent mobilities, which is illustrated in Fig. 8 by the **"+"** and **"-"** molecules. For cations, which move in the same direction as the electroosmotic flow, the electrophoretic mobility (μ_{ep}) and the electroosmotic mobility (μ_{eo}) have the same sign (both are positive). On the other hand, the electrophoretic mobility of anions is in the opposite direction of electroosmosis, so for anions, μ_{ep} is substracted from μ_{eo}. At pH around 2.7 and higher, electroosmotic velocity is higher than electrophoretic velocity causing anions to migrate towards the cathode, which is where the detector is located [66]. The electropherogram in Fig. 9 shows the order of CZE separations (i.e., cations > neutrals > anions) at pH > 3.

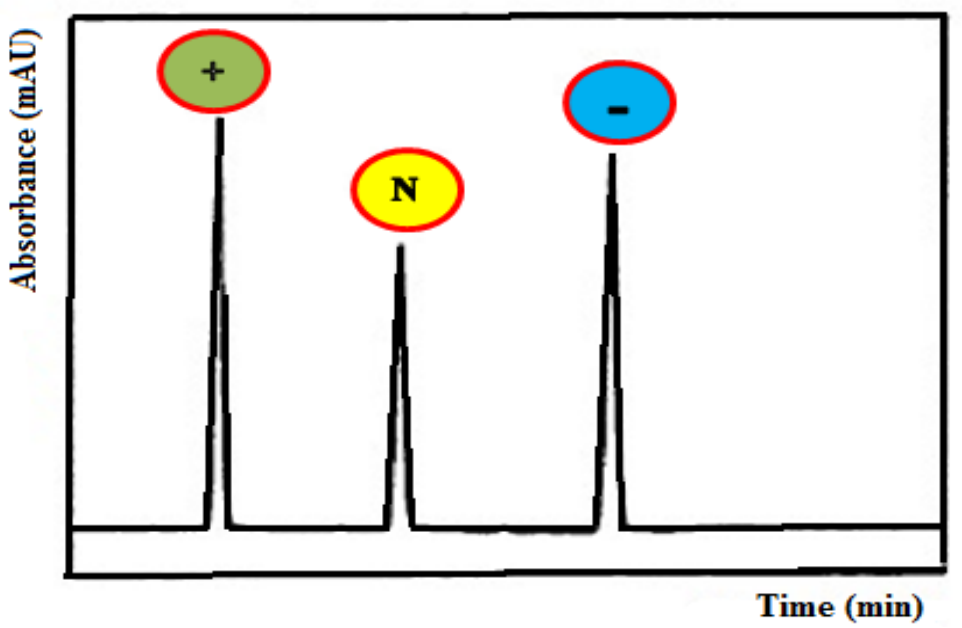

Figure 9. *Schematic representation of an electropherogram showing the order of elution of CE separation at pH > 2.7 [64].*

At low pH, electroosmosis is weak (EOF = 0) and anions cannot reach the detector, only electrophoretic mobility is responsible which depends on charge (q) and radius (r), which is related to the mass of the ion. The separation pH used in this project was 2.5, so only cations are detected, where small and mulit-charged cations elute faster, followed by large cations, as shown in Fig. 10. Throughout the remainder of this thesis, the term CE is used rather than CZE.

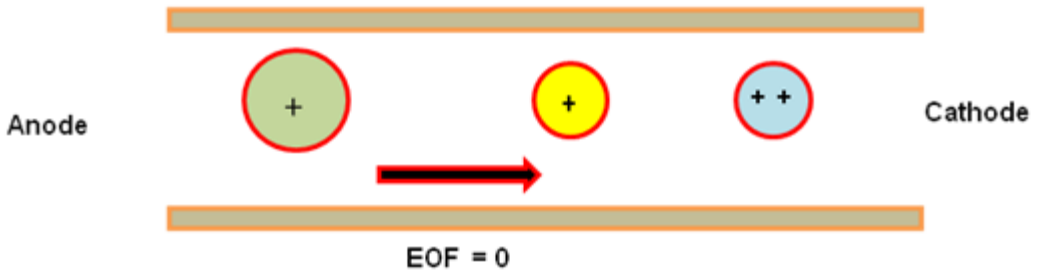

Figure 10. *Schematic representation of the migration of cations in a capillary at pH 2.5.*

1.4. Goals of studies

The hypothesis is that immobilized chymotrypsin (CT) can effectively digest protein substrates relative to free CT, and also reduce or prevent autoproteolysis. Previous studies from our group by Migneault *et al*. [43] showed that it was possible to do peptide mapping using GA-cross-linked trypsin. Nguyen used a similar method to immobilize chymotrypsin via GA cross-linking (i.e., GA-CT) with CE-UV as the separation technique used for her analysis of human hemoglobin [22] and Ghafourifar *et al*. [23] demonstrated peptide mapping of BSA and myoglobin with GA-CT. However, some basic experiments had not yet been done as outlined in more detail in the next paragraphs.

In the previous work done by Nguyen [22], the autoproteolysis of soluble CT without substrate was followed. The soluble CT was incubated at 37ºC for 240 min and then analyzed by CE-UV. Her result showed only a few autoproteolysis peaks. However, when Ghafourifar [23] studied autoproteolysis using a blank substrate (water as sample) "denatured" with urea, then reduced, alkylated, and incubated for 24 h at 37ºC with soluble CT, the results showed many autoproteolysis peaks for the soluble CT. the same experimental procedure but using GA-CT showed essentially no autoproteolysis peaks. These studies by Nguyen and Ghafourifar in our group showed the importance of how the substrate is prepared before digestion and that the residual reagents for denaturation/reduction/alkylation increase autoproteolysis of the free enzyme. Therefore, it was deemed interesting to see the effects of using only denaturation by heating of substrates for free (i.e., soluble) versus immobilized CT, which is explored in the current work.

The main goals of this project were to compare the performance of GA-immobilized CT to that of free CT by looking at: a) the extent of autoproteolysis for various digestion times (30 and 240 min) and temperatures (4, 24, and 37ºC), and b) whether mild substrate denaturation conditions (i.e., heating at 60, 75 and 90ºC) made a difference in enzyme digestion efficiency. For the second goal, two model proteins were used: BSA and myoglobin. Additional studies were carried out to support the main goals: i) choosing the best buffer (ammonium bicarbonate and Tris-HCl) for digestion and peptide mapping by CE-UV, ii) choosing a method for terminating the digestion that was compatible with CE-UV, and iii) finding the best capillary conditioning protocol for repeatable peptide maps.

Chapter 2. Materials and Methods

2.1. Reagents and consumables

α-Chymotrypsin from bovine pancreas type II, bovine serum albumin (BSA), and horse myoglobin-α and glutaraldehyde (25% grade ll, aqueous solution of GA), Tris(hydroxy methyl) amino methane hydrochloride, Tris base, monobasic sodium phosphate, dibasic sodium phosphate were from Sigma Aldrich (St-Louis, MO, USA). Methanol and acetone were from Fisher Scientific. Sodium chloride was from BIO BASIC INC (Torbay Road, Markham Ontario. Canada). Ammonium bicarbonate, glycine and phosphoric acid were from Sigma Aldrich (Oakville, ON, Canada). Sodium dodecyl sulphate (SDS) and sodium hydroxide were from Fisher Scientific. Hydrochloric acid was from EMD Millipore (Gibbstown, NJ, USA). Fused silica capillary tubing for CE separation (75 μm inner diameter ID, 360 μm O.D. outer diameter) was from Polymicro Technologies (Phoenix, AZ, USA). A multi cartridge Milli-Q filtration/deionization system (Millipore, Bedford, MA, USA) was employed for water purification that was used for all solutions and buffers preparation. 250 μL PP (polypropylene) insert bottom spring, with diameter 6x29 mm product from Canadian Life Science was used for CE separation in all experiments.

2.2. Sample preparation

2.2.1. Soluble chymotrypsin autoproteolysis

Chymotrypsin in Milli-Q water was added to either ammonium bicarbonate (25 mM, pH 8) or Tris-HCl (25 mM, pH 8) for autoproteolysis experiments on chymotrypsin. The final concentration of chymotrypsin for both experiments was (0.12 mM) and digestion was performed at 37ºC for 240 min. We evaluated 6 different conditions: time (30 and 240 min), and temperature (4, 24, and 37ºC) and digestion was stopped using two different methods, as described in Section 2.2.3.

2.2.2. Synthesis of immobilized chymotrypsin particles

Chymotrypsin immobilization by GA-cross-linking was carried out based on a procedure described previously for trypsin and chymotrypsin [22, 23]. Briefly, in a 1.5 mL micro centrifuge vial, 80 µL of aqueous chymotrypsin solution (1.3 mM) was added to 594 µL of 50 mM phosphate buffer, pH 6.4 and 156 µL of GA, diluted to 2.5% v/v in water and added drop wise to the enzyme solution. The mixture was reacted at room temperature for 120 min and the solid or immobilized GA-CT formed, was centrifuged for 2 min at 3000 rpm and the supernatant was decanted off. The immobilized enzyme cross-linked-GA particles were washed 3 times with 400 µL phosphate buffer (50 mM, pH 6.4), then 3 times with 400 µL of sodium chloride (500 mM), and again with 400 µL of buffer. All washing steps were to remove unreacted enzyme and excess GA. Next, 400 µL glycine (200 mM) was added to react with any remaining aldehyde groups of GA and the solution was allowed to stand at room temperature for 180 min. The final product, which gave a yellow colour with irregular shape (Fig. 11) was washed 3 times with 400 µL phosphate buffer and then 3 times with 400 µL Milli-Q water. The GA-cross-linked chymotrypsin was stored in 400 µL Milli-Q water at -20^0C in 400 µL until used.

To determine the amount of enzyme (CT) that reacted with glutaraldehyde after the cross-linking reaction (GA-CT), Ghafourifar *et al.* [23] reported two methods: Forth Derivative Spectroscopy and Analysis of a Mixture, which are commonly used quantitative methods in analytical chemistry [10]. Ghafourifar *et al.* [23] indicated that the amount of CT that reacted with GA was 94±2% by these two quantification methods. Since the GA-CT immobilization procedure used in this study was the same that used by Ghafourifar, it was assumed that we also have a 94±2% mass immobilization efficiency. It is important to point out that the activity of an enzyme usually decreases when immobilized, compared with the free (soluble) enzyme.

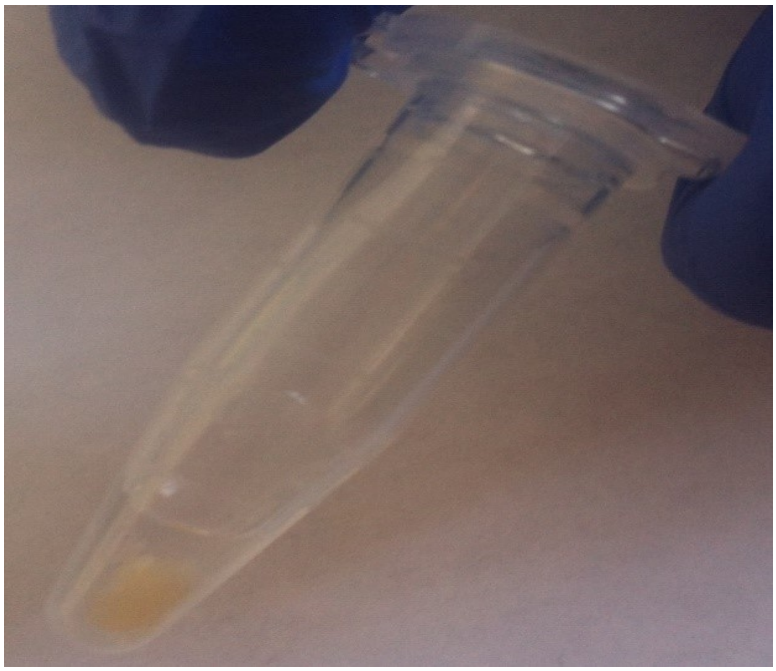

Figure 11. *Photograph of immobilized chymotrypsin (GA-CT) particle in centrifuge tube after storage in 400 μL water.*

2.2.2.1. Immobilized chymotrypsin autoproteolysis

A solution of 400 μL of GA-CT (having 0.24 mM apparent concentration based on the initial moles of CT reacted with GA and 94% immobilization efficiency) was used for digestion in two different buffers (ammonium bicarbonate or Tris-HCl). The solutions were incubated at different temperature (4, 24, and 37ºC) for different times (30 and 240 min). Digestion products were gently shaken by hand, then 200 μL of digestion solution were collected for CE separation after stopping digestion by two methods as describe below.

2.2.3. Termination of chymotrypsin digestion

For in-solution and immobilized CT (in Sections 2.2.1 and 2.2.2), the enzymatic reactions were stopped by adding 1 μL of 12 M HCl to the digestion solution or by using a dry ice / acetone bath at very low temperature (-78ºC) prior to peptide analysis by CE.

2.2.4. Heat-induced denaturation of protein substrates

A solution of 0.013 mM substrate (BSA or myoglobin) was dissolved in ammonium bicarbonate (25 mM, pH 8), heated at 60, 75, and 90ºC for 45 min, then cooled at room temperature for 15 min. Digestion was carried out immediately before the reversible re-folding process could be complete. For all studies, BSA and myoglobin were denatured only by heating without adding any chemicals (i.e., urea). No reduction/alkylation reactions were carried out either.

2.2.5. In-solution digestion of substrates by free chymotrypsin

Heat-induced denaturated protein substrates (Section 2.2.4) were added to 400 µL free chymotrypsin (0.0013 mM final concentration) to reach an enzyme-to-substrate ratio of 1:10 and a final concentration of substrate of 0.013 mM. Digestion was carried out in 1.5 mL microcentrifuge tube at 37ºC for 240 min.

2.2.6. Digestion of substrates by immobilized chymotrypsin particles

BSA and myoglobin were heat denatured (Section 2.2.4). And digestions were carried out in 1.5 mL micro centrifuge tube by adding protein substrate immobilize chymotrypsin as described in Section 2.2.2 to reach enzyme to substrate ratio of 18:1 (mol:mol). The digestion solutions of 0.013 mM BSA or myoglobin and an effective concentration of 0.24 mM immobilized enzyme (in 400 µL) were incubated at 37ºC for 240 min. The digestion solution was decanted off by gentle shaking and 200 µL digestion solution was placed in a dry ice/acetone bath to stop reaction, before CE separation.

2.3. CE separation conditions

Separations were carried out on an HP^{3D}CE System (Agilent Technologies, Santa Clara, CA, USA) equipped with an ultraviolet-visible (UV/Vis) Diode Array Detector (DAD). All separations were performed in f.s. capillary of 75 µm inner diameter (ID) and 360 µm outer diameter (OD). The total capillary length was 46 cm with effective length to

the detection window of 36 cm from the inlet. Background electrolyte (BGE) separation buffers (25 and 75 mM) were made in purified water and the pH was adjusted to 2.5 by using sodium phosphate and phosphoric acid, with concentration of 25 or 75 mM as indicated in Table 1. All BGEs and rinsing solutions were passed through 0.22 μL Nylon syringe filters from (Thermo Scientific, Waltham, MA) to fill the reservoirs in HP^{3D}CE instrument. The current, +15 kV electric potential, was switched on for 30 min with the anode plunged into BGE buffer at the inlet vial and the cathode into the outlet BGE buffer vial. A SDS solution was dissolved in Milli-Q water and passed through 0.22 μL filter before use. For all separations detections were performed at $\lambda = 200$ nm.

In this project, a new capillary was conditioned by rinsing sequentially 1M NaOH for 10 min (flush = 950 mbar), pure water for 10 min (flush), and phosphate buffer for 10 min (flush). Between each new sample, the capillary was rinsed (flushed) with 0.1 M NaOH for 3 min, pure water for 3 min and phosphate buffer for 3 min.

The method for capillary conditioning was modified a few times during the study. For convenience, the different methods used are shown in Table 1. All autoproteolysis and digest samples were run (injected) at least three times. According to the injection conditions in Table 1, the volume of sample injected into the capillary (29 nL, determined by using the Poiseuille equation) was accomplished by applying pressure of 34.5 mbar for 5 s. Electropherograms (i.e., the peptide maps) were compared either visually or by measuring peak heights and migration times as a way to evaluate the efficiency of digestion (or autoproteolysis).

Table 1. Initial capillary conditioning parameters without SDS rinsing (Method A), those with SDS in pre-conditioning (Method B), and with SDS in post-conditioning (Method C), to optimize the reproducibility of peptide separations.

	Action [a]	**Solution**[b] **and duration for each method**		
		Method A	Method B	Method C
Pre-conditioning				
1	Flush		**SDS, 3 min**	NaOH, 3 min
2	Flush			H_2O, 2 min
3	Flush	HCl, 2 min	HCl, 3 min	HCl, 2 min
4	Flush			H_2O, 2 min
5	Flush	Buffer, [c] 3 min		
CE injection				
4	Inject	Sample, 5 s		
5	Inject	Buffer, 2 s		
Post-conditioning				
	Flush			**SDS, 3 min**
5	Flush	NaOH, 1 min	NaOH, 2 min	NaOH, 2 min
6			Wait, 0.2 min	Wait, 0.2 min
7	Flush	H_2O, 1 min	H_2O, 2 min	H_2O, 2 min
8	Flush	HCl, 2 min		

[a] Flush carried out at 950 mbar; injection carried out at 34.5 mbar;

[b] HCl at 0.1 M; NaOH at 0.1 M; sodium phosphate buffer at 25 mM, pH 2.5; water was always Millipore polished; SDS at 25 mM in water.

[c] Phosphate buffer at 75 mM for digestion of BSA and myoglobin studies.

Chapter 3. Results and Discussion

During the initial experiments of chymotrypsin (CT) autoproteolysis, we suspected that the digestion buffer composition and the method for stopping the digestion might affect the quality of the peptide maps. It was also evident that residual enzyme in digest solutions was affecting the CE separations so capillary rinsing with an SDS solution, which denatures proteins, was added in order to improve reproducibility of the peptide maps. These three experimental parameters, explored for soluble CT only, are described in the first three sections of Chapter 3.

To evaluate the extent of proteolysis of immobilized versus soluble CT, several different digestion temperatures and times were studied, as described below in Section 3.4. The hypothesis that heat-denatured substrates can be digested by immobilized CT to the same extent as soluble CT is evaluated in Section 3.5 for the protein substrates BSA and myoglobin.

3.1. Choice of digestion buffer: ammonium bicarbonate versus Tris-HCl

The choice of digestion buffer is important because its composition and pH affect the activity of the enzyme [38, 67]. As mentioned before, the structure of a protein substrate can be modified by its environment, which could impair or improve the effectiveness of the enzyme [22, 43]. In addition, since digested samples are injected directly into the CE without any solid phase extraction "clean-up" or enrichment, the presence of digestion buffer in the sample matrix can greatly affect the peak shapes and selectivity in CE because a high matrix ionic strength causes reverse stacking leading to peak broadening. The optimal buffer should provide the best digestion (including CT autodigestion) and should also not affect the separation of individual peaks in an electropherogram. Typically, digestion buffers are volatile and often used in biochemistry studies where buffer exchange is required. In the current study, enzyme digestion in two different buffer solutions (ammonium bicarbonate and Tris-HCl) was investigated to determine their effects on autoproteolysis and on the quality of the peptide maps by CE. Our group had previously used these buffers when investigating trypsin and CT digestion [7, 23, 43]. Ammonium bicarbonate is a buffer used in the pH 8-10 range, and Tris-HCl in the pH 7.3–9.3 range [47, 68].

Aqueous ammonium bicarbonate solution was added to soluble CT to give final concentrations of 25 mM for the buffer and 0.12 mM for CT. The solution was incubated at 37ºC for 240 min, and then analyzed by CE. The same procedure was followed for Tris-HCl. Both digestion buffer solutions were 25 mM and prepared at a pH of 8. The CE Method A (Table 1) was used for peptide mapping in a pH 2.5 phosphate buffer, as described in Section 2.3.1. Figs. 12A and B show the CE-based peptide maps resulting from the autoproteolysis of soluble CT carried out in ammonium bicarbonate and in Tris-HCl, respectively. By visual inspection, autodigestion performed in Tris-HCl buffer (Fig. 12B) resulted in much weaker signals (approx. 30 mAU on average), compared to autodigestion done in the ammonium bicarbonate buffer (approx. 75 mAU on average). The experiments shown in Fig. 12 were repeated 3 times and reproducible electropherograms were obtained for both buffers, giving confidence to the noticeable difference between the two digestion buffers. The 25 mM ammonium bicarbonate buffer at pH 8 (Fig. 12A). consistently provided the highest number of peaks with the best resolution and was thus used in all subsequent CE analyses.

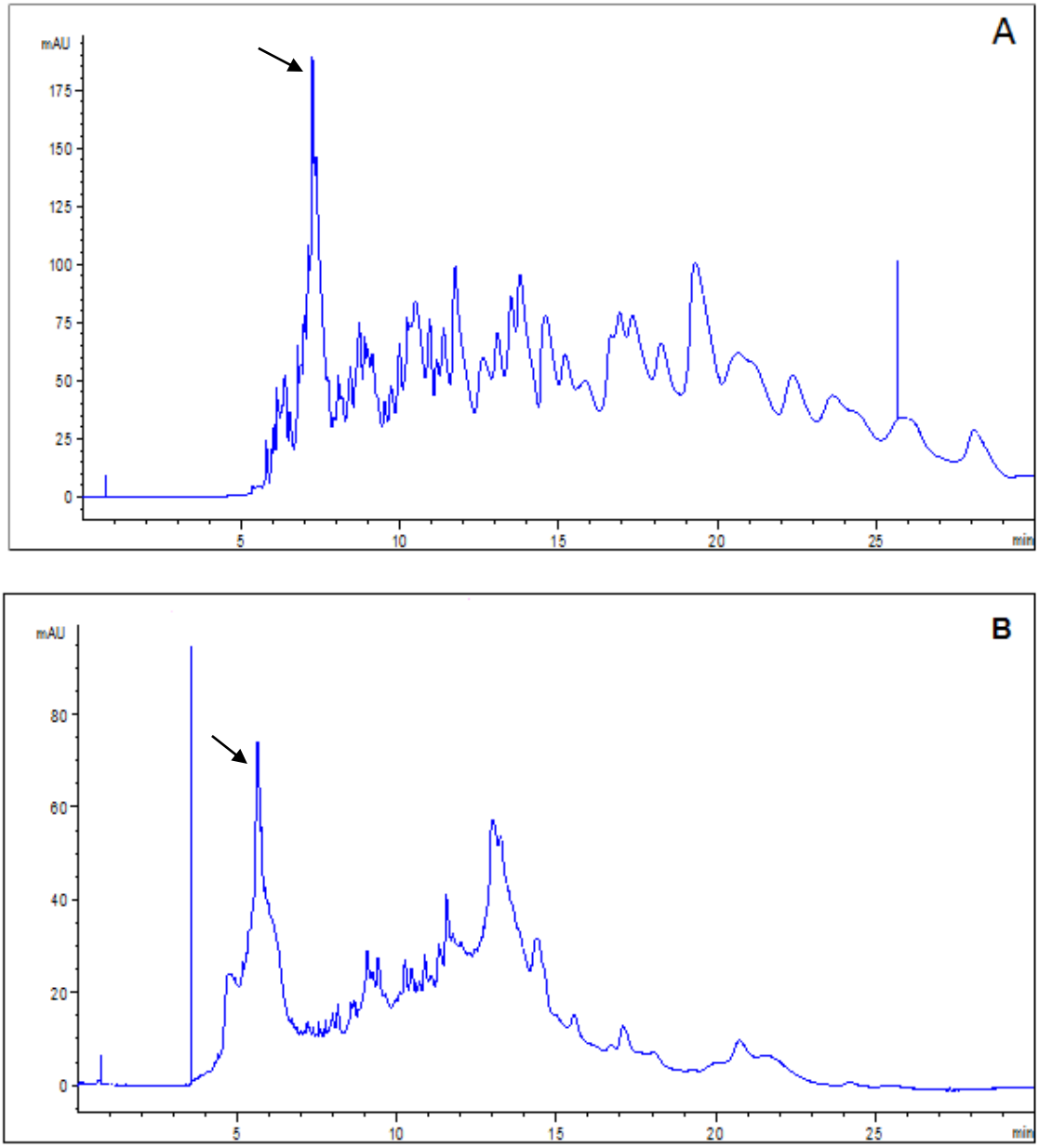

Figure 12. *Electropherograms showing autoproteolysis of 0.12 mM soluble CT digested in 25 mM of ammonium bicarbonate (A) and in 25 mM Tris-HCl (B), both at pH 8. Both solutions were incubated at 37ºC for 240 min. The separations were performed using a 25 mM phosphate buffer, pH 2.5, V_{app}= +15 kV, L_t = 46 cm, L_d = 36 cm, using the conditioning and injection method A (Table 1) as described in Section 2.3.1. Note that the scale is different in each graph, for clarity. Arrows indicate undigested CT.*

3.2. Effect of SDS rinsing on CE separation reproducibility

The peptide maps (i.e., electropherograms) were not as reproducible in Section 3.1 as we expected, maybe because of the large protein concentration in the samples, so we decided to investigate a better method for conditioning the capillary. The effect of SDS (sodium dodecyl sulfate) on the reproducibility of CE separation was therefore investigated. SDS is anionic surfactant used as a detergent in biochemistry because it can help dissolve large proteins in solution by denaturing them [69]. Therefore, SDS was used to remove any proteins that may be adsorbed onto the capillary wall, which would affect the reproducibly of the migration time of the peptides being separated. Three different CE capillary conditioning procedures were compared, as described below:

- No addition of SDS rinsing (Method A in Table 1, in Section 2.3).
- Addition of 25 mM SDS in the rinsing step during pre-conditioning (Method B, Table 1, in Section 2.3).
- Addition of SDS rinsing in the post-conditioning step (Method C, Table 1, in Section 2.3).

The sample used to test the capillary conditioning procedures was the autoproteolysis product of soluble CT, obtained after incubation at 37°C for 240 min in ammonium bicarbonate buffer (25 mM, pH 8). To compare the results, certain peaks were numbered, which is important for comparison of peptides from separations across multiple injections and for different conditions. If the separation doesn't show sufficient resolving power, one signal could include more than one peptide.

The reproducibility of the migration times and peak heights for 15 peaks was monitored for 3 separate injections (Fig. 13) without including SDS in any of the capillary conditioning steps (Method A in Table 1). In contrast, Figures 14 and 15 show the electropherograms obtained when using SDS in pre-conditioning (Method B) and post-conditioning (Method C) of the capillary, respectively.

We obtained the lowest numbers of resolved peaks when using SDS rinsing in pre-conditioning (Method B, Table 1). Even though using SDS in pre-conditioning showed greater peak intensity, it was excluded due to the reduction in the number of peaks from 15

to 8. In this case, there is a possibility that SDS persistence in the capillary after rinsing in pre-conditioning impaired the separation of the autodigestion peptides. As seen in Method B of Table 1 (Section 2.3), there was only 3 min of HCl rinsing and 3 min of buffer rinsing after the SDS and before sample injection whereas Method C provided 16 min of total rinsing between SDS and sample injection. The poor separation of peptides in Fig. 14 (SDS rinse in pre-conditioning) may also result from persistence of high ionic strength matrix in the capillary before injection as there were no water rinse steps after SDS and HCl. It would be interesting to see if a longer rinsing period of buffer and water after the SDS pre-conditioning rinse would improve the peptide separation. This should be investigated further.

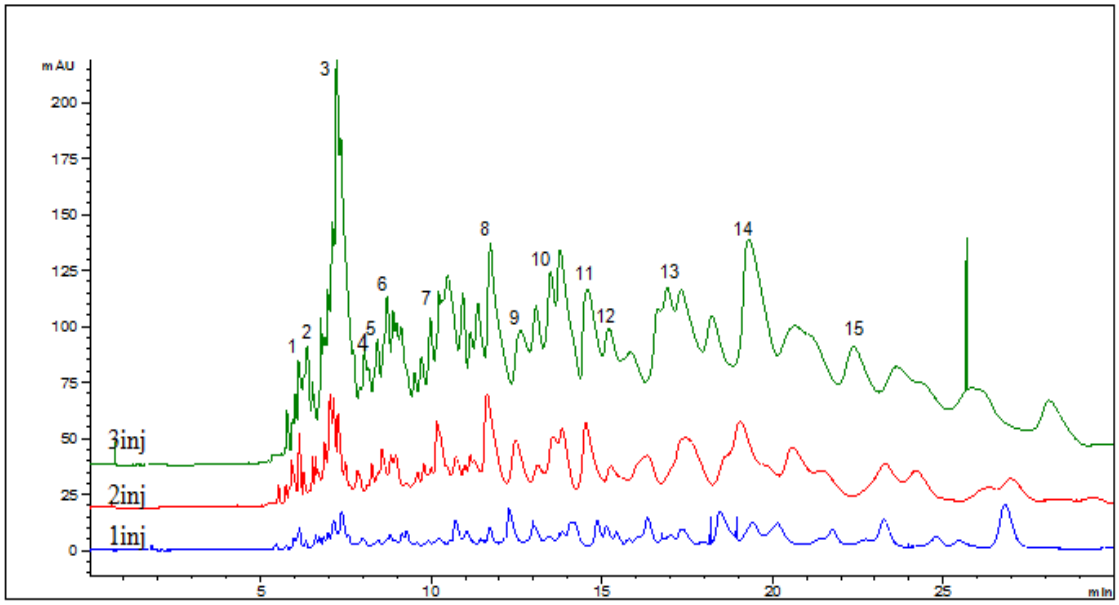

Figure 13. *Electropherograms for triplicate injections showing peptide maps for soluble CT (0.12 mM) autoproteolysis. The digestion and separation conditions were the same as shown in Fig. 12, where no SDS rinsing of the capillary was used.*

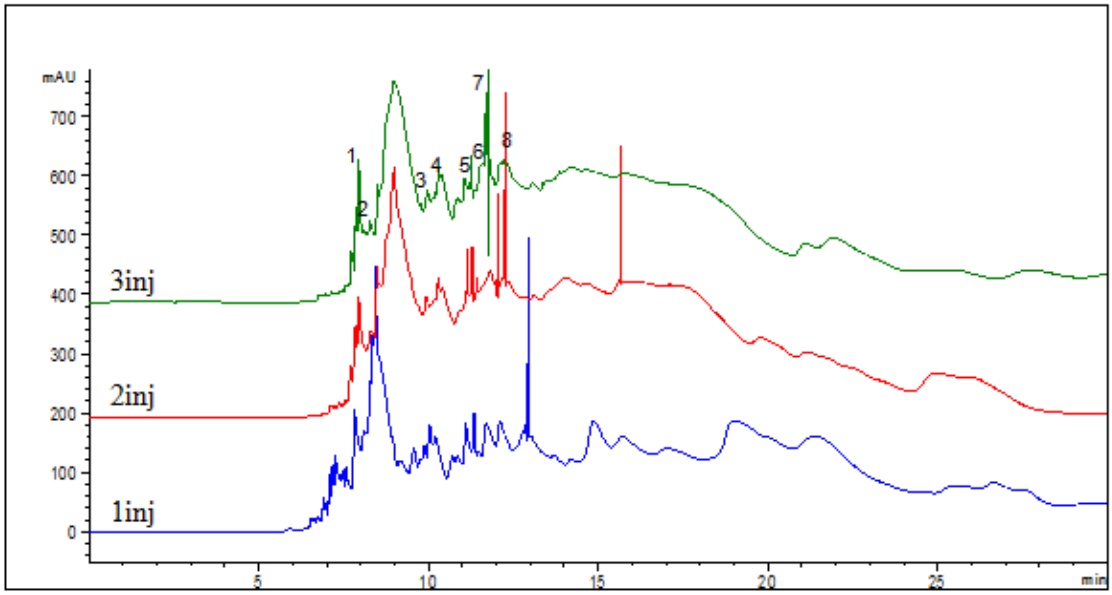

Figure 14. *Electropherograms for triplicate injections showing peptide maps for 0.12 mM soluble CT autoproteolysis. The digestion and separation conditions were the same as in Fig. 12 except that SDS rinsing was used in the capillary pre-conditioning (Method B, Table 1, in Section 2.3).*

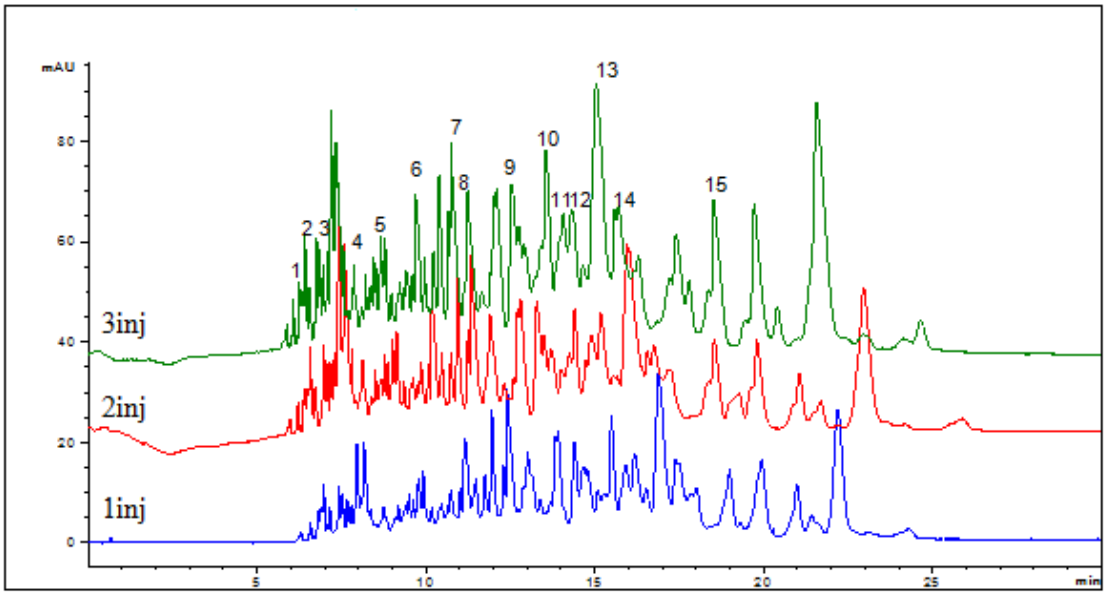

Figure 15. *Electropherograms for triplicate injections showing peptide maps for 0.12 mM soluble CT autoproteolysis. The digestion and separation conditions were the same as in Fig. 12 except that SDS rinsing was used in the capillary post-conditioning (Method C, Table 1, in Section 2.3).*

Therefore, excluding the results from Fig. 14, where 15 peaks could not be clearly identified, a more quantitative comparison of reproducibility was made only between using SDS in post-conditioning (Method C, Table 1) and without using SDS during capillary conditioning (Method A, Table 1). The graphs in Figs. 16 and 17 show the reproducibility in migration time and peak height, respectively, for the autoproteolytic peptides of two different samples of soluble CT (0.12 mM) incubated at 37°C for 240 min.

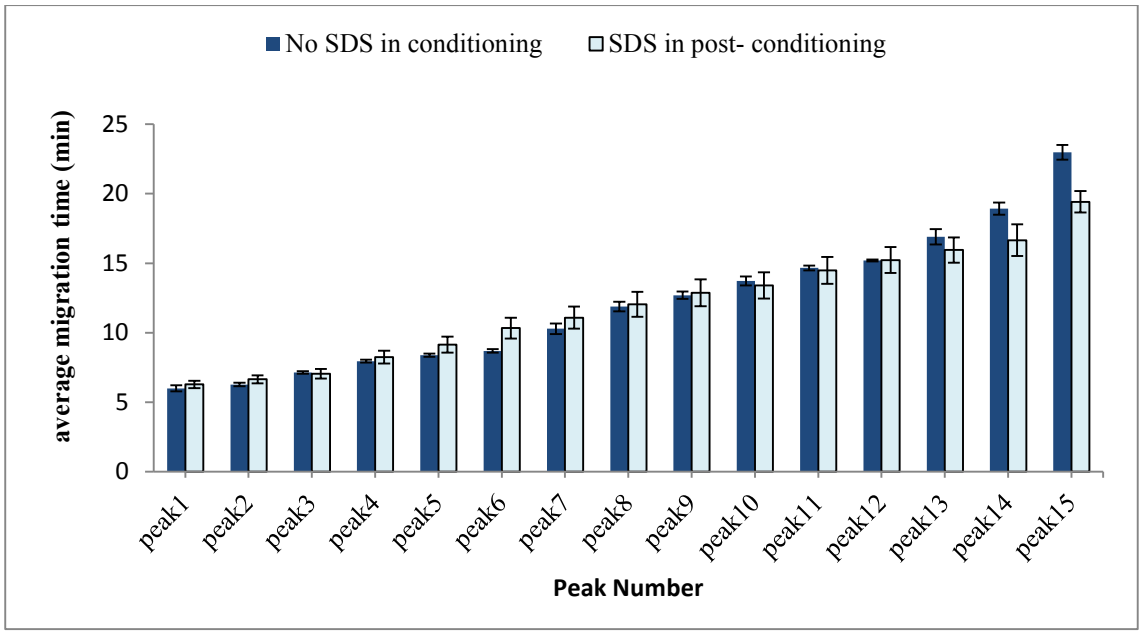

Figure 16. *Bar chart showing the migration time reproducibility of 15 peaks as identified in Figs. 13 and 15 resulting from autoproteolysis of 0.12 mM soluble CT using identical CE separation conditions as in Fig. 12 except for the omission of SDS (dark blue bars) and addition of SDS (light blue bars) in capillary post-conditioning rinses. Errors bars represent the standard deviation (STD) of the migration time (n=3).*

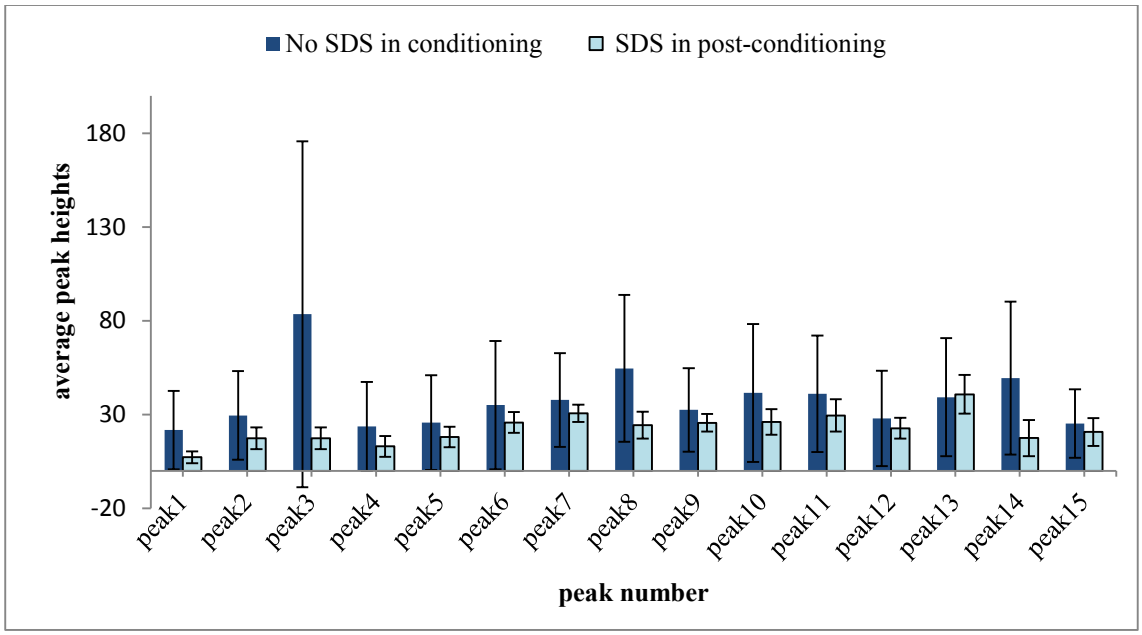

Figure 17. *Bar chart showing the migration time reproducibility of 15 peaks as identified in Figs. 13 and 15 resulting from autoproteolysis of 0.12 mM soluble CT using identical CE separation conditions except for the omission of SDS (dark blue bars) and addition of SDS (light blue bars) in capillary post-conditioning rinses. Errors bars represent the standard deviation (STD) of the migration time (n=3).*

The bar charts in Figs. 16 and 17 show that adding SDS in the capillary post-conditioning steps did not greatly affect the migration time reproducibility, although inspection of Figure 13 and 15 showed a distinct improvement in peak resolution when SDS post-conditioning was used. In addition, it improved the peak height reproducibility as seen by the smaller error bars in Fig. 17 obtained from the digested soluble CT. The average relative standard deviation (RSD) across all the numbered peptide peaks after autodigestion was calculated for all three methods of capillary conditioning, as summarized in Table 2.

Table 2. Reproducibility of peptide maps showing the effect of rinsing with SDS during capillary conditioning.

Type of SDS rinsing for capillary treatment [a]	Average RSD	
	Migration times	Peak heights
No SDS (Method A)	2%	85%
SDS in pre-conditioning (Method B)	2% [b]	23% [b]
SDS in post-conditioning (Method C)	6%	30%

[a] treatment methods A, B and C are given in Table 2, Section 2.3.1.
[b] Only 8 peaks could be identified in triplicate injections.

As seen in Table 2, peak heights showed poor reproducibility in general, with RSD values ranging from 23 to 85%. This could possibly be due to residual CT and/or peptides adsorbed on the capillary walls, or due to the fact that all three injections were not necessarily made on the same day, or due to the method employed to stop digestions, which consisted only of putting the digestion solution in the freezer at -20ºC. The time required for solutions to actually freeze solid would be > 1 h, allowing for autodigestion to continue. The best results for the peak height reproducibility were obtained when SDS rinsing was used in pre-conditioning, with a very large reduction in the RSD value compared with not using SDS. However, only 8 peptide peaks were consistently identified with this CE analysis method because resolution was so bad.

It was observed in Fig. 15 with SDS rinsing in capillary post-conditioning that the efficiency was much better and the peak capacity increased, which improved peptide mapping, compared with using SDS in pre-conditioning or not using it at all. Peak widths appeared reduced and likely resulted in higher theoretical plates (N). In summary, using SDS rinsing in the capillary post-conditioning procedure showed the best compromise for maximizing the number of peptides detected and for migration time and peak height reproducibility.

3.3. Choice of method for terminating the digestion

According to the results shown in Table 2, there was a large variation in the RSD of the peak heights with values ranging from 23 to 85% across the 3 methods for capillary conditioning (Section 2.3, Table 2), and this could come from incomplete or irreproducible digestion. The proposed solution is to stop the reaction at a predetermined point, and then no significant difference should be observed between different analyses of similar samples. Two methods of stopping the enzymatic digestion reaction were investigated: i) adding 12 M HCl to the digestion solution to rapidly change the pH ,and ii) putting the digestion solution in a dry ice/acetone bath (-78ºC) for rapid freezing.

For these experiments, 200 μL of 0.12 mM soluble CT was incubated at 37°C for a 240 min period in ammonium bicarbonate buffer, then the reaction was stopped by adding either 1 μL of 12 M HCl or by putting the micro tube in the -78ºC cooling bath for about 1 min; samples were then put into the freezer at -20°C until CE analysis (i.e., peptide mapping). Figs. 18 and 19 show the peptide maps from autoproteolysis of soluble CT after stopping the reaction with a solution of HCl or with rapid freezing, respectively. These results show that better peak separation and resolution are observed when terminating the digestion by using rapid freezing in a dry ice/acetone bath (-78ºC) (Fig. 19). The addition of HCl to the sample, even small amounts, affects the CE separation by reducing separation efficiency. This is due to the increased ionic strength of the sample solution compared to the concentration of the solutes, i.e., the peptides. Therefore, using a dry ice/acetone bath was the preferred procedure for stopping digestions for the rest of the project.

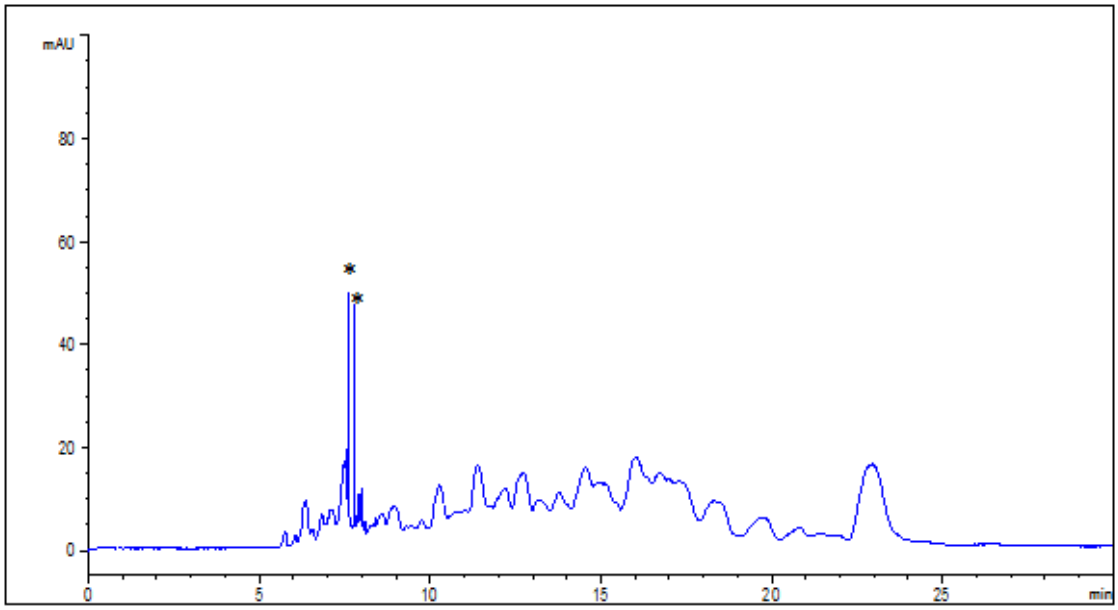

Figure 18. *Electropherogram showing peptide maps for 0.12 mM soluble CT autoproteolysis. The digestion and separation conditions were the same as in Fig. 15 except that the reaction was stopped by adding 1 µL 12 M HCl (method in Section 2.2.3). Peaks labeled with a star (*) are noise: they are too narrow to be dissolved species and appear randomly.*

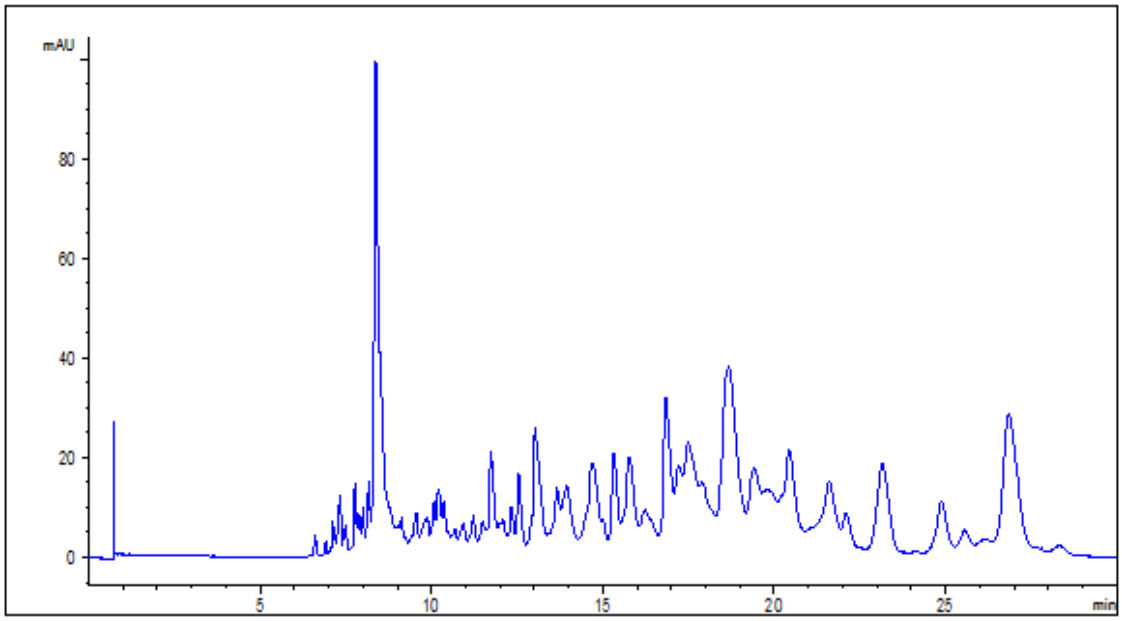

Figure 19. *Electropherogram showing peptide maps for 0.12 mM soluble CT autoproteolysis. The digestion and separation conditions were the same as in Fig. 15 except that the reaction was stopped by putting the digestion solution in a dry ice/acetone bath (-78ºC) (method in Section 2.2.3).*

3.4. Effect of time and temperature on autoproteolysis of soluble and immobilized chymotrypsin

The aim of this section was to investigate the effect of incubation time (30 vs 240 min) and temperature (37, 24, and 4°C) on the extent of autoproteolysis for soluble versus GA-cross-linked (immobilized) CT. Specifically, this involved studying the influence of these parameters on the enzyme and the autoproteolytic peptide peak heights and the reproducibility of the peptide maps. In all cases, the digestion reaction was terminated using a dry ice/acetone bath (-78°C) and the CE separation method was the same as that used previously (Method C in Table 1, Section 2.3). Section 3.4 is divided into two subsections for the study of time and temperature on autoproteolysis: soluble CT and immobilized CT (GA-CT). The hypothesis is that immobilized CT has better thermal stability and thus reduced autoproteolysis compared to soluble CT.

3.4.1. Soluble chymotrypsin

Figs. 20 and 21 show the peptide maps for 240 and 30 min incubation, respectively, of 0.12 mM CT at the three temperatures. The peak heights are directly proportional to the concentration of the components in the solution. The enzyme (i.e., chymotrypsin) and the autoproteolysis peaks (i.e., autoproteolytic peptides) are labeled in both figures. To identify the enzyme peak, an undigested solution of free CT was injected in the CE and the migration time determined (t_m = 6.64 ± 0.08min) as is shown in the inset of Fig. 20A. The migration time of the enzyme peak varied slightly between experiments, which is not uncommon in CE. The reproducibility of the results, in general, is discussed below.

Fig. 20A shows the full scale peptide maps by CE separation for incubation temperatures of 37, 24 and 4ºC (all for 240 min) whereas Fig. 20B is the "zoomed in" version of A to show the many peptides. These results show that, in general, the autoproteolytic peptides increase in abundance with increasing temperature, because the enzyme activity is increased with temperature, while the enzyme peak decreased as it was self-digested, as expected.

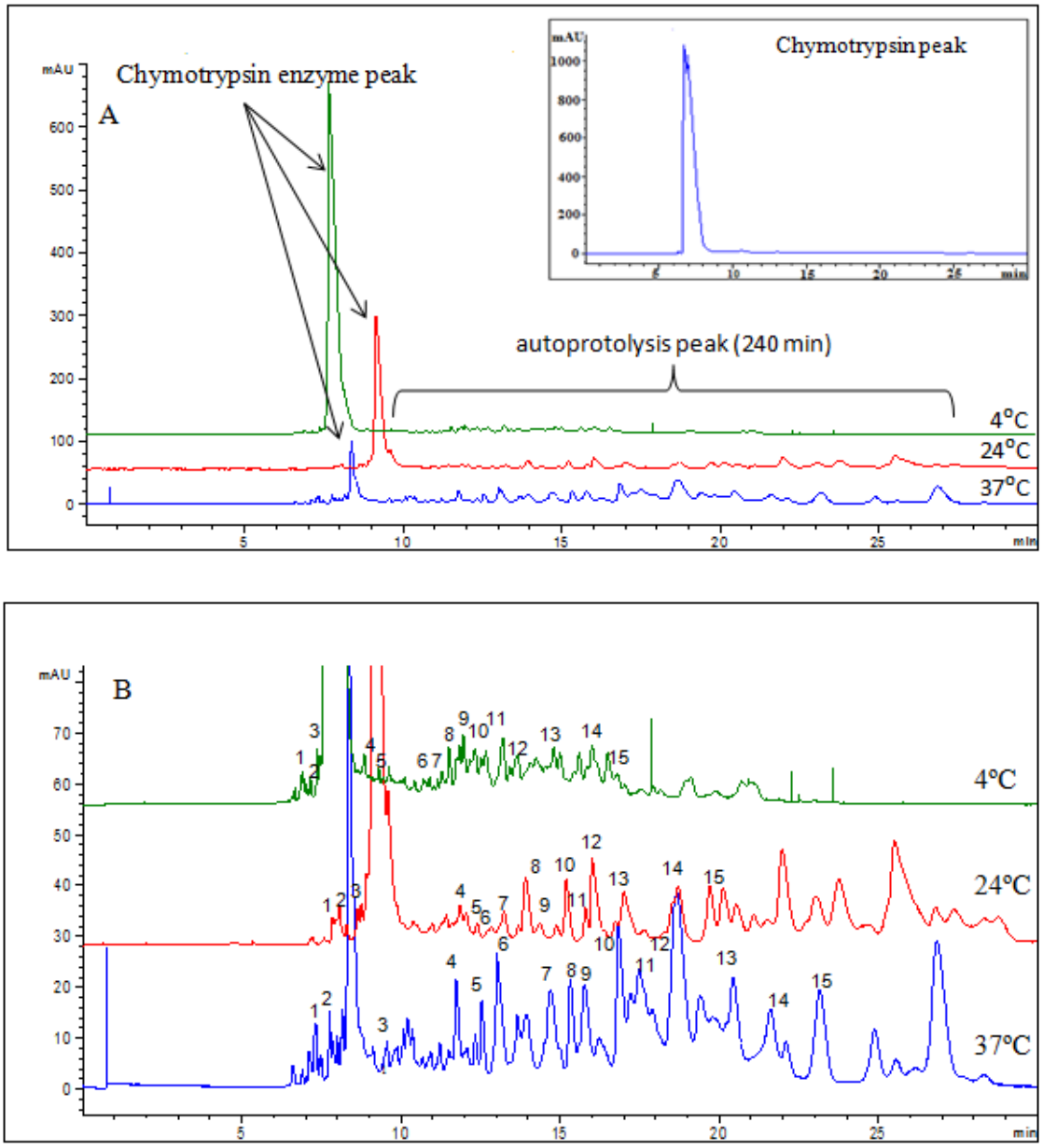

Figure 20. *Electropherograms showing peptide maps for autoproteolysis of 0.12 mM soluble CT (A) at three different temperatures, 37, 24 and 4ºC, for 240 min and the zoomed-in electropherograms (B). The experiment was repeated 3 times at each temperature and a reproducibility study is shown in Figs. A1 to A3 in the Annex. The peaks labeled with numbers in the electropherograms are those followed for reproducibility studies. The separation condition was the same as shown in Fig. 15.*

The experiments were then done for 30 min incubation at the same three temperatures. Fig. 21A shows the results of this series of measurements with the baseline zoomed in for Fig. 21B. The relationship between the incubation temperature and the peak height of the

peptides is generally the same as it was with the longer digestion of 4 h. It can also be seen that the autoproteolysis peak heights decreased with the decreasing digestion time to 30 min, while the enzyme peak height decreased for each temperature studied as it did for the 240 min digestions. The experiments were repeated 3 times at each temperature and incubation time and the corresponding maps are shown in Figs. A1- A6 (Annex).

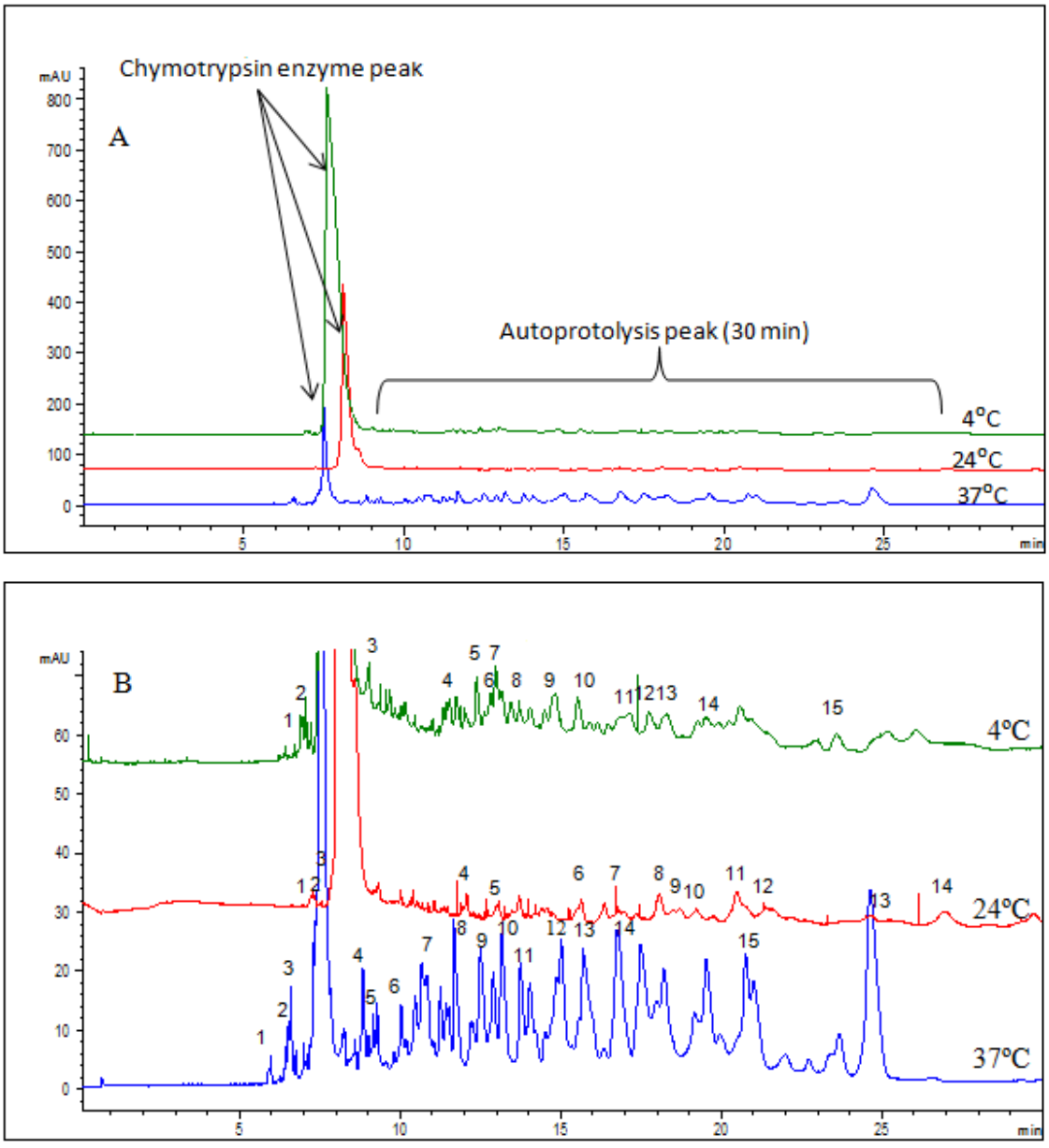

Figure 21. *Electropherograms showing peptide mapping for autoproteolysis of 0.12 mM soluble CT in three temperatures (A) at three different temperatures 37, 24 and 4°C, for 30 min. (B) is a zoomed-in version of the same electropherogram. The experiment was repeated 3 times at each temperature and a reproducibility study is shown in Figs. A4 to A6 in the Annex. The separation conditions were as shown in Fig. 15.*

By comparing Figs. 20 and 21, it can be seen that when the digestion time was increased, the enzyme peak height decreases substantially, except at 4ºC. This can be explained by the slow rate of digestion at such a low temperature. In other words, the rate of digestion is so slow that increasing the time from 30 to 240 min is not enough to cause a significant difference in autoproteolysis.

The relationship between the digestion time and the extent of autoproteolysis was as expected and can be explained by the fact that autoproteolysis is more extensive for longer incubation times [23] as shown below in Fig. 22.

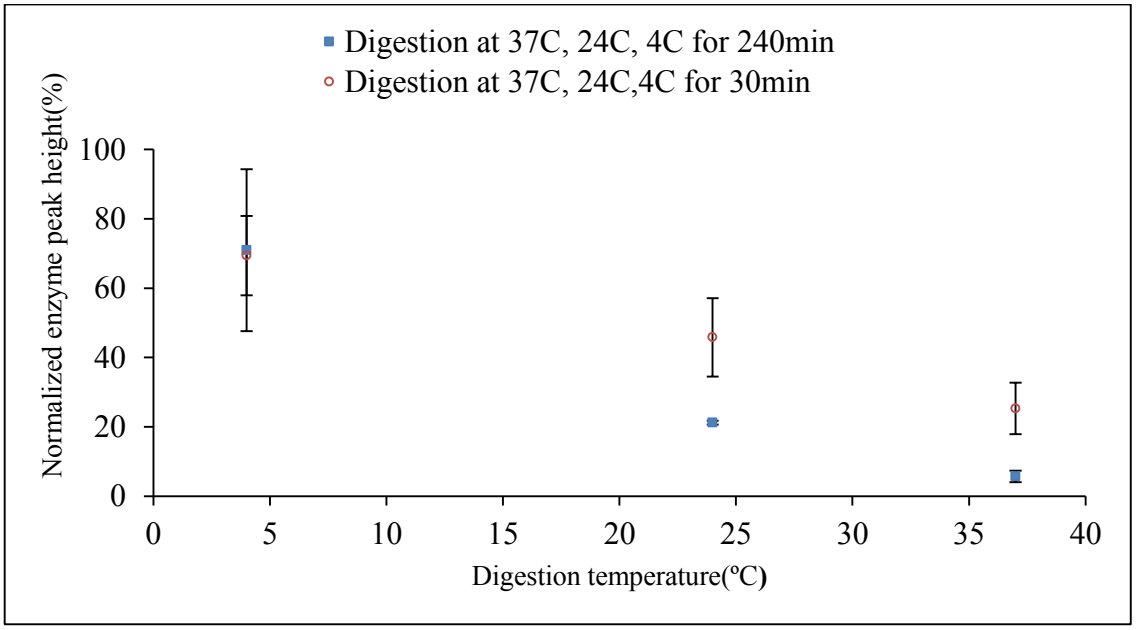

. Figure 22*. A plot of the average enzyme peak height versus digestion temperature for 0.12 mM soluble CT digestion at 37, 24 and 4ºC for 240 min (the red data points, and 30 min (blue data points) compared with free enzyme (same concentration) without any digestion. Errors bars represent the standard deviation (n = 3 injections) of the peak heights.*

Fig. 22 demonstrates the effect of temperature on enzyme autodigestion: at higher temperatures there is less enzyme concentration left in the solution because it has undergone more autodigestion. The peak heights were normalized relative to the undigested free

enzyme's peak height, i.e., this means peak heights after digestion were divided by the height of the free enzyme without digestion. Fig. 22 also shows that when the peak height for CT is smaller, the CE reproducibility is better, as seen by the smaller error bars. This is because the peaks are more Gaussian and not broadened by sample overloading.

The reproducibility of peptide separations with respect to migration time and peak height was investigated by following 15 arbitrarily-selected peaks per digestion temperature and time. A different set of peaks was chosen for each digestion temperature-time to spread them across the elution window (see Figs. A1-A6, Annex). These are summarized in Fig. 23 below, which shows bar charts of the average migration time and average peak height, respectively, for the 240 min incubation study. Fig. 24 shows the analogous data for the 30 min incubation study.

The overall reproducibility of the separation was measured by calculating the relative standard deviation (RSD) of peak heights and then calculating the average RSD across the 15 peaks for the experimental data given above. Table 3 shows that reproducibility in peak heights was very poor, with RSD values ranging from 18 to 67%. This similar problem was reported by Bonneil who studied peptide mapping reproducibility for digestion in a trypsin microreactor [6].

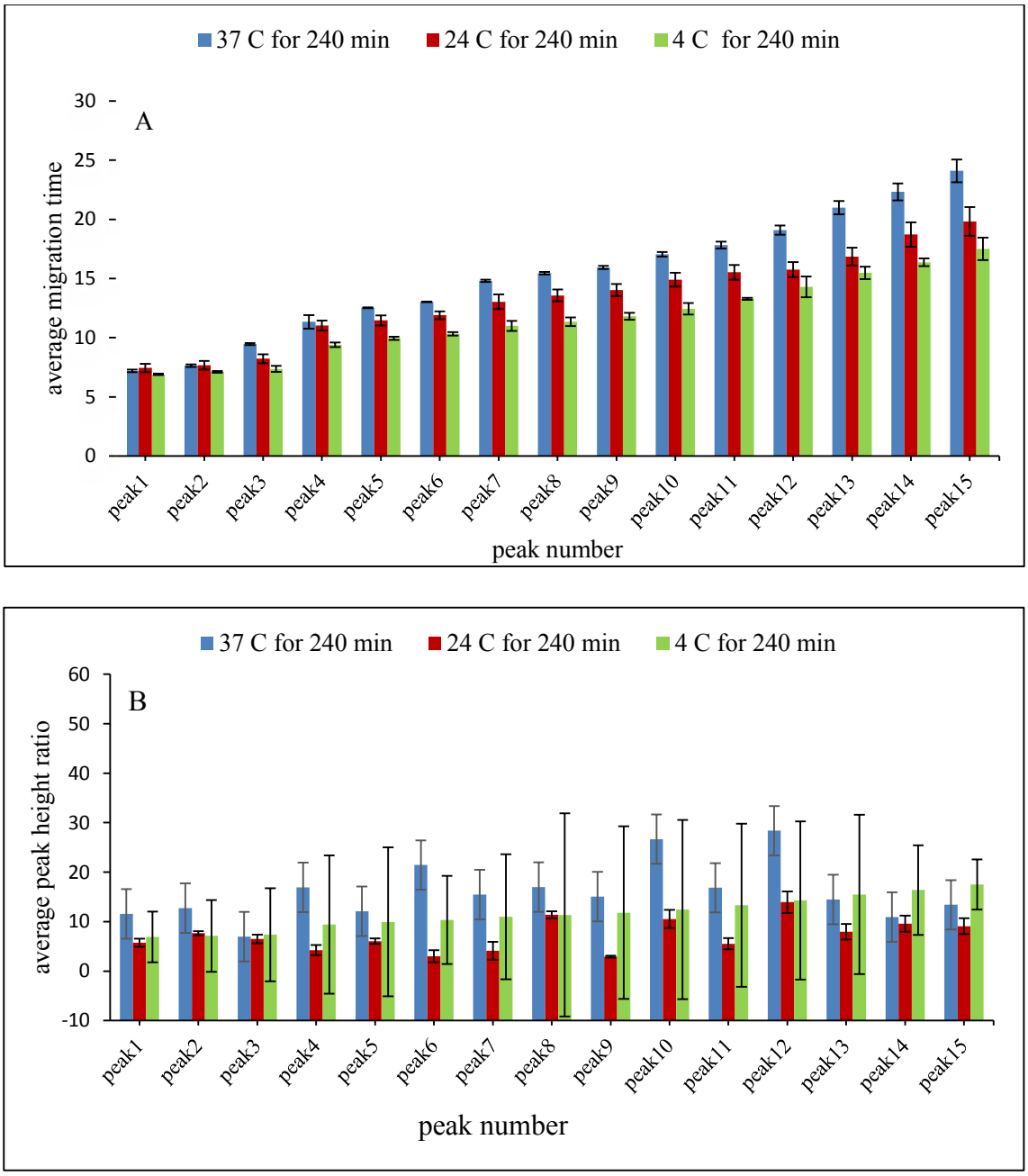

Figure 23. *Bar charts showing the variation of migration time (A) and the variation of the peak height (B) across 15 peaks, where the blue bars, the red bars and the green bars represent digestions at temperatures of 37, 24 and 4ºC, respectively, for 240 min. The peptide maps (separations) are presented in Figs. A1-A3 (Annex). Error bars represent the standard deviation of the three analyses (injections).*

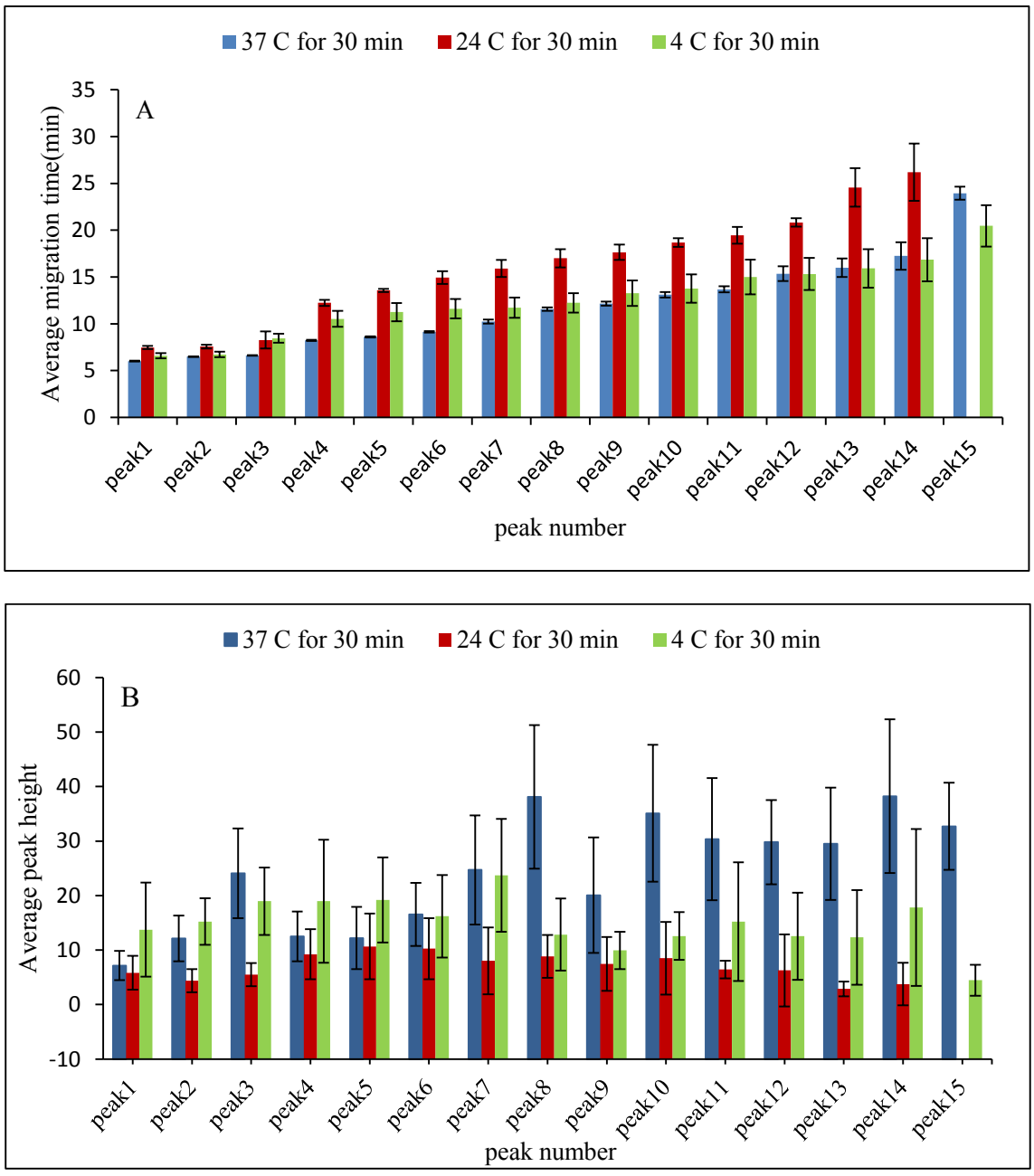

Figure 24. *Bar chart showing the reproducibility of average migration time (A) and reproducibility of peak heights (B) across 15 peaks, where the blue bars, the red bars and the green bars represent digestions at temperatures of 37, 24 and 4°C, respectively, for 30 min. The peptide maps (separations) are presented in Figs. A4-A6 (Annex). Error bars represent the standard deviation of the three analyses (injections).*

Table 3. Summary of migration time and peak height reproducibility across 15 peaks[a] as a function of digestion time and temperature[b] for triplicate injections.

Digestion temperature (°C) [b]	Average RSD for migration time [a]		Average RSD for peak height	
	30 min digestion	240 min digestion	30 min digestion	240 min digestion
37	2.4 %	1 %	36 %	23 %
24	5 % [c]	4 %	61 % [c]	18 %
4	9 %	3 %	52 %	67 %

[a] Peak numbers correspond to those labeled in Figs. 20 and 21.
[b] The sample analyzed was the digestion product of 0.12 mM soluble CT incubated at 37, 24 or 4ºC for either 240 or 30 min.
[c] Only 14 peaks out of 15 peaks could be identified in triplicate injections.

Good migration time reproducibility is required in analytical separations to establish a method that either confirms the presence of analytes, or possibly discards them as contamination or noise. For peptide mapping, a high degree of migration time reproducibility is required to distinguish peptides from a normal protein from those carrying a post-translational modification or a mutation. It is also essential for quantitative mass spectrometry analysis where peak height is used to determine an increase or decrease in abundance. The examination of error bars for average migration time in Figs. 23 and 24 shows fairly small variations, suggesting that the 15 peaks selected could be good candidates for peptides from CT and not just background or random peaks. Also, the RSD values (shown in Table 3) show variation going from 1 to 5% (excluding the 30 min incubation at 4°C), which confirms the acceptable reproducibility of the CE separation.

The relationship between time, temperature of digestion and extent of autoproteolysis was also determined by monitoring the peak representing the free enzyme. The high variability in this peak did not allow us to confirm this relationship quantitatively, so results will be discussed qualitatively only. We observed that the enzyme peak height decreased with increasing temperature of digestion, which resulted from increased autoproteolysis. A similar trend was observed for increased digestion time, except at 4ºC, where the very slow rate of reaction means that increasing the digestion time has little effect. Overall, the results

suggest that for autoproteolysis of soluble CT, the peptide map reproducibility is best at 240 min digestion at 37ºC, but that a 30 min digestion at 37ºC could also give peptide maps with good reproducibility and that these conditions could be applied for a real protein substrate.

The method reproducibility of the autoproteolysis (i.e., digestion) was also evaluated for three separate samples of soluble CT, when incubated at 24ºC for 240 min. We used the RSD of peak heights from triplicate injections for each sample and then calculated the overall RSD across the 15 peaks for the three samples. Table 4 shows that the reproducibility in peak heights was not very good, with RSDs reaching 38% for the 9 injections (3 samples digested, with 3 injections each for CE separation), whereas reproducibility of migration time was better, with a global RSD of 5%. These results indicate that better control of the experimental conditions for digestion are needed.

Table 4. Summary of migration time and peak height reproducibility across 15 peaks as function of digestion time and temperature for triplicate injections of each of 3 samples of free CT.

CT sample (digested at 24ºC for 240 min) [a]	Average RDS for migration time	Average RDS for peak height
Sample 1	4%	18%
Sample 2	2%	31%
Sample 3	9%	66%
Overall	**5%**	**38%**

[a] The sample analyzed was the digestion product of 0.12 mM soluble CT incubated at 24ºC for 240 min for 3 batches, each then injected into CE in triplicate.

3.4.2. Immobilized chymotrypsin

In the present work, CT immobilized by GA-mediated cross-linking (GA-CT) was investigated as a means to limit unwanted auto-digestion compared to soluble CT due to better thermal stability of GA-CT. Therefore, the effects of incubation time and the temperature on the autodigestion peptide maps for the immobilized enzyme were studied under the same conditions as in Section 3.4.1 for soluble CT.

The cross-linked GA-CT was made following the procedure described previously by our group [22, 23] as described in the experimental section. The apparent concentration of immobilized CT is 0.24 mM, which is twice that used for the free enzyme (0.12 mM) autoproteolysis studies described above.

Previous studies that compared autoproteolysis of the free and immobilized CT at the same concentration (0.12 mM) for incubation time of 240 min at 37ºC reported a significant reduction of the autoproteolysis peaks upon immobilization [23]. Therefore, increasing the concentration of the immobilized CT will help to confirm this observation and verify whether autoproteolysis peaks were not observed simply because they were not detectable (i.e., the immobilized enzyme resists autoproteolysis) or because the activity of the GA-CT is much lower than that of the soluble CT. Fig. 25 shows the resulting electropherograms (i.e., peptide maps) of the three injections of one sample digested at 37ºC for 240 min. For the same incubation time, immobilized CT was also digested at 24ºC and 4ºC as shown in Figs. 26 and 27, respectively.

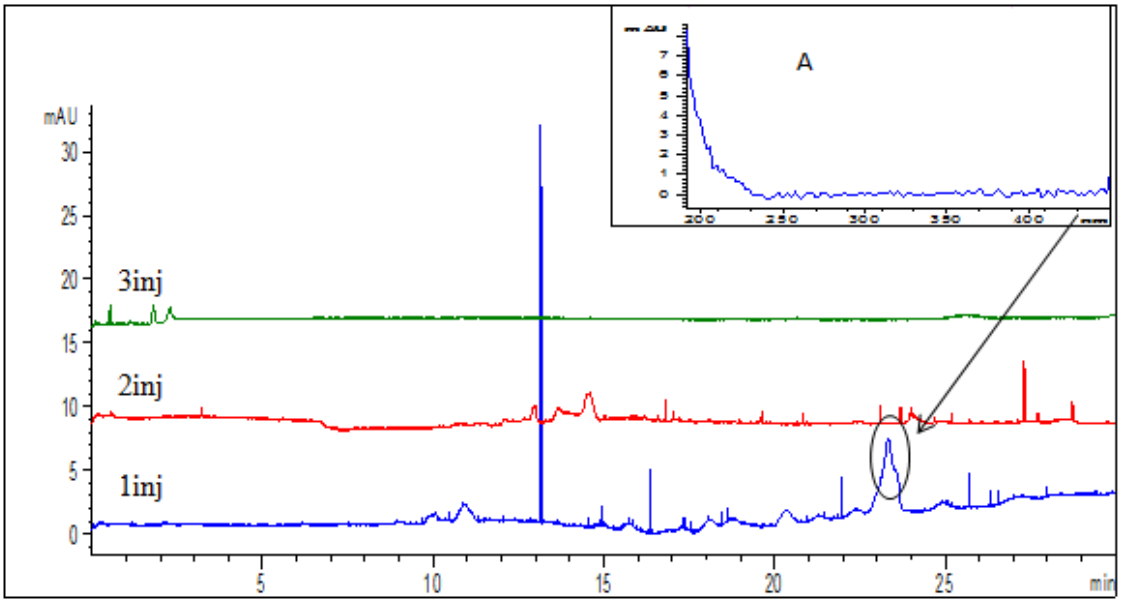

Figure 25. *Electropherograms showing peptide maps for three analyses of 0.24 mM immobilized CT (i.e., GA-CT; same batch) with incubation time of 240 min at 37°C. The separation conditions were the same as shown in Fig. 15. Panel A is the UV-visible spectrum from the DAD detector of the peak circled in the electropherogram of the 1st injection.*

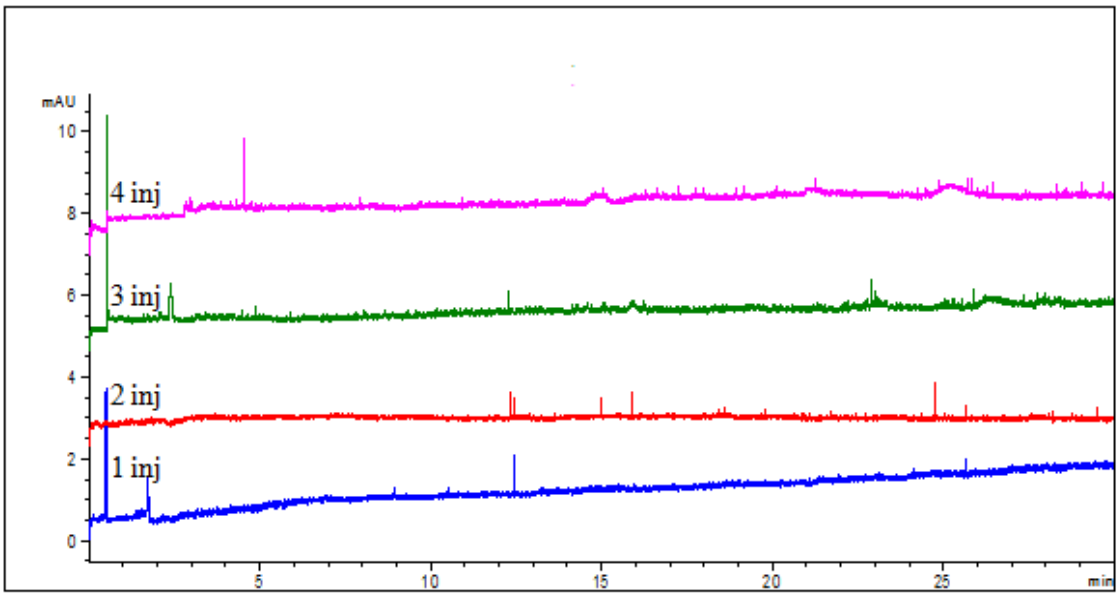

Figure 26. *Electropherograms showing peptide maps for four analyses of 0.24 mM GA-CT (same batch) with incubation time 240 min at 24ºC. The separation conditions were the same as shown in Fig. 15.*

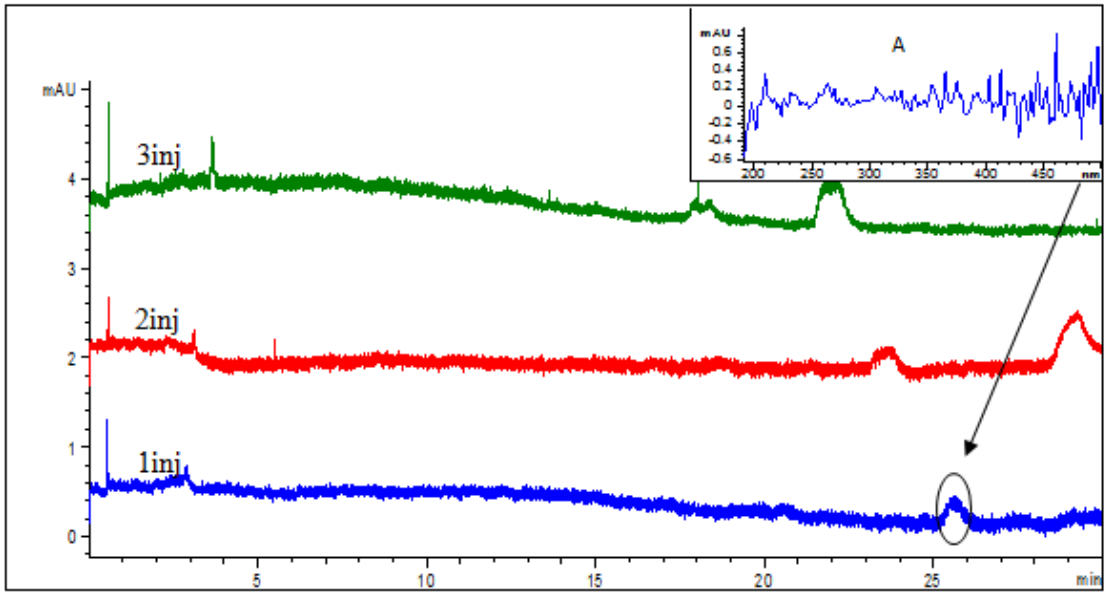

Figure 27. *Electropherograms showing peptide maps for three analyses of 0.24 mM GA-CT (same batch) with incubation time 240 min at 4°C. The separation conditions were the same as shown in Fig. 15. Panel A is the UV-visible spectrum from the DAD detector of the peak circled in the electropherogram of the 1st injection.*

Figs. 25, 26 and 27 show that no major peak for either the enzyme or its autoproteolysis peptides were detected within the detection limits for CE-UV separation, except for one peak that was detected in Fig. 25 (at 23.5 min in the 1st injection). This peak shows a peptide-like absorbance spectrum (i.e., similar to the spectrum of the peptide at 18.5 min for soluble CT digestion, shown in Fig. A1, Annex), and it is only present in one injection. The other small peaks in Figs. 25 to 27 are noise, which was verified by inspection of their absorbance spectra. Therefore, it shows that there is little or no autoproteolysis even when the digestion temperature is increased.

The experiment was repeated, and the incubation time was changed from 240 to 30 min. The same thee temperatures were investigated. Figs. 28, 29 and 30 show the effect on GA-CT autoproteolysis of the different incubation temperatures of 37, 24 and 4ºC, respectively, for 30 min.

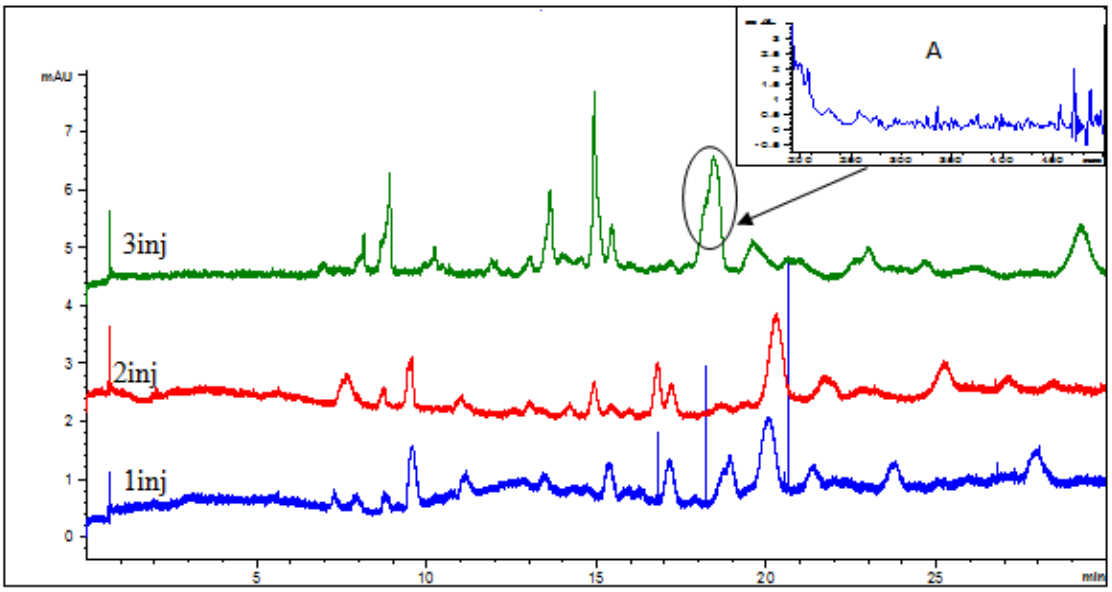

Figure 28. *Electropherograms showing peptide maps for three analyses of 0.24 mM GA-CT (same batch) with incubation time 30 min at 37°C. The separation conditions were the same as shown in Fig. 15. Panel A is the UV-visible spectrum from the DAD detector of the peak circled in the electropherogram of the 3rd injection.*

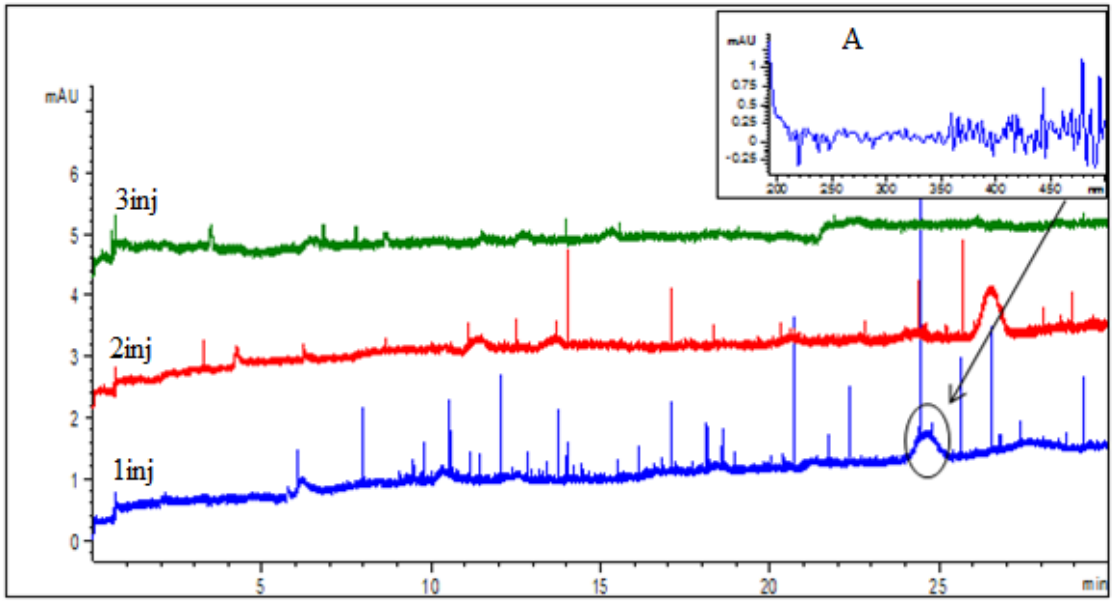

Figure 29. *Electropherograms showing peptide maps for three analyses of 0.24 mM GA-CT (same batch) with incubation time 30 min at 24°C. The separation conditions were the same as shown in Fig. 15. Panel A is the UV-visible spectrum from the DAD detector of the peak circled in the electropherogram of the 1st injection.*

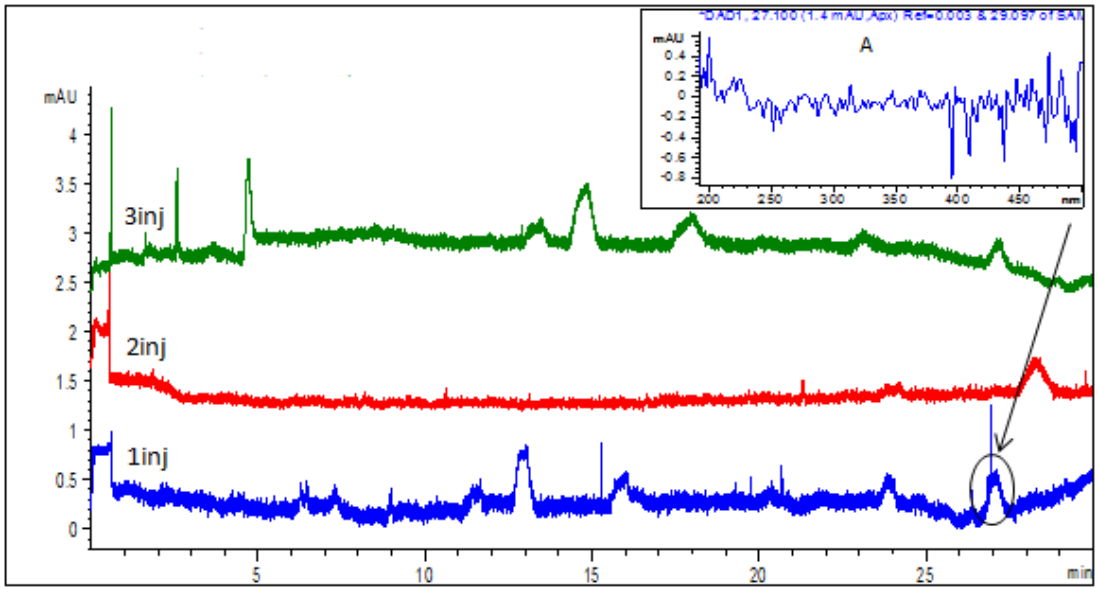

Figure 30. *Electropherograms showing peptide maps for three analyses of 0.24 mM GA-CT (same batch) with incubation time 30 min at 4°C The separation conditions were the same as shown in Fig. 15. Panel A is the spectrum of the peak circled in the electropherogram of the 3rd injection.*

According to Figs. 28, 29, and 30, more peaks were detected in the digests incubated for 30 min than for 240 min, but most were identified as noise by their UV-Vis absorbance

spectra. The peaks in Fig. 28 may be peptides, but the concentrations are so small that the spectra are not reliable for identification. Generally, all apparent peaks have similar spectra, suggesting they are noise and not peptides. It is important to see the zoomed-in absorbance scale. No major peaks were detected in any of the experimental conditions for incubation of immobilized CT, and no CT peak was seen, suggesting again that the autoproteolysis is highly suppressed for immobilized enzymes.

To compare the autoproteolysis of the soluble enzyme to the immobilized enzyme, the electropherograms for each at 37ºC × 240 min incubation were overlaid, as shown in Fig. 31. For comparisons of the effect of other times and temperatures on soluble versus immobilized CT, results from each were also overlaid and can be seen in Figs. A7 to A11 in the Annex.

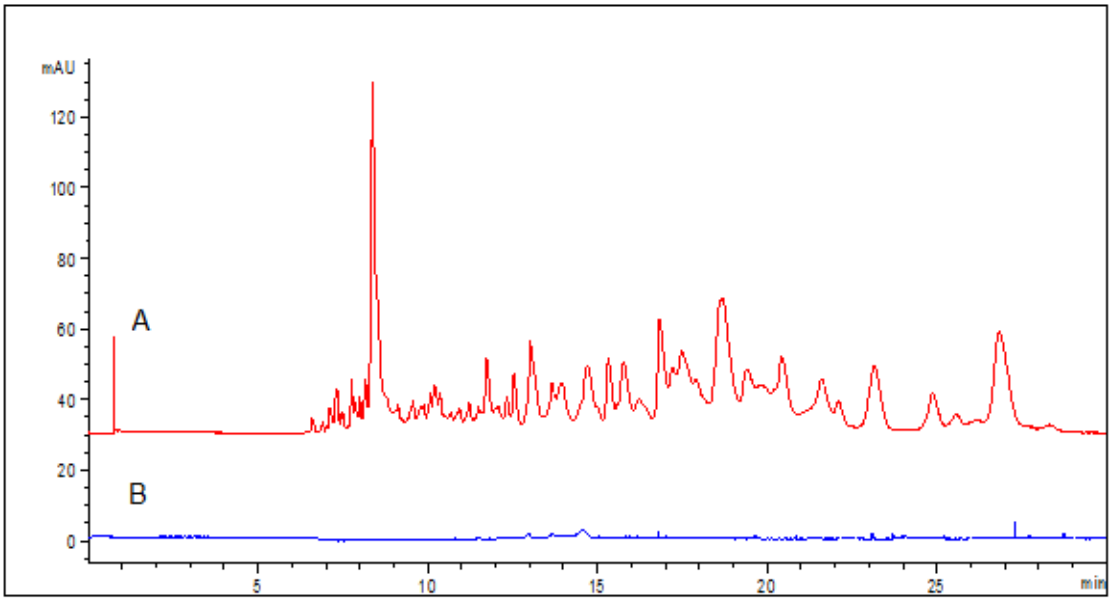

Figure 31. *Electropherograms (peptide maps) showing the comparison between autoproteolysis of free (soluble) CT (A) and immobilized CT (B). Both were incubated at 37ºC for 240 min. The separation conditions were the same as shown in Fig. 15.*

Fig. 31A shows a large number of peptides, while Fig. 31B shows mainly low level noise when viewed on the same scale. These results confirm that the immobilization of CT through GA-mediated cross-linking strongly reduces autoproteolysis. Likewise, under the other five time and temperature conditions, autoproteolysis was observed for the free but not

the immobilized enzyme suggesting that the GA-CT does not permit auto-digestion of chymotrypsin.

3.5. Effect of heat-induced denaturation time on substrate digestion

As described in the introduction, a protein substrate is typically denatured by chemically induced unfolding followed by reduction and alkylation of disulfide bonds before the cleavage by enzyme for peptide mapping. Substrates prepared this way have been successfully digested by GA-immobilized trypsin and chymotrypsin as shown in previous studies in our group [7, 23, 43]. Recent autoproteolysis studies in our group showed that when digestions using free CT and "blank" substrate samples that had been taken through the full denaturation/reduction/alkylation process were made, several CT autoproteolysis peptides were seen. This was likely due to residual denaturing reagents that denatured some CT and caused it to undergo more rapid autodigestion. The same experiment using GA-CT showed practically no autoproteolysis [70]. Since reduction and alkylation of a substrate is time consuming and more difficult to automate, it is interesting to look instead at using heating only for partial substrate denaturation, especially when complete digestion is not needed for protein identification by MS/MS-based peptide mapping. Therefore, we wanted to see whether the immobilized GA-CT could digest heat-induced denatured substrates to the same extent as free CT, with the knowledge that protein refolding occurs upon cooling and that the presence of disulfide bridges limit the amount of substrate unfolding. The following sections describe the comparison of immobilized to soluble (free) CT for digestion of two protein substrates (BSA and myoglobin) denatured at three different temperatures but not reduced/alkylated.

3.5.1. BSA digestion by immobilized chymotrypsin

In this section, the effect of substrate denaturation temperature (60, 75 and 90°C) on peptide maps of BSA digested with GA-CT was studied. The free CT digestion studies are presented in the next section. The details of BSA concentration and digestion parameters are described in Chapter 2.

Increasing the denaturation temperature of the substrate should lead to more unfolding of the protein, even when disulfide brides are still present, and allow the enzyme to access some digestion sites [8, 26]. The results expected should be a higher number of peptide peaks and with higher concentrations (peak heights) coming from the digestion of BSA along with a decrease in the substrate concentration as heat-denaturation temperature is increased. However, during the first study at 90ºC denaturation of BSA for 45 min, very poor resolution of the BSA peptides was observed, as shown in Fig. 32A. It was suspected that the problem was related to the CE analysis and not the digestion.

The buffer concentration in CE separations should be at least 100 times higher than the sample concentration. As noted by Baker's group, "low buffer concentration or ionic strength should be avoided because this may cause distortion of electric field and broadened peaks, or also allow adsorption of solute such as protein on capillary walls" [71]. The CE buffer used up to this point in the studies was 25 mM sodium phosphate, pH 2.5, which was suspected of being too low, even though the BSA concentration used in digestion was only 0.013 mM. Therefore, the effect of increasing the CE buffer concentration from 25 to 75 mM was evaluated. Figs. 32A and B compare the effects of two separation buffers (25 and 75 mM) on the peptide map of BSA denatured at 90ºC for 45 min and digested with GA-CT. The peptide map shown in Fig. 32B suggests that 75 mM phosphate buffer with pH 2.5 is the better choice, since the peaks were less broadened. Therefore, 75 mM phosphate buffer was used in the remaining experiments.

The heat-induced denaturation experiment was repeated for 0.013 mM BSA at 60 and 75ºC for 45 min, and then samples digested by GA-CT with an enzyme:substrate ratio of 18:1 (mol/mol). Digestions were at 37ºC for 240 min after allowing the denatured BSA to cool down for approx. 15 min at room temperature. The results are shown in Fig. 33.

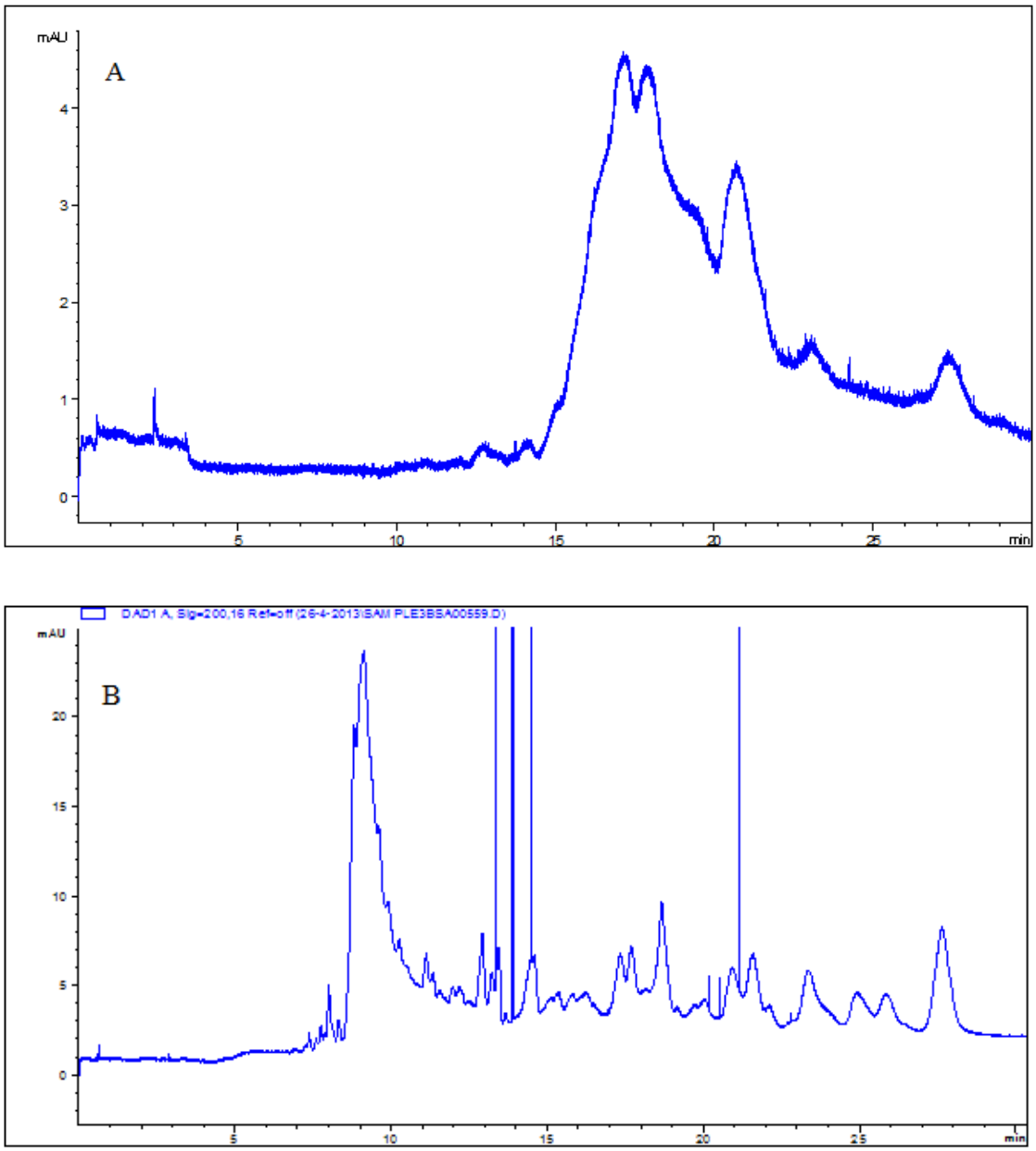

Figure 32. *Electropherograms showing effect of different concentration of CE separation buffer on peptide maps of BSA: (A) 25 mM sodium phosphate buffer, pH 2.5; (B) 75mM sodium phosphate buffer, pH 2.5. The sample was the same in both separations: 0.013 mM BSA digested with GA-CT at 37ºC for 240 min after BSA denaturation at 90ºC for 45 min. The separation conditions were the same as shown in Fig. 15, except the separation buffer concentration.*

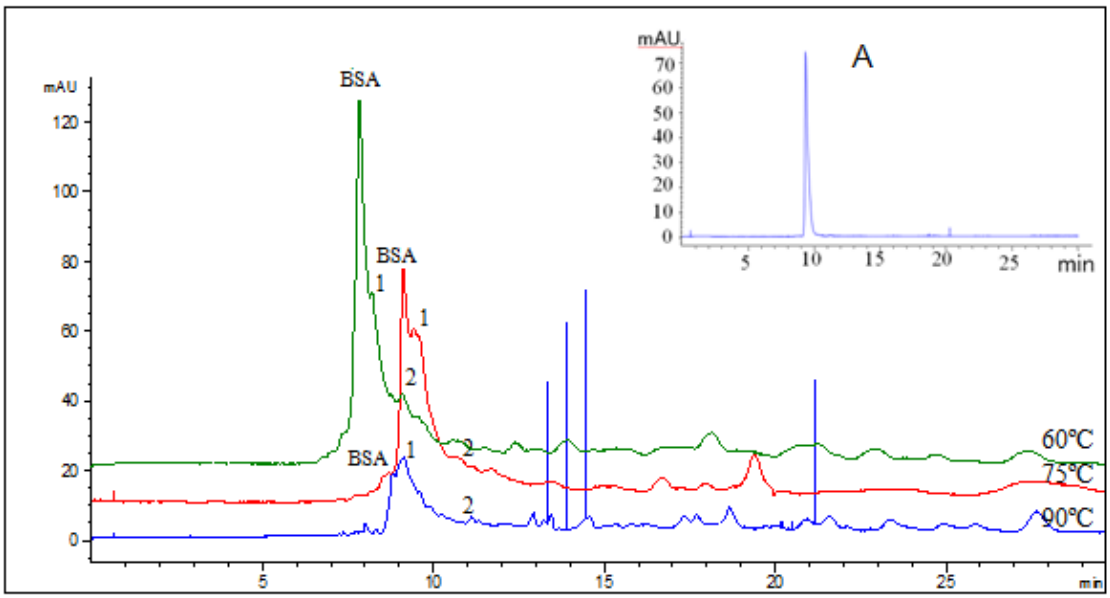

Figure 33. *Electropherograms showing peptide maps of BSA (0.013 mM) with three different temperatures of denaturation for 45 min: 60, 75 and 90ºC. The digestion was made with GA-CT at 37ºC for 240 min and the enzyme to substrate ratio was 18:1 (mol:mol). The separation conditions were the same as shown in Fig. 15, except for CE buffer concentration, which was now 75 mM. The inset image (Fig. 33A) presents the injection of undenaturated BSA to identify its migration time (9.35 min) in this CE separation. Peaks 1 and 2 for each denaturation temperature were selected for quantitative comparison.*

To quantitatively evaluate the effect of three different denaturation temperatures of native BSA on the peptide mapping, the heights of two selected peaks were considered as an indication of the concentration. The two peaks selected to follow the evolution of the digestion are identified as 1 and 2 in Fig. 33. However, when the heights of peaks 1 and 2 were plotted against temperature of denaturation, the opposite trend was seen to what was expected: peak heights decreased as denaturation temperature increased. We expected that more denaturation (i.e., at 90°C compared to 60°C) would make digestion easier and thus higher (or more) peptide peaks would be seen for triplicate injections.

This is likely explained by the poor resolution between the peaks numbered 1, 2 and the BSA peak (Fig. 33) and also by the high variability in peak heights, even between injections of a given sample (as seen in Table 3). Therefore, by calculating the peak height ratios of peaks 1 and 2 relative to the BSA peak, these negative experimental effects were taken into account and, as shown in Fig. 34 (and Table A1 in Annex), as denaturation

temperature increased, digestion by GA-CT was facilitated and more of the peptides 1 and 2 were formed.

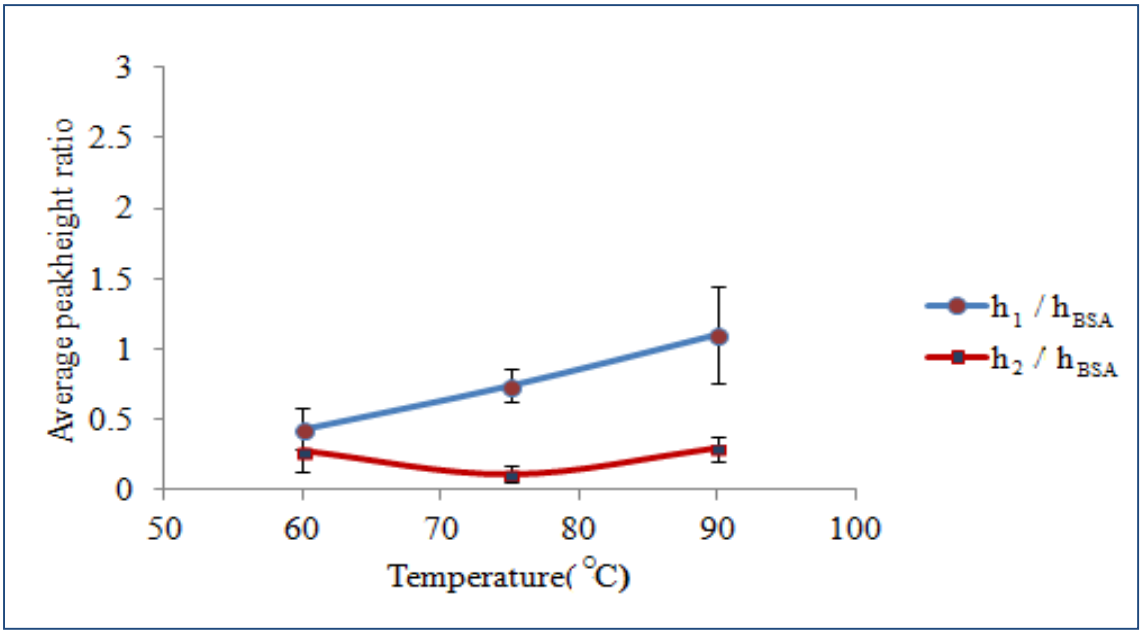

Figure 34. *Plot of the average peak height ratios of h_1/h_{BSA} and h_2/h_{BSA} versus denaturation temperature for BSA denatured at 60, 75 and 90ºC for 45 min and digested at 37ºC for 240 min, for triplicate injections. Peaks 1, 2 and BSA are those labeled in Fig. 33. Data for this graph are shown in Table A1 in the Annex.*

The relationships observed in Fig. 34 shows acceptable linearity for peak number 1 with a R^2 of 0.999, but not for the peak number 2 with a R^2 of 0.6624. The slopes shown for both 1 and 2 suggest that the increase in temperature of denaturation did not significantly increase digestion product.

The reproducibility of CE separations for the three different temperatures of denaturation of BSA then digestion with GA-CT are shown by the error bars in Fig. 34, which were improved by taking the ratios h_1/h_{BSA} and h_2/h_{BSA}.

According to the results above, the digestion of heat-induced denatured BSA by GA-CT was not satisfactory for peptide mapping. Contrary to our expectation of more peptides at 90ºC denaturation, Fig. 33 showed very few peptide peaks and no large differences

between three different temperatures, even though more BSA seems to have been reacted when denatured at 90ºC for 45 min because the BSA peak decreased. The lack of digestion is obviously due to the fact that the substrate BSA contains 17 disulfide bonds and therefore heat-induced denaturation was not effective without reduction of these bonds and alkylation of cysteine residues. The BSA is still too highly folded as a substrate to react with the active site of CT whose mobility is very restrained because of the cross-linking in the GA-CT particles.

3.5.2. BSA digestion by soluble chymotrypsin

As a comparison to GA-CT, and for an equal substrate concentration, soluble CT (0.0013 mM) was used to digest BSA after its heat-induced denaturation at the same three temperatures used above: 60, 75 and 90ºC. It is important to note that the amount of immobilized CT was 180 times more than the free CT because the process of immobilization is known to decrease an enzyme's specific activity (i.e., activity per gram of immobilized material) [54]. The same procedure was used: heating for 45 min and cooling for 15 min before digestion at 37ºC for 240 min. The enzyme:substrate ratio was 1:10 (mol/mol), which is about five times higher amount of soluble enzyme than usually used in protein digestion protocols but similar to previous experiments in our group (unpublished). The results expected were an increase of the digestion products when the temperature of denaturation was increased owing to the unfolding of BSA that increases the access of the enzyme to digestion sites, and to improved activity of soluble compared to immobilized CT. However, the digestion of BSA with soluble CT did not present a clear increase of digestion products with increasing the temperature from 60 to 90ºC (Fig. 35). To better investigate the effects of substrate denaturation temperature, the peak from native undigested BSA was identified by injecting BSA standard solution (see Fig. 35A inset). Using the UV absorbance spectra from the DAD detector, undigested BSA in the peptide maps was identified in Fig. 35. Two peaks representing peptides (numbered 1 and 2 in Fig. 35) were selected by choosing peaks that were repeated for the three different denaturation conditions and the same graphical analysis described in Section 3.5.1 above was carried out: the average peak height ratios from

the selected peaks relative to the BSA peak (h_1/h_{BSA}) were plotted against denaturation temperature (Fig. 36). The data for this graph are shown in Table A2 in the Annex.

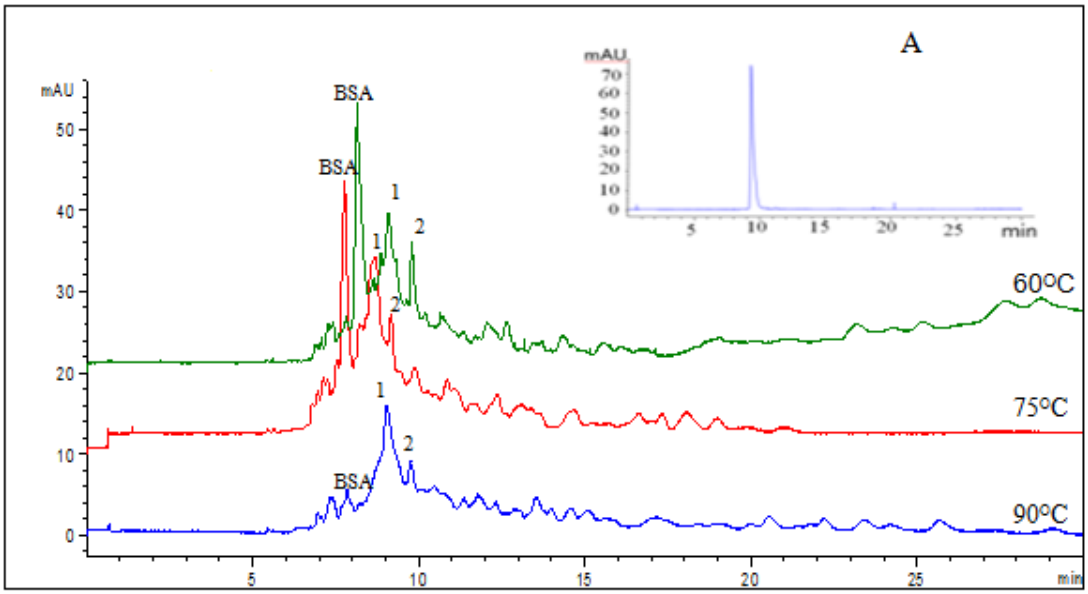

Figure 35. *Electropherograms showing peptide maps of BSA (0.013 mM) for three different temperatures of denaturation: 60, 75 and 90ºC. The digestion was made with free CT at 37ºC for 240 min and the enzyme to substrate ratio was 1:10 (mol:mol). The separation conditions were the same as in Fig. 33. The inset, Fig. 35A, presents the injection of undenatured BSA, showing that migration time for a standard solution injected into the CE has a different migration time than when in a digest. Peaks 1 and 2 are peptides identified by their UV absorbance spectra.*

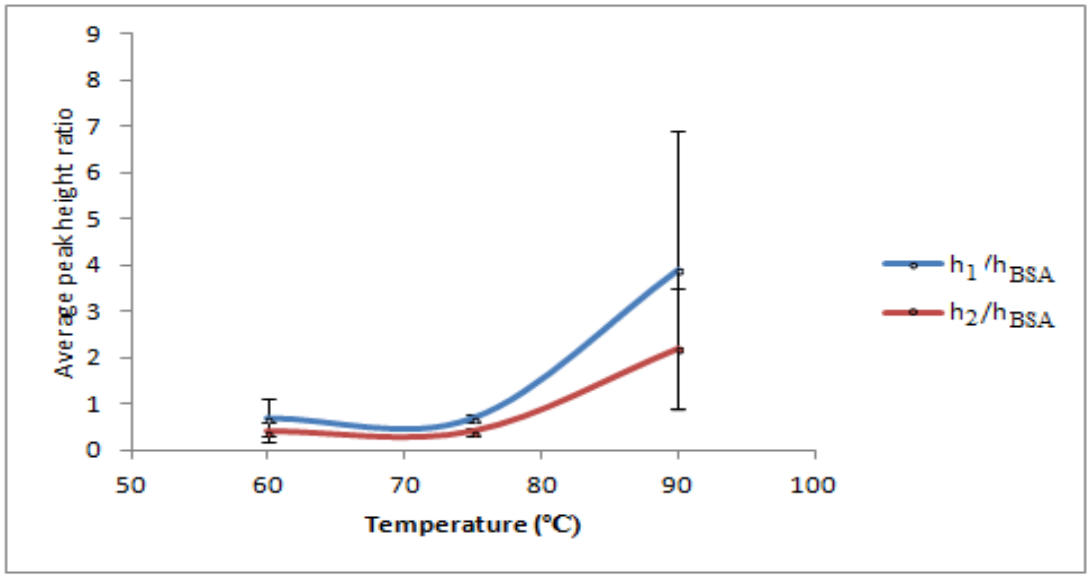

Figure 36. *Plot of the average peak height ratios of h_1/h_{BSA} and h_2/h_{BSA} versus denaturation temperature for BSA denatured at 60, 75 and 90ºC for 45 min and digested* ***at*** *37ºC for 240 min, for triplicate injections. Peaks 1, 2 and BSA are those labelled in Fig. 35. Data for this graph are shown in Table A2 in the Annex.*

The graph in Fig. 36 shows that increasing the heating temperature of BSA from 60 to 75ºC did not significantly affect the BSA digestion (for both peak ratios). However, the BSA denaturation at 90ºC led to much better BSA digestion than the other two temperatures because the amounts of peptides 1 and 2 increased relative to the substrate.

According to these results shown above, heating the substrate at 90ºC improves the unfolding of BSA and thus the digestion, which was expected. It is important to mention that for the enzyme, which is soluble, the peptide map should also contain the CT autoproteolysis peptide peaks, although the concentration was much less (100×) than for the experiments in Section 3.4. Nonetheless, blank experiments were conducted consisting of the injection of the digestion solution without BSA substrate. The digestion followed the same four steps mentioned in the experimental section, where the blank heat-denatured solution was ammonium bicarbonate buffer without any substrate.

Fig. 37 shows the overlay of the soluble CT and GA-CT digestion of BSA after its denaturation at 90ºC for 45 min, and the blank experiment (no BSA), all incubated at 37ºC for 240 min. This was conducted to distinguish which peptide peaks were from CT

autoproteolysis and which were from BSA digestion. The blank experiments were conducted for the other two denaturation temperatures also, and are shown in Figs. A12 - A14 in the Annex.

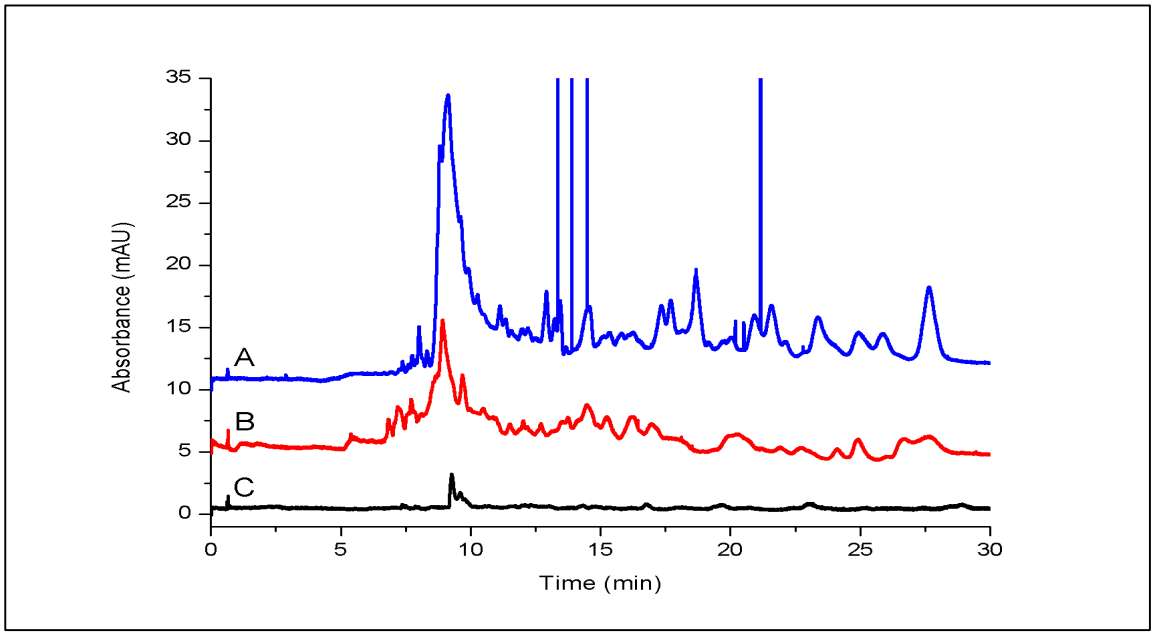

Figure 37. *Electropherograms showing peptide maps of heat-denatured BSA (0.013 mM) at 90ºC digested for 240 min at 37ºC with: (A) GA-CT (enzyme:substrate = 18:1), (B) soluble CT (enzyme;substrate = 1:10), and (C) soluble CT but without BSA (blank experiment). The separation conditions were the same as shown in Fig. 33.*

Fig. 37C shows that the enzyme (free CT, 0.0013 mM) elutes at the same time as a peptide from the BSA digest. The CT and its small autoproteolysis peaks also contribute to the peptide maps in Fig. 35 for 60 and 75ºC denaturation temperatures for BSA. The blank experiment shows the contribution coming both from the enzyme and the autoproteolysis product in the peptide maps. It is important to underline that in Fig. 37, we compared only the effect of digestion by soluble versus immobilized CT on heat-induced (90ºC) denatured BSA by comparing their peptide maps; the effect of heat-induced versus chemically-induced denaturation was not addressed. The results showed very little BSA digestion when using immobilized CT because there are too many disulfide bonds and the tertiary structure remaining after heat-induced denaturation shielded the BSA cleavage sites from GA-CT. When using free CT however, we observed slightly more digestion compared to with GA-

CT, which means some unfolding of BSA at 90ºC occurred and free CT could access some of BSA's cleavage sites.

3.5.3. Myoglobin digestion by immobilized chymotrypsin

Myoglobin is a single polypeptide containing 153 residues and a heme group [72]. In the present study, myoglobin was used as a smaller substrate without disulfide bridges to investigate the effect of different temperatures of denaturation on peptide mapping with immobilized versus soluble CT. The details of myoglobin concentration and digestion parameters are described in Chapter 2.

The results were somewhat as expected, with an increase in denaturation temperature permitting native myoglobin to become partially unfolded and undergo better digestion, as shown by a decrease in the substrate peak in Fig. 38. To identify which peak was myoglobin, blank experiments were made consisting of the substrate (myoglobin) solution denatured at 90ºC and "blank digested" at 37°C for 250 min with no CT enzyme present. Fig. 39 shows the electropherogram of this blank experiment with a very large peak for myoglobin at 9.4 min.

Surprisingly, there seemed to be fewer distinctive peptides for the 90ºC heat-denatured sample as seen in Fig. 38, where peptide maps did not improve with denaturation temperature under GA-CT digestion conditions. For myoglobin heated at 90ºC, the digestion definitely occurred because very little myoglobin was remaining (Fig. 38, bottom trace) and we know that the disappearance of myoglobin was not from heating at 90ºC because the blank digestion in Fig. 39 (90ºC heat-denatured but no CT during digestion incubation) shows the myoglobin peak.

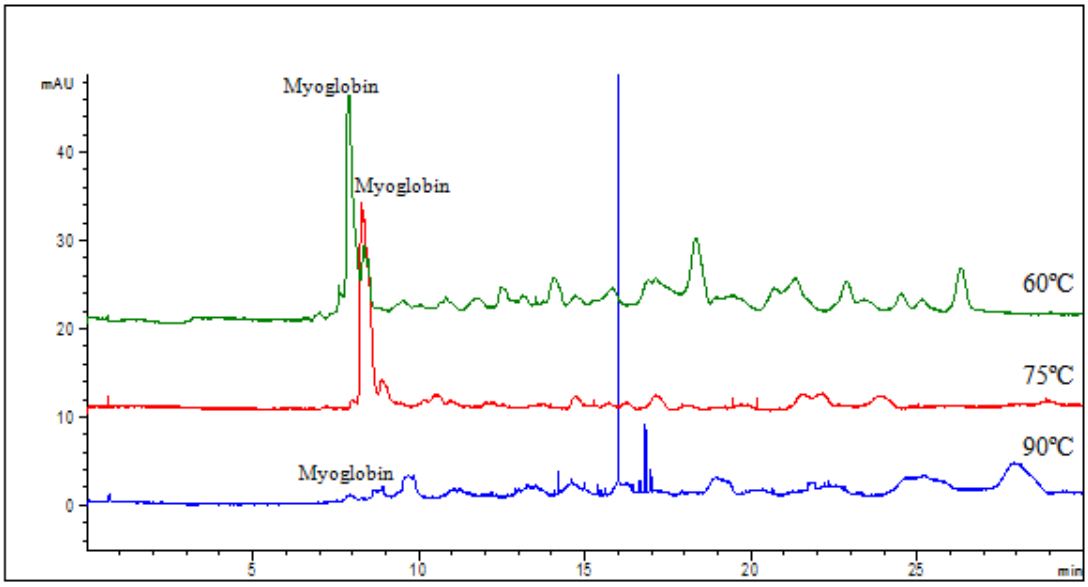

Figure 38. *Electropherograms showing peptide maps of myoglobin (2 mg/ml) at three different temperatures of denaturation: 60, 75 and 90ºC. The digestion was made with GA-CT at 37ºC for 240 min and the enzyme to substrate ratio was 18:1 (mol:mol). The separation conditions were the same as shown in Fig. 33.*

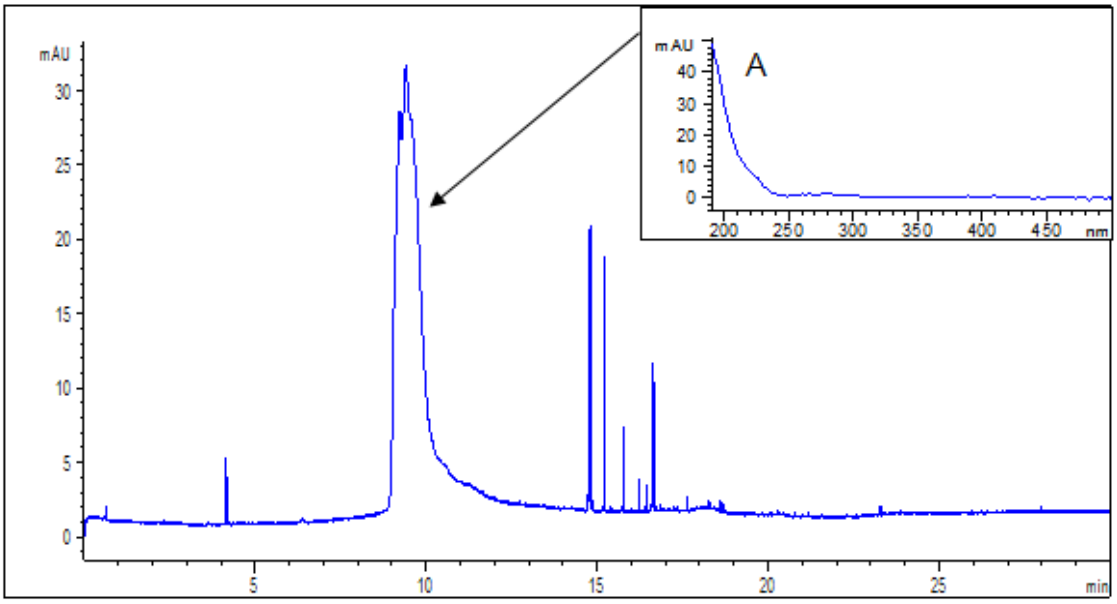

Figure 39. *Electropherogram showing the blank digestion of 0.013 mM myoglobin heat-denatured at 90ºC, then incubated with no CT at 37ºC for 240 min. The inset, Fig. 39A, presents the UV absorbance spectrum of myoglobin from the DAD detector. The separation conditions were the same as shown in Fig. 33.*

3.5.4. Myoglobin digestion by soluble chymotrypsin

As with the BSA, the aim in this section was to evaluate the effect on peptide maps of three different heat-induced denaturation temperatures of myoglobin prior to digestion with 0.0013 mM soluble CT. The concentration of myoglobin was 0.013 mM (2 mg/ml) and the enzyme:substrate ratio was 1:10 (mol/mol).

The results, as expected, were an increase in digestion products and a decrease in substrate when the temperature of denaturation was increased, as shown in Fig. 40. The heating of substrate leads to its unfolding and increases access to the digestion sites of the enzyme in its soluble form. There was unfortunately a large shift in EOF in the 90ºC experiment, which may be caused by the fact the sample was analyzed by CE two weeks after the other two (60 and 75ºC) in Fig. 40.

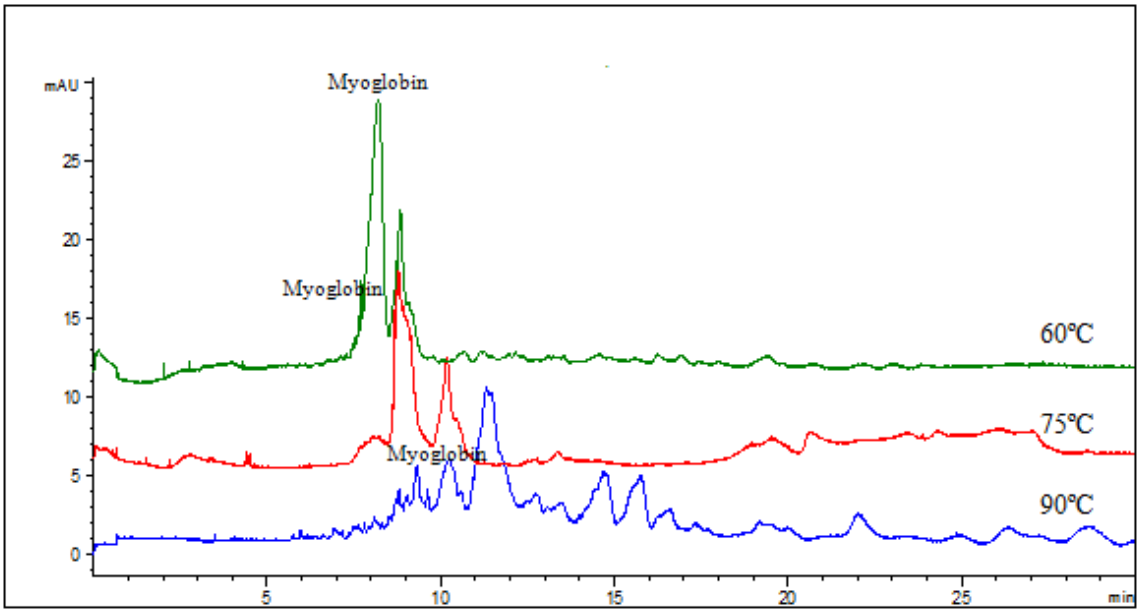

Figure 40. *Electropherograms showing peptide maps of myoglobin (0.013 mM) at three different temperatures of heat-induced denaturation: 60, 75 and 90 ºC. The digestion was made with soluble CT at 37ºC for 240 min and the enzyme to substrate ratio was 1:10 (mol:mol). The separation conditions were the same as in Fig. 33.*

The use of free (soluble) CT means that autoproteolysis peaks from the enzyme are expected and may overlap with myoglobin peptides. Therefore, blank experiments consisting

of the injection of the digestion solution without myoglobin substrate were carried out. The digestion followed the same 4 steps as described in Chapter 2 and the heat-denatured solution consisted of buffer only, without substrate, digested with free CT after simulated denaturation at 90ºC. Fig. 41 shows the result of the blank digestion, with CT eluting around 11.5 min. Few autoproteolysis peptides are seen, mostly just the enzyme peak, because the CT concentration is so small compared with the autoproteolysis experiments presented at the beginning of Chapter 3.

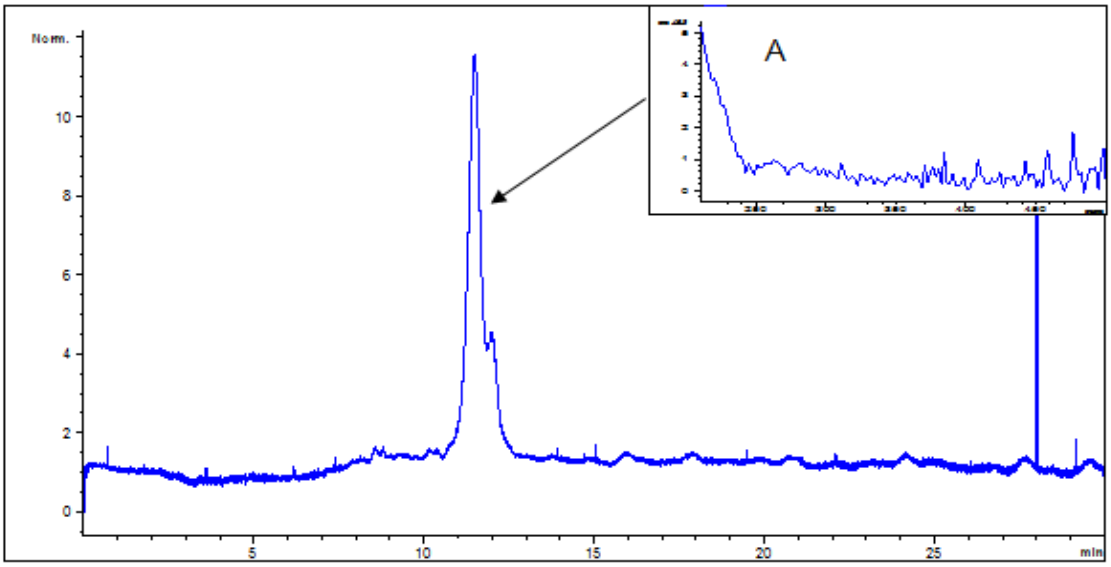

Figure 41. *Electropherogram of a blank experiment (no myoglobin substrate) heated at 90ºC and incubated with soluble CT at 37ºC for 240 min. The separation conditions were the same as shown in Fig. 33. Panel A (inset) is the DAD spectrum of the CT peak.*

The results in Fig. 40 show that the height of the myoglobin peak decreases with increasing the denaturation heating from 60 to 90ºC before digestion with soluble CT. However, increasing the denaturation temperature from 60 to 75ºC did not improve peptide mapping. This is probably because the denaturation state of myoglobin is not unfolded enough at 75ºC. Heating of myoglobin at 90ºC for 45 min before digestion led to a large decrease of the myoglobin peak, which is better revealed in Fig. 42, where the myoglobin digest is overlaid with the CT blank experiment in Fig. 41 (i.e., buffer denatured at 90ºC then

incubated with free CT). Fig. 40 also shows an improved peptide map for the 90°C denatured myoglobin sample compared to the other two samples heat-denatured at 60 and 75°C.

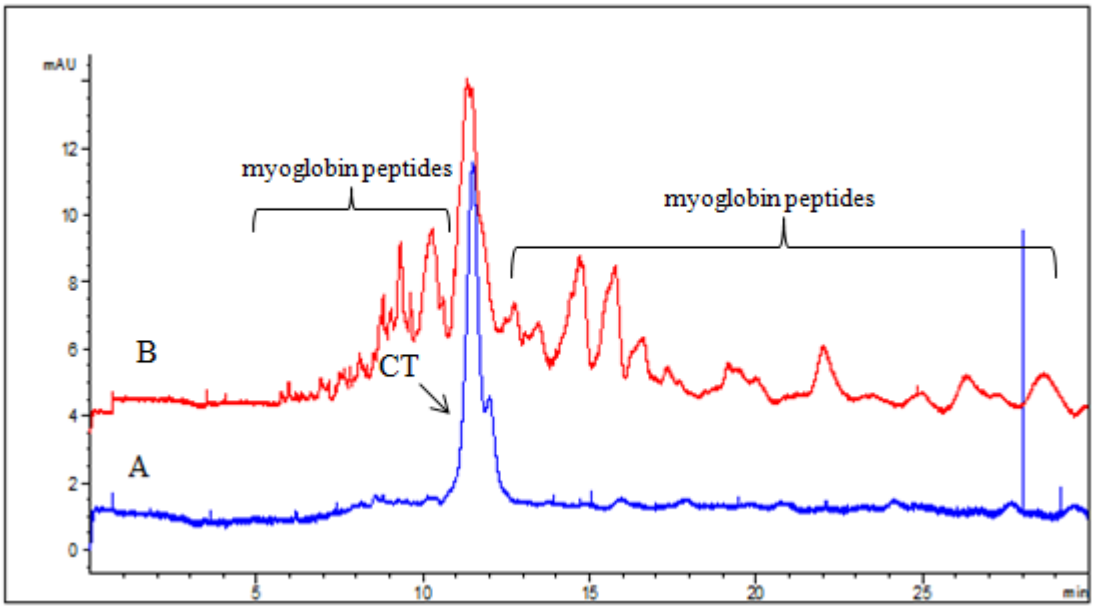

Figure 42. *Electropherograms showing peptide maps of myoglobin (0.013 mM) heat-denatured at 90ºC (Panel B), and the blank experiment (no myoglobin; Panel A). Both digestions were made at 37ºC for 240 min. The separation conditions were the same as in Fig. 33.*

According to the results above, heat-induced denaturation at 90ºC for myoglobin permitted its partial digestion with soluble CT. The GA-immobilized CT did not yield as good a peptide map for myoglobin, even though there was evidence of digestion due to the reduced substrate remaining after digestion. It should be noted that all experiments were repeated in triplicate and results were consistent within the precision shown in Table 4.

Chapter 4. Conclusions and Future Work

The present research aimed to investigate some of the experimental parameters related to the enzyme and the protein substrate to improve peptide mapping with immobilized chymotrypsin (CT). CT was immobilized by cross-linking it with glutaraldehyde (GA) using a procedure similar to that described previously by our group [22, 23]. In the present project, autoproteolysis of soluble CT and GA-CT were investigated under six different conditions of time (30 and 240 min) and temperature (4, 24 and 37ºC), whereas traditional enzymatic digestion is done overnight (16 h) at 37ºC. To improve peptide mapping, some parameters were evaluated including the buffer for digestion, the use of SDS to improve reproducibility of capillary conditioning, the method to stop digestion, and the concentration of the CE separation buffer, all of which affect peptide mapping by CE. These parameters were explored by following CT autoproteolysis with both free (soluble) and immobilized CT and comparing peptide maps obtained by CE with UV absorbance detection. The results showed that ammonium bicarbonate, pH 8, was the better digestion buffer than Tris-HCl because it resulted in better CE separation with more digestion peaks resolved. This may be an effect of sample ionic strength, but it was not investigated further. Tris-HCl had been used by our group for peptide mapping with immobilized trypsin [44]. The buffer selection is important because it affects enzyme digestion as well as separation of the peptides. For detection with mass spectrometry, buffer volatility is also an important aspect and thus ammonium bicarbonate is a good choice for future CE-MS experiments. When analyses of soluble CT autoproteolysis showed poor resolution and poor reproducibility in intensity of the peak heights, a modification of the capillary conditioning was done. It was found that adding a rinse step of 25 mM SDS after each separation improved the RSD of peak heights of the peptides by almost 3 times (from 85 to 30% RSD). Similarly, the method used to stop a digestion affects the peptide map when using CE separations, especially when it involves addition of strong acid. Therefore, the dry ice/acetone bath was selected for these experiments because the results showed better separation. In later experiments with the substrate BSA, it was noticed that the CE separation buffer concentration of 25 mM sodium phosphate (pH 2.5) was too low so it was increased to 75 mM to improve resolution of the peptides.

After choosing the previous parameters (buffer for digestion, CE separation improvement, method for stopping the digestion), autoproteolysis of soluble and GA-immobilized CT was studied as a function of the different incubation times and temperatures

of the enzyme itself. The results showed that with increased time and temperature (i.e., 240 min for 24 or 37ºC), autoproteolysis of soluble CT increased, as expected. The comparison between autoproteolysis of soluble and immobilized CT confirmed that the immobilization reduces autoproteolysis. In other words, it confirms the thermal stability of the GA-CT.

To investigate heat-induced denaturation of substrate as a simple alternative to traditional chemical denaturation methods, which have been used successfully for digestion by GA-CT [22, 23], peptide mapping of two model substrates (BSA and myoglobin) was compared for soluble CT versus GA-CT. Prior to the digestion, 0.013 mM (2 mg/mL) BSA or myoglobin was denatured by heating at different temperatures (60, 75, and 90ºC) for 45 min. After denaturation, protein substrate was incubated at 37ºC for 240 min with free (soluble) CT with an enzyme to substrate ratio of 1:10 and with GA-CT with enzyme to substrate ratio of 18:1. The results showed that heat-induced denaturation of BSA up to 90ºC did not produce much digestion product (peptides) when immobilized CT or even free CT was used. This is due to the fact that BSA is still too highly folded as a substrate to react with the active site of CT and that it is necessary to break disulfide bonds chemically rather than just use heat-induced denaturation of BSA, which is a reversible process on cooling. On the other hand, digestion of 90ºC heat-induced denatured BSA with soluble CT decreased the substrate peak in the peptide map and this could be explained by the small percentage of unfolding of BSA that allowed soluble CT access for cleavage at a few sites.

Under the same conditions as for BSA experiments, the peptide maps of myoglobin, a smaller protein substrate without disulfide bonds, were compared for digestion by immobilized and soluble CT after heat-induced denaturation. Again, GC-CT was not able to adequately digest myoglobin even after heat-induced denaturation at 90ºC. Digestion of myoglobin with soluble CT did not improved peptide mapping when substrate was heated to 75ºC, whereas heating at 90ºC improved the digestion of myoglobin by soluble CT and detection of peptides was achieved.

During the present study, GA-CT was evaluated for its thermal stability and potential to provide peptide maps for protein substrates denatured only by heating. It would be interesting to try immobilizing the enzyme with different cross-linking agents to evaluate the

effects on digestion efficiency, or to add extra non-enzyme spacers to the GA cross-linking method to make the enzyme particles more accessible to the substrate. Future studies should also involve improving the CE separation conditions to remove the protein that adsorbs onto the capillary wall, causing EOF changes, and to improve the separations. The addition of SDS capillary rinsing to the separation method was a noticeable advantage, but it requires rigorous removal before injection, which was not done in the pre-conditioning experiment. The use of permanently coated capillaries should also be interesting to try. This would be important for CE coupled with MS detection, which would be used for identification of peptides by their mass, and not just for comparison of peptide maps due to a change in one or two peptides.

Chapter 5. References

[1] Pandey, A.; Mann, M., Proteomics to study genes and genomes. *Nature*, (2000) ***405***, 837.

[2] Aebersold, R.; Goodlett, D. R, Mass spectrometry in proteomics. *Chemical Reviews*, (2001) ***101***, 269.

[3] Honda, K.; Ono, M.; Shitashige, M.; Masuda, M.; Kamita, M.; Miura, N.; Yamada, T., Proteomic Approaches to the Discovery of Cancer Biomarkers for Early Detection and Personalized Medicine. *Japanese Journal of Clinical Oncology*, (2013) ***43***, 103.

[4] Guo, T.; Lee, C. S.; Wang, W.; Devoe, D. L.; Balgley, B. M., Capillary separations enabling tissue proteomics-based biomarker discovery. *Electrophoresis*, (2006) ***27***, 3523.

[5] Bakry, R.; Huck, C. W.; Najam-ul-Haq, M.; Rainer, M.; Bonn, G. K., Recent advances in capillary electrophoresis for biomarker discovery. *Journal of Separation Science*, (2007) ***30***, 192.

[6] Bonneil, E.; Mercier, M.; Waldron, K. C., Reproducibility of a solid-phase trypsin microreactor for peptide mapping by capillary electrophoresis. *Analytica Chimica Acta*, (2000) ***404***, 29.

[7] Migneault, I.; Dartiguenave, C.; Vinh, J.; Bertrand, M. J.; Waldron, K. C., Two glutaraldehyde-immobilized trypsin preparations for peptide mapping by capillary zone electrophoresis, liquid chromatography, and mass spectrometry. *Journal of Liquid Chromatography & Related Technologies*, (2008) ***31***, 789.

[8] Voet, D.; Voet, J. G.; Pratt, C. W., *Fundamentals of Biochemistry*, 3rd Edition; Wiley & Sons, Inc: Hoboken, NJ, (2008); p 1099.

[9] Kotz, J. C; Treichel, P. M; Townsend, J. R., *Chemistry & Chemical Reactivity*, 7th Edition; Mary Finch: Belmont, CA, (2006).

[10] Harris, D. C., *Quantitative Chemical Analysis*, 7th Edition; W. H. Freeman and company: New York, (2007); p 663.

[11] Edman, P., Method For Determination Of The Amino Acid Sequance In Peptides. *Acta Chemica Scandinavica*, (1950) ***4***, 283.

[12] Berg, J. M; Tymoczko, J. L; Stryer, L., *Biochemistry*, 5th edition; W.H. Freeman: (2002); p 1050.

[13] Chen, M.; Waldron, K. C.; Zhao, Y. W.; Dovichi, N. J., Micellar capillary electrophoresis separaetion and thermo-optical absorbancy detection of products from manual peptide sequencing. *Electrophoresis*, (1994) ***15***, 1290.

[14] Sun, D.; Wang, N.; Li, L., In-Gel Microwave-Assisted Acid Hydrolysis of Proteins Combined with Liquid Chromatography Tandem Mass Spectrometry for Mapping Protein Sequences.*Analytical Chemistry*, (2014) ***86***, 600.

[15] Xie, H.; Gilar, M.; Gebler, J. C., Characterization of Protein Impurities and Site-Specific Modifications Using Peptide Mapping with Liquid Chromatography and Data Independent Acquisition Mass Spectrometry.*Analytical Chemistry*, (2009) ***81***, 5699.

[16] Wang, S.; Bao, H.; Zhang, L.; Yang, P. Y.; Chen, G., Infrared-assisted on-plate proteolysis for MALDI-TOF-MS peptide mapping.*Analytical Chemistry*, (2008) ***80***, 5640.

[17] Fagerquist, C. K.; Miller, W. G.; Harden, L. A.; Bates, A. H.; Vensel, W. H.; Wang, G. L.; Mandrell, R. E., Genomic and proteomic identification of a DNA-binding protein used in the "fingerprinting" of Campylobacter species and strains by MALDI-TOF-MS protein biornarker analysis.*Analytical Chemistry*, (2005) ***77***, 4897.

[18] Wheat, T. E.; Young, P. M.; Astephen, N. E., Use of capillary electrophoresis for the detection of single- residue substitutions in peptide mapping. *Journal of Liquid Chromatography*, (1991) ***14***, 987.

[19] Ross, G. A.; Lorkin, P.; Perrett, D., Separation and tryptic digest mapping of normal and variant haemoglobins by capillary electrophoresis. *Journal of Chromatography*, (1993) ***636***, 69.

[20] Yang, Y.; Boysen, R. I.; Harris, S. J.; Hearn, M. T. W., Peptide mapping with mobile phases of intermediate pH value using capillary reversed-phase high-performance liquid chromatography/electrospray ionisation tandem mass spectrometry. *Journal of Chromatography A*, (2009) ***1216***, 3767.

[21] Bergquist, J.; Palmblad, M.; Wetterhall, M.; Hakansson, P.; Markides, K. E., Peptide mapping of proteins in human body fluids using electrospray ionization Fourier transform ion cyclotron resonance mass spectrometry. *Mass Spectrometry Reviews*, (2002) ***21***, 2.

[22] Nguyen, Q. V., Développement d'un microréacteur à base d'enzyme protéolytique réticulée avec le glutaraldéhyde pour la cartographie peptidique, M.Sc., Thesis, Université de Montréal (2008).

[23] Ghafourifar, G.; Fleitz, A.; Waldron, K. C., Development of glutaraldehyde-crosslinked chymotrypsin and an in situ immobilized enzyme microreactor with peptide mapping by capillary electrophoresis. *Electrophoresis*, (2013) ***34***, 1804.

[24] Amankwa, L. N.; Kuhr, W. G., Trypsin- modified- silica capillary microreactor for peptide mapping by capillary zone electrophoresis. *Analytical Chemistry*, (1992) ***64***, 1610.

[25] Krenkova, J. Foret, F., Immobilized microfluidic enzymatic reactors. *Electrophoresis*, (2004) ***25***, 3550.

[26] Lin, Y.; Chen, Y.; Yang, X.; Xu, D.; Liang, S., Proteome analysis of a single zebrafish embryo using three different digestion strategies coupled with liquid chromatography-tandem mass spectrometry. *Analytical Biochemistry*, (2009) ***394***, 177.

[27] Guzman, N. A.; Park, S. S.; Schaufelberger, D.; Hernandez, L.; Paez, X.; Rada, P.; Tomlinson, A. J.; Naylor, S., New approaches in clinical chemistry: on-line analyte concentration and microreaction capillary electrophoresis for the determination of drugs, metabolic intermediates, and biopolymers in biological fluids. *Journal of Chromatography B*, (1997) ***697***, 37.

[28] Hu, S.; Dovichi, N. J., Capillary electrophoresis for the analysis of biopolymers. *Analytical Chemistry*, (2002) ***74***, 2833.

[29] Nielsen, R. G.; Riggin, R. M.; Rickard, E. C., Cpillary zone electrophoresis of peptide-fragments from trypsin digestion of biosynthetic human growth-hormone. *Journal of Chromatography*, (1989) ***480***, 393.

[30] Nielsen, R. G.; Rickard, E. C., Method optimization in capillary zone electrophoresis analysis of hGH tryptic diges fragments. *Journal of Chromatography*, (1990) ***516***, 99.

[31] Bujacz, A.; Bujacz, G., Crystal Sturacture of Bovne Serum Albumin, In (2014-02-11).

[32] Tanaka, N.; Nishizawa, H.; Kunugi, S., Structure of pressure-induced denatured state of human serum albumin: A comparison with the intermediate in urea-induced denaturation. *Biochimica et Biophysica Acta-Protein Structure and Molecular Enzymology*, (1997) ***1338***, 13.

[33] Iwakura, M.; Nakamura, D.; Takenawa, T.; Mitsuishi, Y., An approach for protein to be completely reversible to thermal denaturation even at autoclave temperatures. *Protein Engineering*, (2001) ***14***, 583.

[34] Shin, H. C.; Scheraga, H. A., Effect of protein disulfide isomerase on the regeneration of bovine ribonuclease A with dithiothreitol.*Febs Letters*, (1999) ***456***, 143.

[35] Michaux, C.; Pomroy, N. C.; Prive, G. G., Refolding SDS-denatured proteins by the addition of amphipathic cosolvents. *Journal of Molecular Biology*, (2008) ***375***, 1477.

[36] Bennion, B. J.; Daggett, V., The molecular basis for the chemical denaturation of proteins by urea. *Proceedings of the National Academy of Sciences of the United States of America*, (2003) ***100***, 5142.

[37] Patel, S.; Chaffotte, A. F.; Amana, B.; Goubard, F.; Pauthe, E., In vitro denaturation-renaturation of fibronectin. Formation of multimers disulfide-linked and shuffling of intramolecular disulfide bonds. *International Journal of Biochemistry & Cell Biology*, (2006) ***38***, 1547.

[38] Krenkova, J.; Kleparnik, K.; Foret, F., Capillary electrophoresis mass spectrometry coupling with immobilized enzyme electrospray capillaries. *Journal of Chromatography A*, (2007) ***1159***, 110.

[39] Peterson, D. S.; Rohr, T.; Svec, F.; Frechet, J. M. J., High-throughput peptide mass mapping using a microdevice containing trypsin immobilized on a porous polymer monolith coupled to MALDI TOF and ESI TOF mass spectrometers. *Journal of Proteome Research*, (2002) ***1***, 563.

[40] Rosenfeld, J.; Capdevielle, J.; Guillemot, J. C.; Ferrara, P., In-gel digestion of proteins for internal sequence- analysis after 1-dimensional or 2-dimensional gel-electrophoresis *Analytical Biochemistry*, (1992) ***203***, 173.

[41] Gevaert, K.; Vandekerckhove, J., Protein identification methods in proteomics. *Electrophoresis*, (2000) ***21***, 1145.

[42] Calleri, E.; Temporini, C.; Perani, E.; Stella, C.; Rudaz, S.; Lubda, D.; Mellerio, G.; Veuthey, J. L.; Caccialanza, G.; Massolini, G. , Development of a bioreactor based on trypsin immobilized on monolithic support for the on-line digestion and identification of proteins. *Journal of Chromatography A*, (2004) ***1045***, 99.

[43] Migneault, I.; Dartiguenave, C.; Vinh, J.; Bertrand, M. J.; Waldron, K. C., Comparison of two glutaraldehyde immobilization techniques for solid-phase tryptic peptide mapping of human hemoglobin by capillary zone electrophoresis and mass spectrometry. *Electrophoresis*, (2004) ***25***, 1367.

[44] Dartiguenave, C.; Hamad, H.; Waldron, K. C., Immobilization of trypsin onto 1,4-diisothiocyanatobenzene-activated porous glass for microreactor-based peptide mapping by capillary electrophoresis: Effect of calcium ions on the immobilization procedure. *Analytica Chimica Acta*, (2010) ***663***, 198.

[45] Sheldon, R. A., Enzyme immobilization: The quest for optimum performance. *Advanced Synthesis & Catalysis*, (2007) ***349***, 1289.

[46] Wiseman, A., *Handbook of Enzyme Biotechnology*, 2nd Edition; Wiley & Sons: Chichester, UK (1985).

[47] Goradia, D.; Cooney, J.; Hodnett, B. K.; Magner, E., Characteristics of a mesoporous silicate immobilized trypsin bioreactor in organic media. *Biotechnology Progress*, (2006) ***22***, 1125.

[48] Wu, J.; Luan, M.; Zhao, J., Trypsin immobilization by direct adsorption on metal ion chelated macroporous chitosan-silica gel beads. *International Journal of Biological Macromolecules*, (2006) ***39***, 185.

[49] Wu, H. L.; Tian, Y. P.; Liu, B. H.; Lu, H. J.; Wang, X. Y.; Zhai, J. J.; Jin, H.; Yang, P. Y.; Xu, Y. M.; Wang, H. H., Titania and alumina sol-gel-derived microfluidics enzymatic-reactors for peptide mapping: Design, characterization, and performance. *Journal of Proteome Research*, (2004) ***3***, 1201.

[50] Porter, D. H.; Swaisgood, H. E.; Catignani, G. L., Characterization of an immobilized digestive enzyme-system for determination of protein digestibility *Journal of Agricultural and Food Chemistry*, (1984) ***32***, 334.

[51] Zhang, Y., Development of an enzyme immobilization platform based on microencapsulation for paper-based biosensors, Ph.D., Thesis, University de montreal (2011).

[52] Veledo, M. T.; Pelaez-Lorenzo, C.; Gonzalez, R.; de Frutos, M.; Diez-Masa, J. C. , Protein fingerprinting of Staphylococcus species by capillary electrophoresis with on-capillary derivatization and laser-induced fluorescence detection.*Analytica Chimica Acta*, (2010) ***658***, 81.

[53] Hu, S. ; Ye, M. L.; Schoenherr, R. M.; Dovichi, N. J., On-line protein digestion and peptide mapping by capillary electrophoresis with post-column labeling for laser-induced fluorescence detection. *Electrophoresis*, (2004) ***25***, 1319.

[54] Migneault, I.; Dartiguenave, C.; Bertrand, M. J.; Waldron, K. C., Glutaraldehyde: behavior in aqueous solution, reaction with proteins, and application to enzyme crosslinking.*Biotechniques*, (2004) ***37***, 790.

[55] Mohanta, K.; Pal, A. J.; Roy, S.; Das, P.K., A control over accessibility of immobilized enzymes through porous coating layer. *Journal of Colloid and Interface Science*, (2006) ***304***, 329.

[56] Torabi, S. F.; Khajeh, K.; Ghasempur, S.; Ghaemi, N.; Siadat, S. O. R., Covalent attachment of cholesterol oxidase and horseradish peroxidase on perlite through silanization: Activity, stability and co-immobilization. *Journal of Biotechnology*, (2007) ***131***, 111.

[57] Stroink, T.; Ortiz, M. C.; Bult, A.; Lingeman, H.; de Jong, G. J.; Underberg, W. J. M., On-line multidimensional liquid chromatography and capillary electrophoresis systems for peptides and proteins.*Journal of Chromatography B-Analytical Technologies in the Biomedical and Life Sciences*, (2005) ***817***, 49.

[58] Picariello, G.; Iacomino, G.; Mamone, G.; Ferranti, P.; Fierro, O.; Gianfrani, C.; Di Luccia, A.; Addeo, F, Transport across Caco-2 monolayers of peptides arising from in vitro digestion of bovine milk proteins. *Food Chemistry*, (2013) ***139***, 203.

[59] Leadbeater, L.; Ward, F. B., Analysis of tryptic digests of bovine beta-casein by reversed-phase high-performance loquid-chromatography.*Journal of Chromatography*, (1987) ***397***, 435.

[60] Figeys, D.; Aebersold, R., Capillary electrophoresis of peptides and proteins at neutral pH in capillaries covalently coated with polyethyleneimine. *Journal of Chromatography B*, (1997) ***695***, 163.

[61] Castagnola, M.; Cassiano, L.; Rabino, R.; Rossetti, D. V.; Bassi, F. A., Peptide- mapping through the coupling of capillary electrophoresis and high - performance liquid - chromatography - map prediction of the tryptic of the tryptic digest of myoglobin. *Journal of Chromatography-Biomedical Applications*, (1991) ***572***, 51.

[62] Rickard, E. C.; Towns, J. K., Applications of capillary zone electrophoresis to peptide mapping. *High Resolution Separation and Analysis of Biological Macromolecules, Pt B*, (1996) ***271***, 237.

[63] Messana, I.; Rossetti, D. V.; Cassiano, L.; Misiti, F.; Giardina, B.; Castagnola, M., Peptide analysis by capillary (zone) electrophoresis. *Journal of Chromatography B*, (1997) ***699***, 149.

[64] Waldron, K. C., CHIM 6110 Special Topic Course Note in CE, In Université de Montréal, (2007).

[65] Landers, J. P., *Hand book of capillary electrophoresis*, 2 nd Edition; CRC Press, Inc: Boca Raton, Florida, (1994); p 649.

[66] Robert, W., *Practical Capillary Electrophoresis*, 2nd Edition; Academic Press: (2000).

[67] Shieh, I. F.; Lee, C. Y.; Shiea, J., Eliminating the interferences from TRIS buffer and SDS in protein analysis by fused-droplet electrospray ionization mass spectrometry.*Journal of Proteome Research*, (2005) ***4***, 606.

[68] Durst, R. A.; Staples, B. R., Tris/Tris.HCL - standard buffer for use in physiologic pH range.*Clinical Chemistry*, (1972) ***18***, 206.

[69] Zhang, N.; Chen, R.; Young, N.; Wishart, D.; Winter, P.; Weiner, J. H.; Li, Liang, Comparison of SDS- and methanol-assisted protein solubilization and digestion methods for Escherichia coli membrane proteome analysis by 2-D LC-MS/MS. *Proteomics*, (2007) ***7***, 484.

[70] Ghafourifar, G.; Fleury, B.; Fleitz, A.; Waldron, K. C., Immobilized enzyme microreactor development and optimization as evaluated by capillary electrophoretic peptide mapping, In *The 6th Annual Canadian National Proteomics Network Symposium*, Montreal, (2014).

[71] Baker, D. R., *Capillary Electrophoresis*, John Wiley & Sons, Inc: New York, (1995); p 244.

[72] Sykes, P. A.; Shiue, H. C.; Walker, J. R.; Bateman, R. C., Determination of myoglobin stability by visible spectroscopy. *Journal of Chemical Education*, (1999) ***76***, 1283.

Annex

Figures for the six conditions with effect time and temperature (37, 24 and 4^{O}C) for (30 min and 240min) in free CT

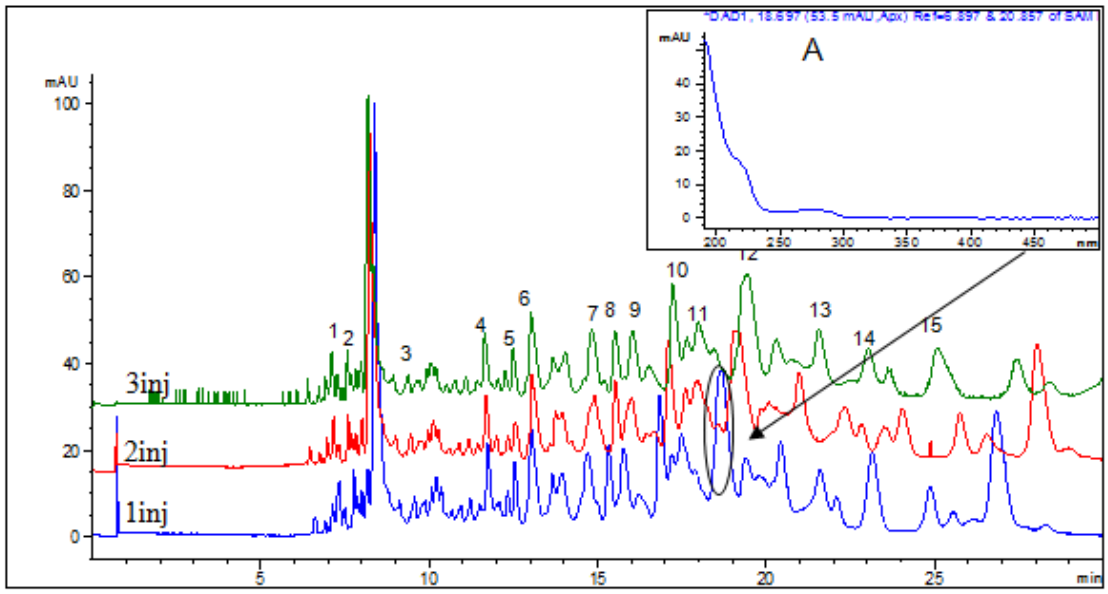

Figure A1. *Electropherograms showing peptide maps of three injections of 0.12 mM soluble CT autoproteolysis (same sample) with incubation time 240 min at 37ºC. The separation conditions were the same as shown in Fig. 15. Panel A is the UV-visible spectrum from the DAD detector of the peak circled in the electropherogram of the 1st injection.*

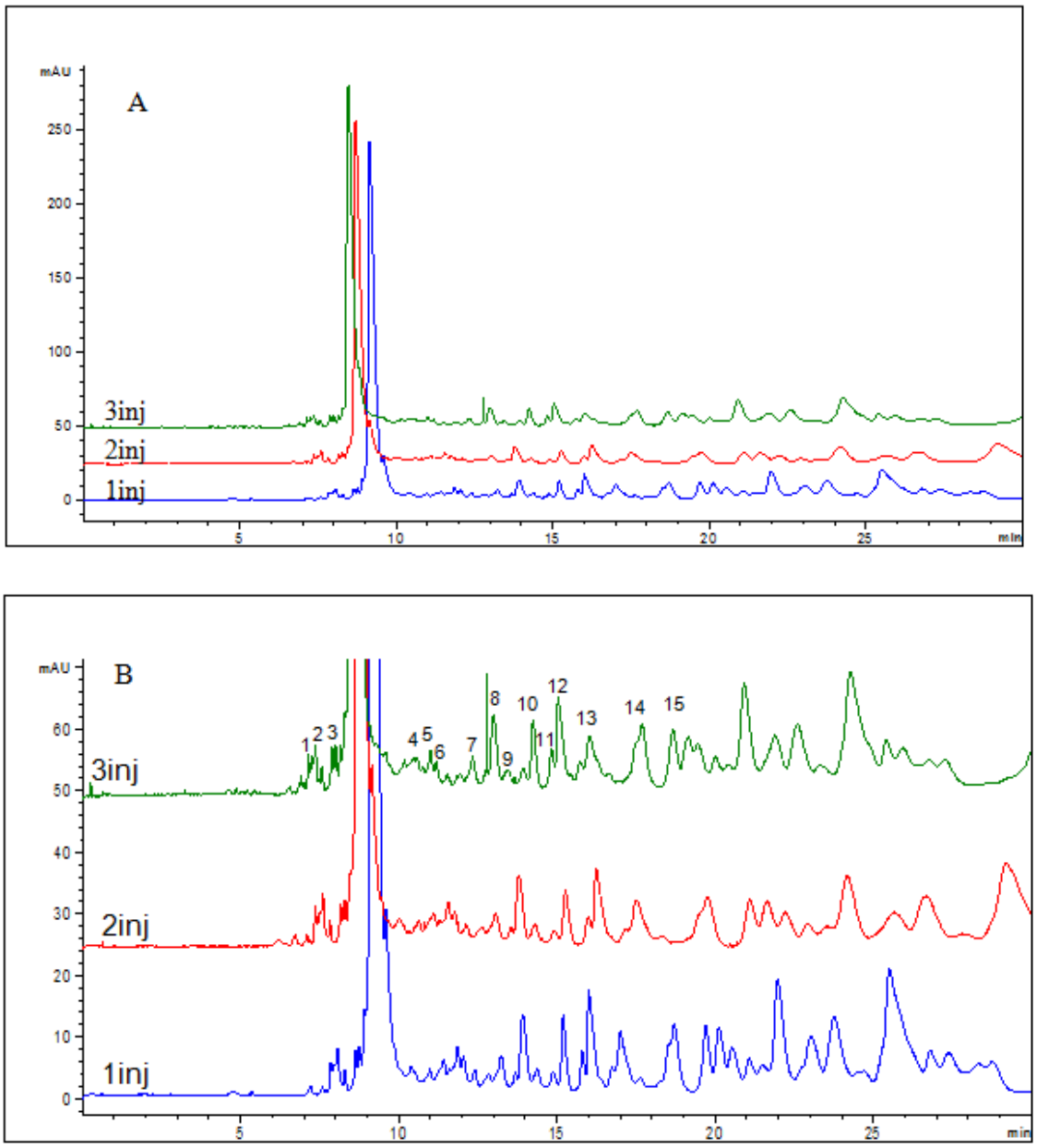

Figure A2. *Electropherograms showing peptide maps of three injection 0.12 mM soluble CT autoproteolysis (same sample) with incubation time 240 min at 24°C (A) and (B) is a zoomed-in version of the same electropherogram. The separation conditions were the same as shown in Fig. 15.*

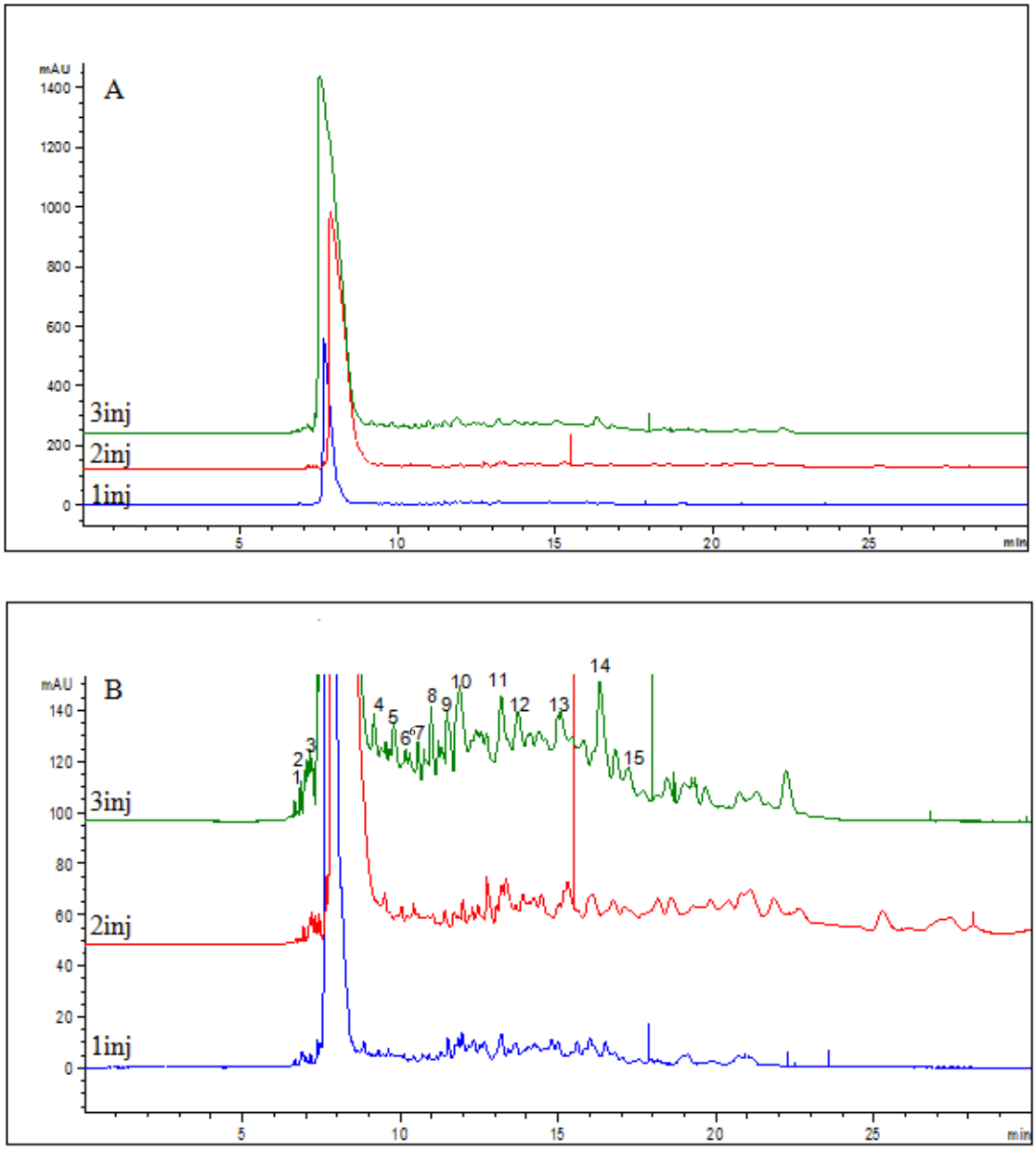

Figure A3. *Electropherograms showing peptide maps of three injection 0.12 mM soluble CT autoproteolysis (same sample) with incubation time 240 min at 4ºC and (B) is a zoomed-in version of the same electropherogram. The separation conditions were the same as shown in Fig. 15.*

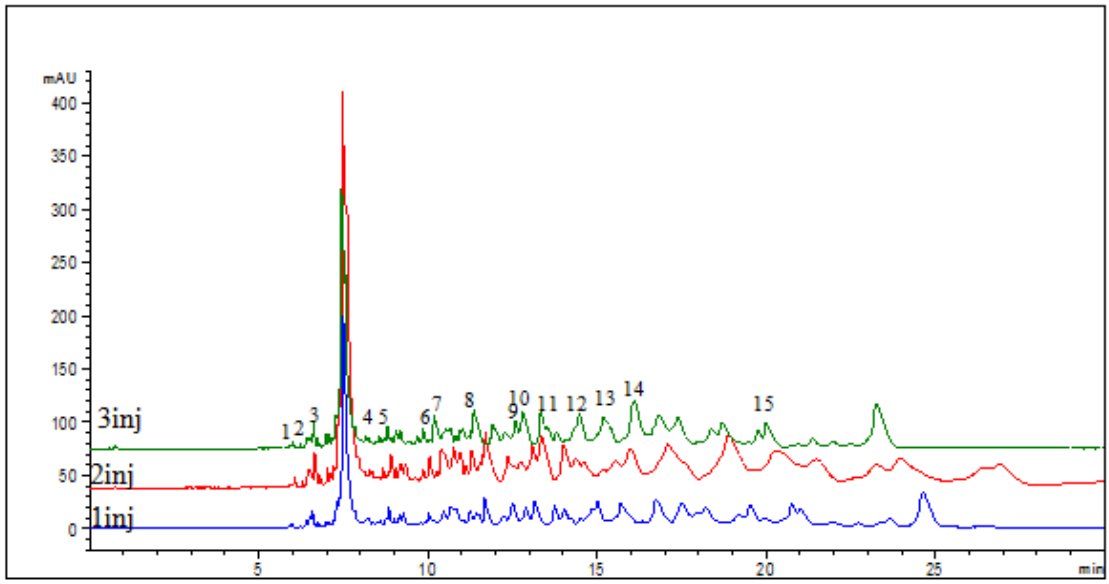

Figure A4. *Electropherograms showing peptide maps of three injections 0.12 mM soluble CT autoproteolysis (same sample) with incubation time 30 min at 37ºC. The separation conditions were the same as shown in Fig. 15.*

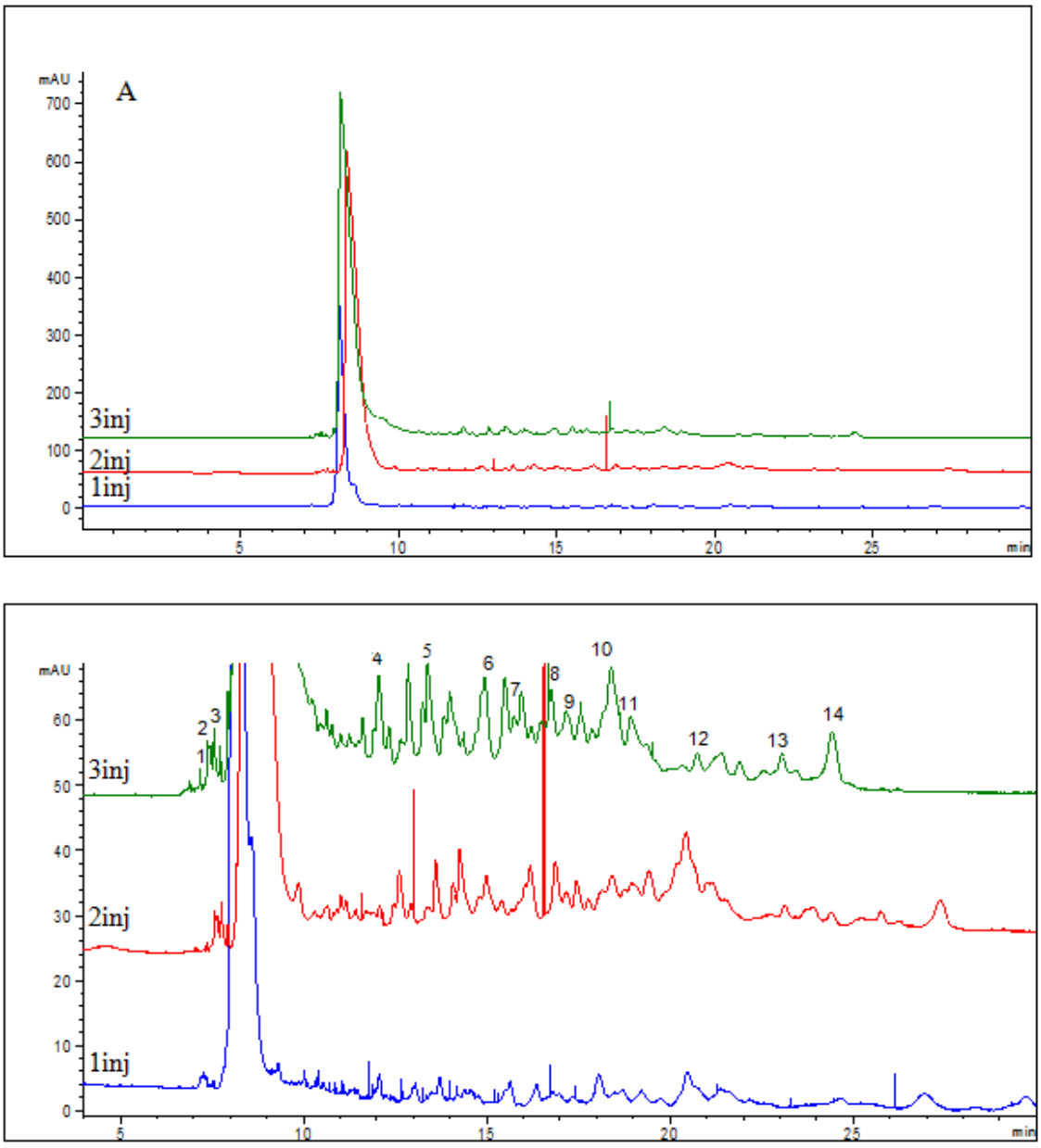

Figure A5. *Electropherograms showing peptide maps of three injection 0.12 mM soluble CT autoproteolysis (same sample) with incubation time 30 min at 24°C (A) and (B) is a zoomed-in version of the same electropherogram. The separation conditions were the same as shown in Fig. 15.*

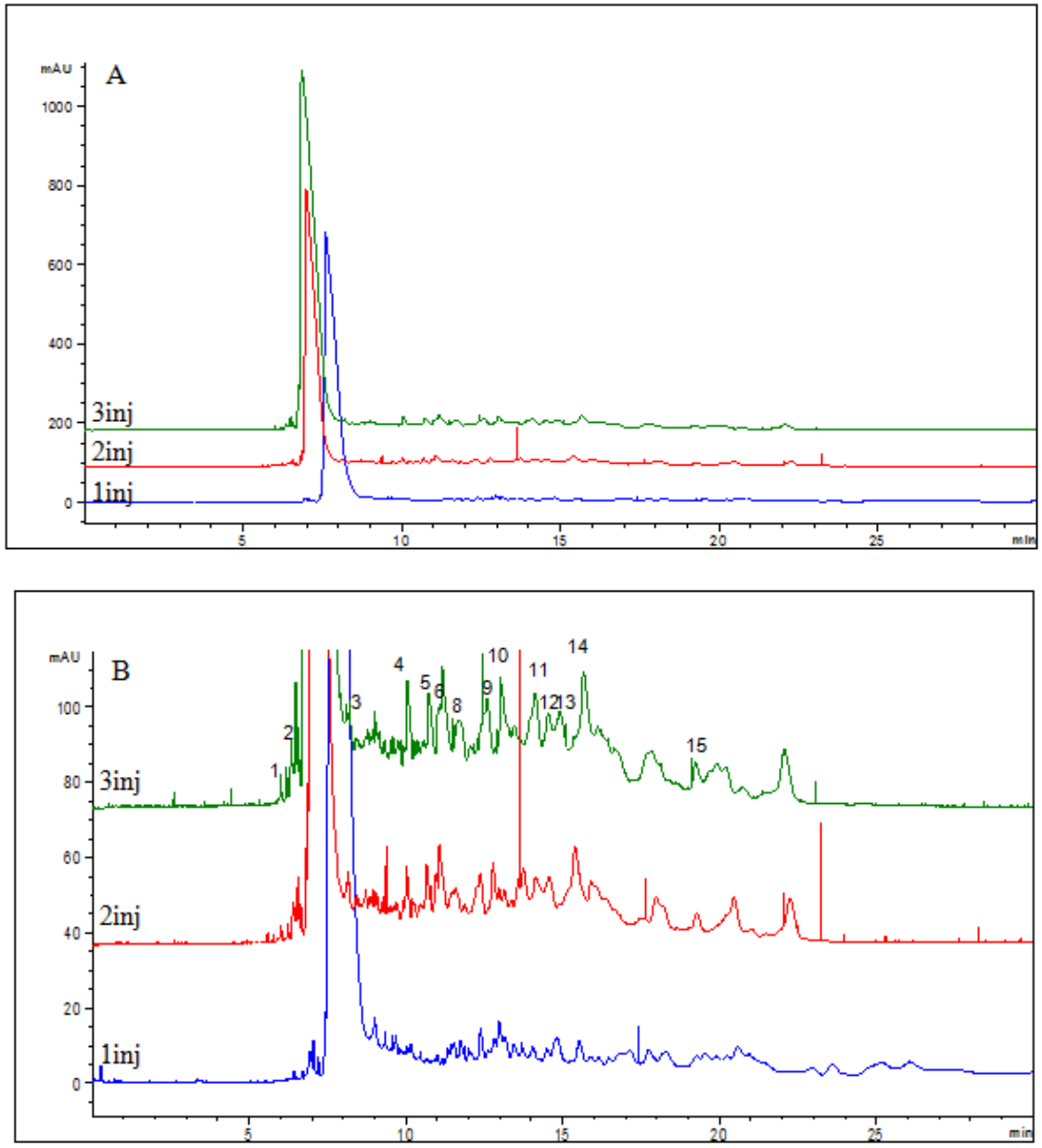

Figure A6. *Electropherograms showing peptide maps of three injection 0.12 mM soluble CT autoproteolysis (same sample) with incubation time 30 min at 4ºC (A) and (B) is a zoomed-in version of the same electropherogram. The separation conditions were the same as shown in Fig. 15.*

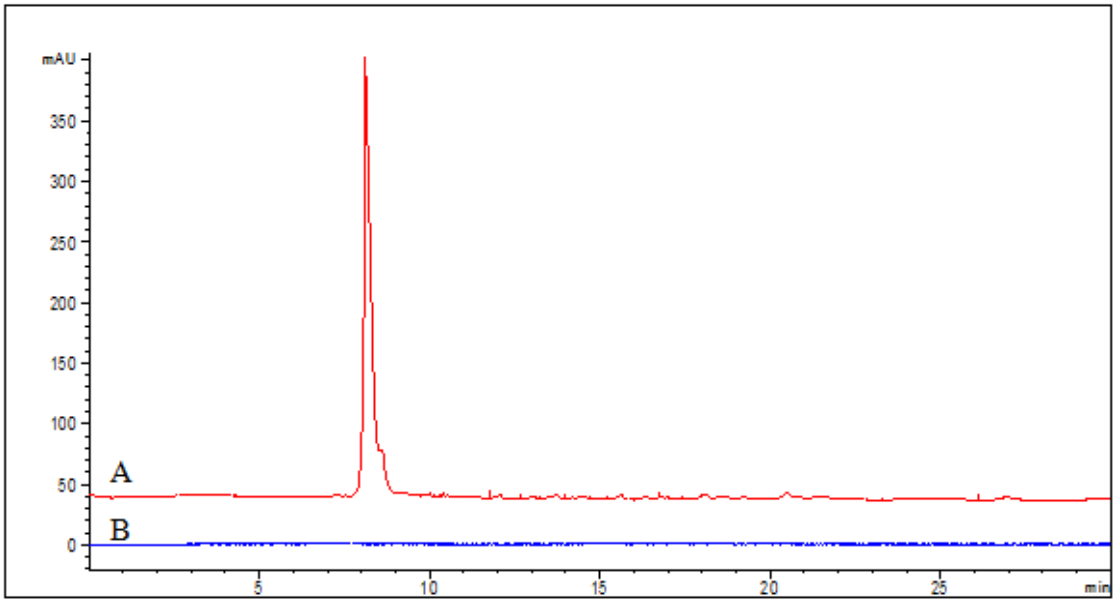

Figure A7. *Electropherograms showing comparison between autoproteolysis of free CT (A), and GA-CT (B). Both incubated at 24 ºC for 240 min and separation conditions were the same as in Fig. 15.*

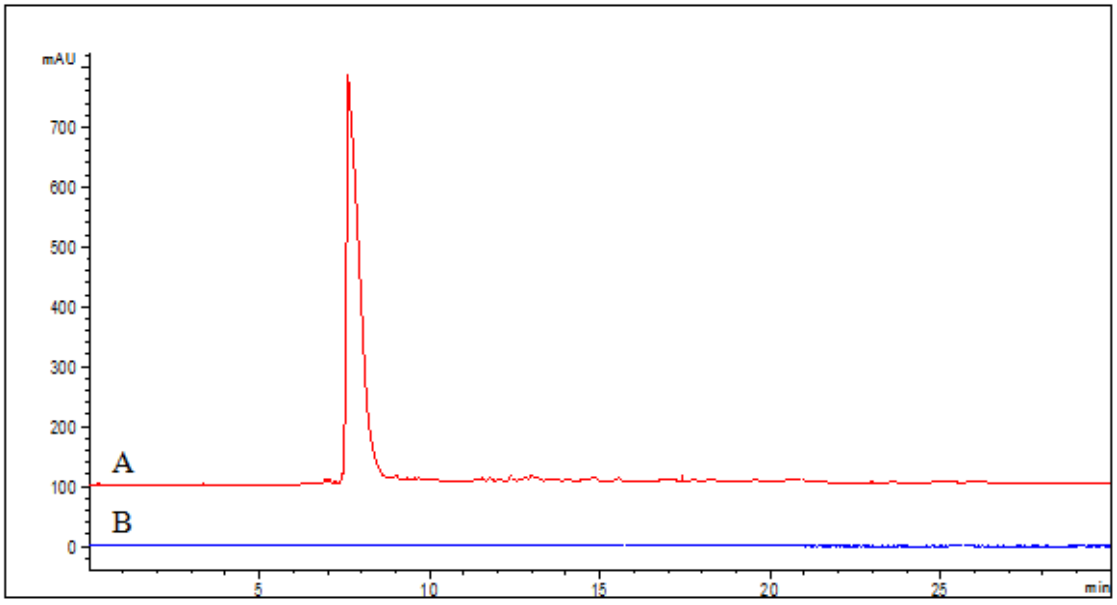

Figure A8. *Electropherograms show comparison between autoproteolysis of free CT (A), and GA-CT (B). Both were incubated at 4ºC for 240 min and the separation conditions were the same as in Figure 15.*

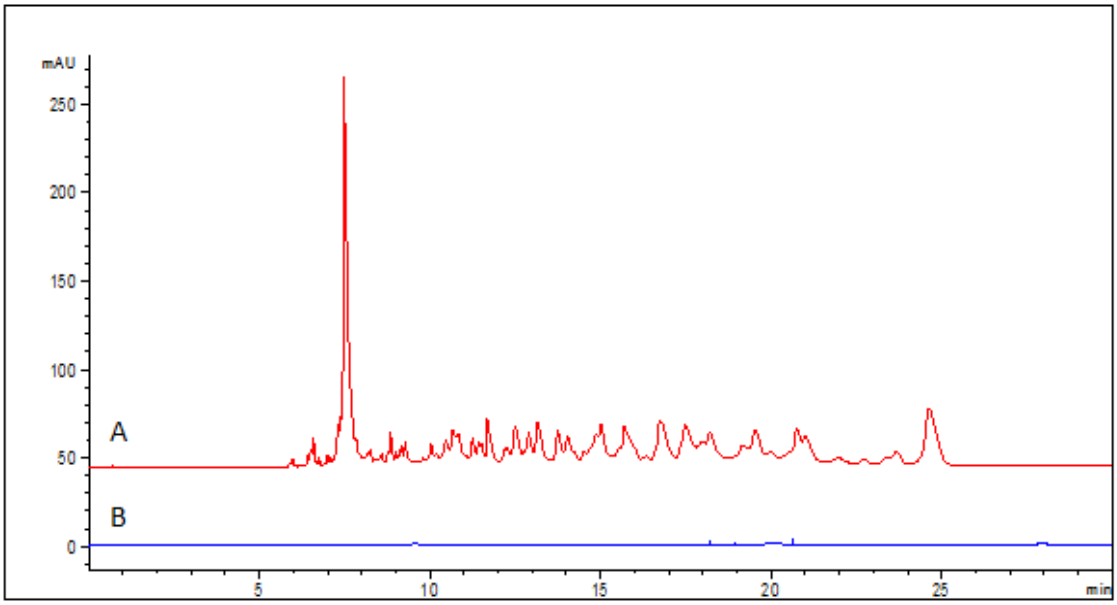

Figure A9. *Electropherograms show comparison between autoproteolysis of free CT (A), and GA-CT (B). Both were incubated at 37ºC for 30 min and the separation conditions were the same as in Fig. 15.*

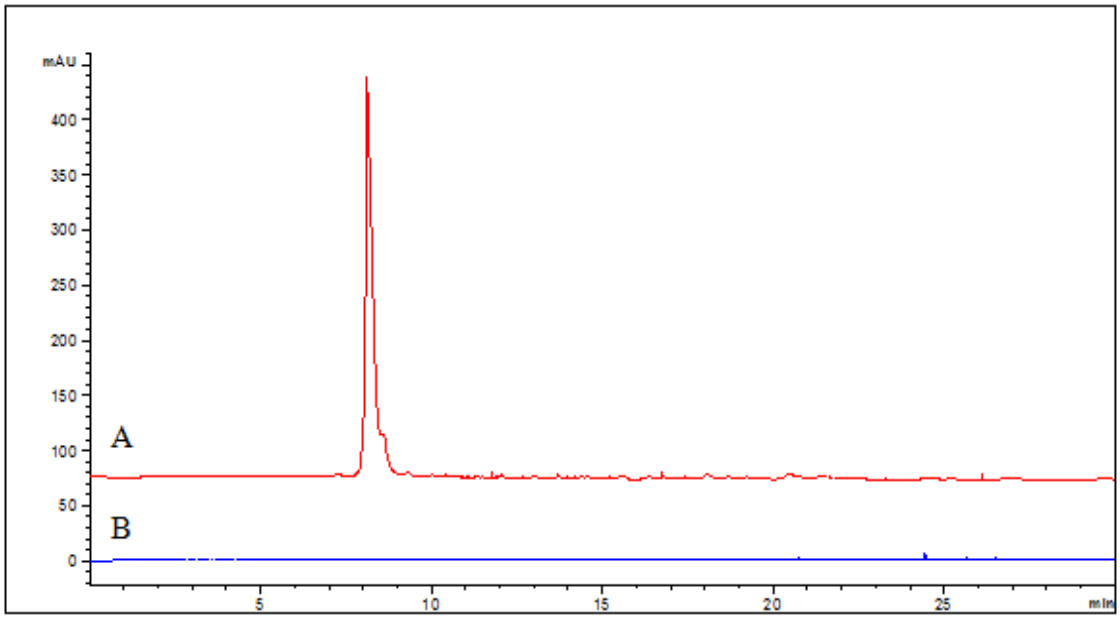

Figure A10. *Electropherograms show comparison between autoproteolysis of free CT (A), and GA-CT (B). Both were incubated at 24ºC for 30 min and the separation conditions were the same as in Fig. 15.*

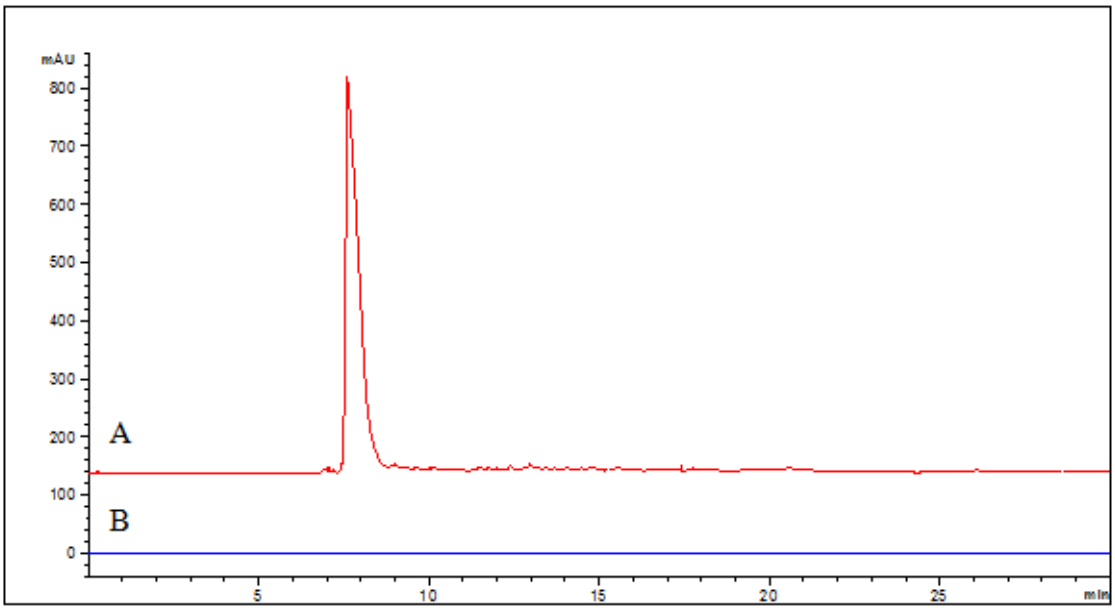

Figure A11. *Electropherograms show comparison between autoproteolysis of free CT (A), and GA-CT (B). Both were incubated at 4 ºC for 30 min and the separation conditions were the same as shown in Fig. 15.*

Figures of blank experiments were conducted for all denaturation temperature and are shown in Figures A-12 to 14 in the Annex A.

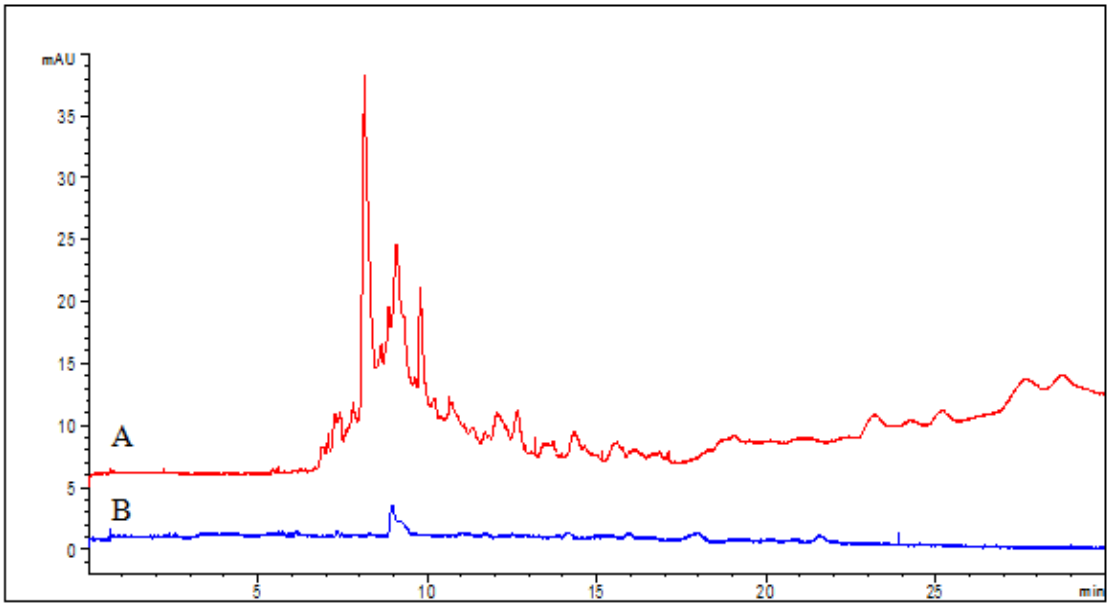

Figure A12. *Electropherograms showing peptide maps of heat-denaturated BSA (2 mg/ml) at 60ºC then digested for 240 min at 37ºC (A), and blank experiment without BSA (B), both cases digested with free CT (enzyme: substrate = 1:10). The separation conditions were the same as in Fig. 33.*

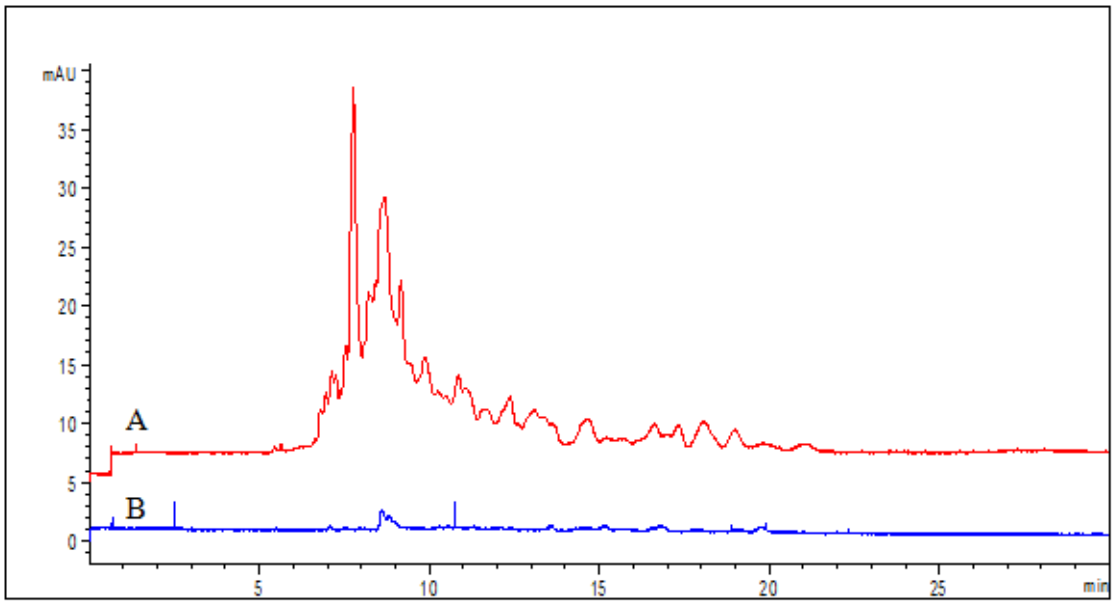

Figure A13. *Electropherograms showing peptide maps of heat-denaturated BSA (2 mg/ml) at 75ºC then digested for 240 min at 37ºC (A), and blank experiment without BSA (B), both cases digested with free CT (enzyme: substrate = 1:10). The separation conditions were the same as in Fig. 33.*

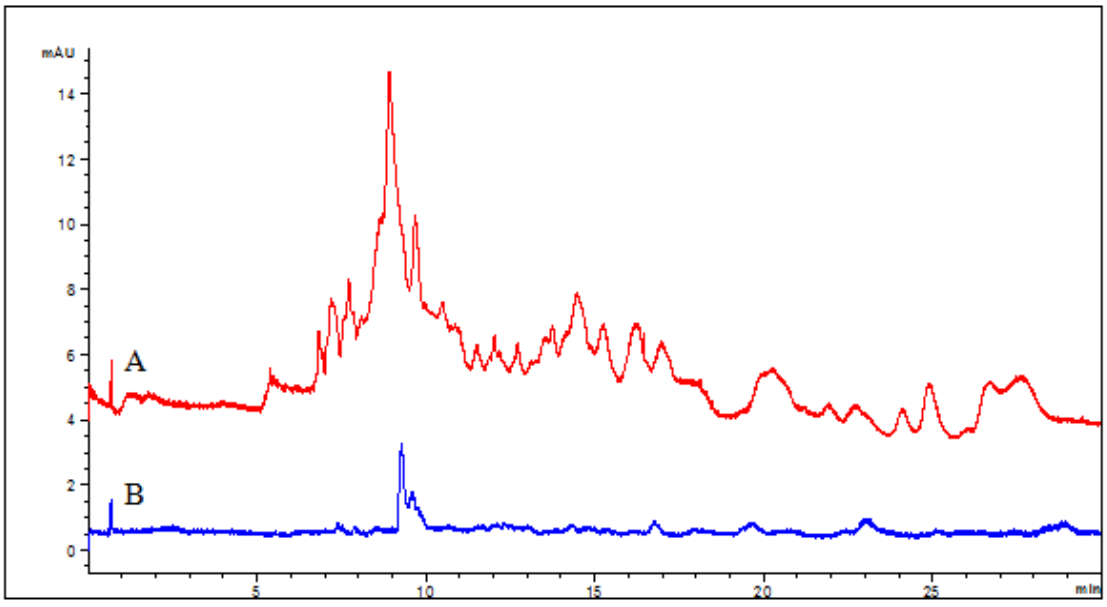

Figure A 14. *Electropherograms showing peptide maps of heat denaturated BSA (2 mg/ml)* ***14****at 90ºC (2 mg/ml) then digested for 240 min at 37ºC (A), and blank experiment without BSA (B), both cases digested with free CT (enzyme: substrate = 1:10). The separation conditions were the same as in Fig. 33.*

Table A1. Summary of CE reproducibility for 0.013 mM BSA digested with immobilized chymotrypsin (GA-CT).

BSA heat-denatured at:	**Retention time (min)**			**Peak height (mAU)**			**Peak height ratio**	
At 60ºC	**Peak 1**	**Peak 2**	**Peak BSA**	**Peak 1**	**Peak 2**	**Peak BSA**	**pk1/BSA**	**pk2/BSA**
Run #1	8.207	8.771	7.835	47.9	17.9	103.1	0.4	0.7
Run #2	9.079	9.795	9.145	17.7	14	31.5	0.5	0.4
Run #3	9.256	9.988	8.325	14.5	11	31.5	0.2	0.2
$\bar{x}$							0.4	0.2
S							0.1	0.1
RSD							32%	53%
At 75ºC	**Peak 1**	**Peak 2**	**Peak BSA**	**Peak 1**	**Peak 2**	**Peak BSA**	**P1/BSA**	**P2/BSA**
Run #1	9.082	10.118	8.659	29.5	3.5	33.8	0.8	0.1
Run #2	9.144	10.641	9.116	42.1	3.9	60.6	0.6	0.1
Run #3	9.810	11.315	9.44	32.4	8.5	49.2	0.6	0.1
$\bar{x}$							0.7	0.1
S							0.1	0.1
RSD							15%	48%
At 90ºC	**Peak 1**	**Peak 2**	**Peak BSA**	**Peak 1**	**Peak 2**	**Peak BSA**	**P1/BSA**	**P2/BSA**
Run #1	10.069	10.933	9.781	8.6	4.3	12.1	0.7	0.3
Run #2	9.13	9.901	8.813	20.8	5.7	17.1	1.2	0.3
Run #3	8.592	10.129	8.186	7.7	1.1	5.6	1.3	0.2
$\bar{x}$							1.1	0.2
S							0.3	0.1
RSD							31%	29%

Table A2. Summary of CE reproducibility for 0.013 mM BSA digested with free CT.

BSA heat-denatured at:	Retention time (min)			Peak heights (mAU)			Peak height ratio	
At 60ºC	**Peak 1**	**Peak 2**	**Peak BSA**	**Peak 1**	**Peak 2**	**Peak BSA**	**Pk1/BSA**	**Pk2/BSA**
Run #1	9.761	10.81	8.619	19.5	10.1	15.5	1.2	0.6
Run #2	9.079	9.795	8.145	17.7	14	31.5	0.6	0.3
Run #3	9.252	10.08	8.325	14.5	8.7	51.4	0.3	0.2
$\bar{x}$							0.7	0.4
S							0.4	0.2
RSD							57%	50%
At75ºC	**Peak 1**	**Peak 2**	**Peak BSA**	**Peak 1**	**Peak 2**	**Peak BSA**	**Pk1/BSA**	**Pk2/BSA**
Run #1	9.052	9.326	7.697	5.6	2.5	6.9	0.8	0.4
Run #2	8.683	9.161	7.760	19.3	11.7	29.4	0.6	0.4
Run #3	8.777	9.376	7.923	19.2	10.4	33.3	0.6	0.3
$\bar{x}$							0.7	0.4
S							0.1	0.1
RSD							14%	25%
At 90ºC	**Peak1**	**Peak 2**	**Peak BSA**	**Peak 1**	**Peak 2**	**Peak BSA**	**Pk1/BSA**	**Pk2/BSA**
Run #1	8.918	9.677	7.713	8.3	3.4	2.7	7.1	3.8
Run #2	10.35	11.15	8.993	8.3	3.1	2.7	1.1	1.4
Run #3	9.035	9.754	7.838	12.2	4.5	3.3	3.7	1.4
$\bar{x}$							3.9	2.2
S							3.0	1.3
RSD							77%	59%